AALTO UNIVERSITY. SCHOOL OF ENGINEERING.

Department of Civil and Environmental Engineering

JUAN GALLARDO FORÉS

SHEAR RESISTANCE OF BACKFILL COMPONENTS' INTERFACES IN NUCLEAR WASTE DEPOSITION TUNNELS

Master´s Thesis submitted on 29th of August 2012

SUPERVISOR: Professor (fixed term) LEENA KORKIALA-TANTTU

ADVISOR: Lic. Sc. (Tech) MATTI LOJANDER

Aalto University
School of Engineering

Aalto University, P.O. BOX 11000, 00076 AALTO
www.aalto.fi

Abstract of master's thesis

Author	Juan Gallardo Forés
Title of thesis	Shear resistance of backfill components' interfaces in nuclear waste deposition tunnels
Department	Civil and Environmental Engineering
Professorship	Soil Mechanics and Foundation Engineering
Code of professorship	Rak-50
Thesis supervisor	Professor (fixed term) Leena Korkiala-Tanttu
Thesis advisor(s) / Thesis examiner(s)	Lic. Sc. (Tech) Matti Lojander
Date	29.08.2012
Number of pages	79+8(app)
Language	English

Abstract

The purpose of the study was to investigate the shear strength behaviour of the interface of tunnel backfilling components in nuclear waste deposition tunnels. The studied disposal concept in this project is the KBS-3V, where the holes are drilled vertically into the bedrock from the deposition tunnel floor. The waste deposition tunnels will be excavated into an approximate depth of 420 m.

The determined shear strength parameters will be used in the numerical modelling of the buffer/ backfill interactions. The analysis of the results can also be used in the reliability evaluation of the modelling results. In this case, the tested backfill materials were Friedland clay as block material, bentonite pellets, mixtures of granulated bentonite and crushed rock as foundation bed material and granite stones. Investigated granite stones were classified to three different types depending on their surface roughness.

The followed test method was direct shear box test using large scale equipment. The side dimension of the square test box was 300 mm. A large testing program of 26 shear box tests was carried out in the laboratory of Soil Mechanics and Foundation Engineering. Seven different interfaces were tested: block / block, block / pellets, block / granulated bentonite, block / foundation bed material, smooth stone / pellets, intermediate roughness stone / pellets and rough stone / pellets. Calculations of some material properties (bulk density, dry density, water content, grain distribution) were also implemented.

On the basis of the shear box tests made, it seems that the interface between granite stone and bentonite pellets have the highest value for friction angle. The interface between blocks got the lowest friction angle. The obtained values for the strength parameters in the interfaces block / granulated bentonite and block / foundation material are quite similar. Moreover, not important differences can be observed in the smooth and intermediate roughness granite stone.

Keywords backfill, interface, shear box test, bentonite clay, granite stone, pellets, block

PREFACE

I would like to thank Professor Leena Korkiala-Tanttu and Laboratory Manager Matti Lojander for teaching, guidance, advice, time and giving me the opportunity to work on this research project. I would also like to thank Practical Training Supervisor Jarmo Vihervuori, for helping me in the laboratory tests and for his patience.

In addition, I would like to thank the personnel of the Laboratory of Soil Mechanics and Foundation Engineering at Aalto University, School of Engineering and everybody else who have supported me in my work and above all had welcome and treated me so warmly at the department.

Espoo, the 29th of August 2012

Juan Gallardo Forés

LIST OF SYMBOLS

R_a	Average roughness parameter
S_R	Degree of saturation
c	Cohesion
e_0	Initial void ratio
w	Water content
Δx	Horizontal displacement
Δy	Vertical displacement
ρ	Bulk density
ρ_d	Dry density
ρ_s	Grain density
ρ_w	Water density
τ	Shear stress
τ_{max}	Maximum shear stress
φ	Friction angle

Contents

1. INTRODUCTION

This laboratory study is part of Aalto University's research project 'Block-shear' and its funding is provided by the State Nuclear Waste Management Fund (VYR) and Aalto University. Block-shear is an acronym of "The mechanical behaviour of bentonite and backfill block surfaces in shear stress". Block-shear is a subproject of coordination project BOA (Assessment of bentonite characteristics), which is one project in KYT2014 (Finnish Research Programme on Nuclear Waste Management) research programme 2011-2014.

The aim of this study is to provide reliable values for the strength parameters that are needed to modelling the interaction between different components in the deposition holes. The most important requirement of the deposition tunnel is that the backfill material should have enough stiffness, even if the buffer swells and compress the backfill, the buffer density must not decrease substantially. So, the main point is to avoid the penetration of the buffer to the backfill and for that reason it is important to keep buffer density in high values. The effectiveness of the buffer/backfill system depends on the global system rigidity, and especially on the stiffness of its single component and the interfaces between them. For this reason, a study of the mechanical behavior of the interactions in the tunnel backfilling of nuclear waste deposition tunnels, mainly shearing, was carried out. This document evaluates and reports the interface shear strength behavior of different materials and components that can be used in the tunnel backfilling. The friction angle (φ) and cohesion (c) of the interfaces are the evaluated strength parameters in this study. The Direct Shear Box Test (ISO/TS 17892-10:2004) was employed to test the interface shear strength behavior.

The tested backfill materials were Friedland clay blocks, bentonite pellets, mixtures of granulated bentonite and crushed rock as foundation bed material and granite stones. Investigated granite stones were classified into three depending on their surface roughness. A series of 26 shear box tests were carried out at the Soil Mechanics and Foundation Engineering laboratory at Aalto University. Seven different interfaces were tested: block / block, block / pellets, block / granulated bentonite, block / foundation material, smooth stone / pellets, intermediate roughness stone / pellets and rough stone / pellets. Calculations of some material properties such as bulk density, dry density, water content and grain distribution were also performed.

2. BACKGROUND

2.1. General

Nuclear waste management of Finnish nuclear power plants is regulated by the Nuclear Energy Act (990/1987) and the Nuclear Energy Decree (161/1988) which entered into force in 1988. The above legislation determines, for example, the liabilities of nuclear energy producers, the enforcement of nuclear waste management, permit procedures and supervision rights. According to the Nuclear Energy Act which was rectified in 1994, all nuclear waste created in Finland must be disposed within Finland. (Posiva 2010.)

According to Finnish nuclear energy legislations, each producer of nuclear waste is responsible for the safe handing, management, and disposal of its waste, as well as for the costs arising. Posiva, the company owned by the nuclear energy-producing power companies, is in charge of spent nuclear fuel management in Finland. For this purpose, the Ministry of Trade and Industry established the decision 9/815/2003. In that decision, Teollisuuden Voima Oyj (TVO) and Fortum Power and Heat Oy, as parties under nuclear waste management obligation shall, either separately, together, or through Posiva Oy, prepare to present all reports and plans required to obtain a construction license for a disposal facility for spent nuclear fuel as stated in the Nuclear Energy Decree by the end of 2012. The disposal facility is expected to become operational by 2020. (Posiva 2010.)

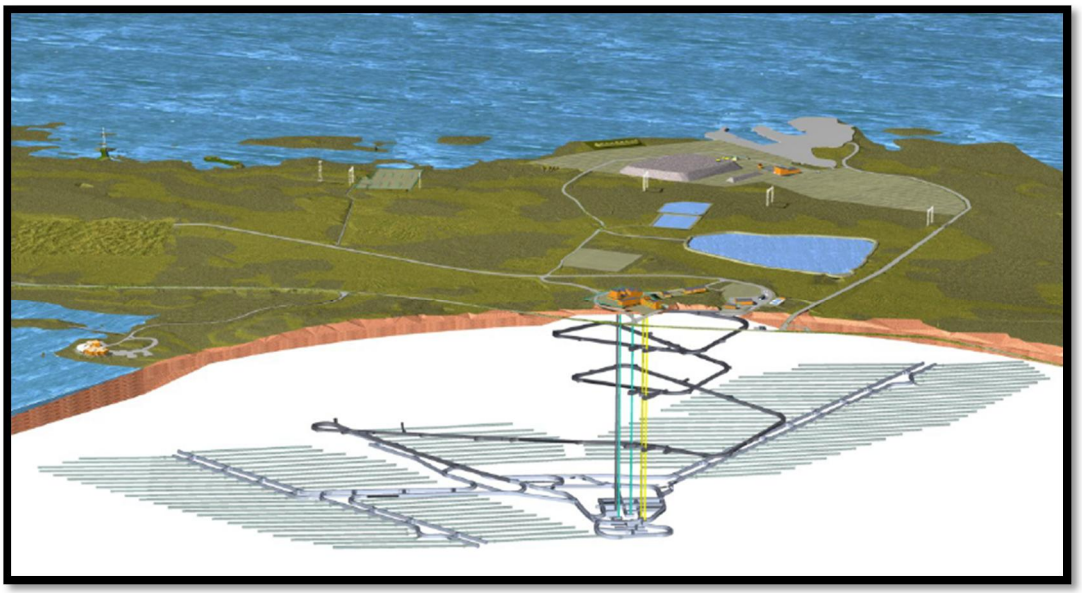

***Figure 2-1**. Disposal facility at Olkiluoto island (Posiva 2010, p. 21).*

The disposal facility planned by Posiva consists of two parts: the aboveground encapsulation plant and the underground repository. In the encapsulation plant, the spent nuclear fuel is encapsulated in disposal canisters. The disposal canisters are then transferred from the encapsulation plant to the underground disposal facility, which comprises the repository facilities, the central tunnels connecting the repository facilities, an access tunnel, a number of shafts and other underground auxiliary and technical facilities. Furthermore, the disposal facility provides a repository for low and intermediate level waste mainly generated in connection with the operation and decommissioning of the encapsulation plant. (Posiva 2010.)

Features of the repository facilities in the basic plan consist of deposition tunnels and deposition holes. Deposition tunnels have to be bored into the floors of the tunnels. The excavation of deposition tunnels will be performed gradually over the operational phase of the repository, with an average tunnel excavation of 10 to 20 at a time. The disposal depth is around 500 meters from the ground surface. After the placement of canisters into the deposition holes, the deposition tunnel will be backfilled and sealed as soon as possible. (Posiva 2010.)

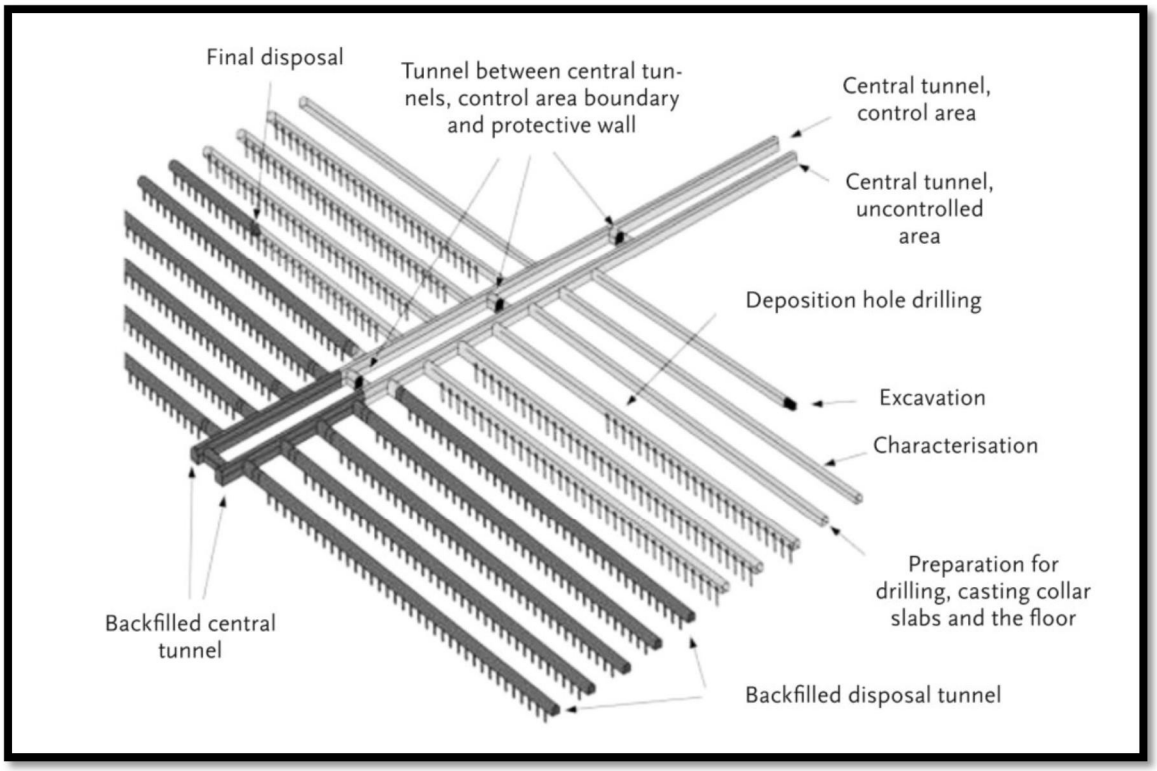

Figure 2-2*. Construction detail of the deposition tunnels underground (Posiva 2010, p.26).*

2.2. KBS-3V concept

This document is focused on the KBS-3 system. The KBS is an abbreviation of KärnBränsleSäkerhet and that means “nuclear safety”. This is referred to the technology for safe disposal of high-level radioactive waste which was developed in Sweden by Svensk Kärnbränslehantering SKB AB (SKB 1998).

Different principles and strategies for the disposal of spent nuclear fuel and high-level waste have been studied in many countries ever since nuclear power began to be used for large-scale electricity production in the 1960s and 1970s. In the 1980s, a new view arose in Sweden on reprocessing as the main point for dealing with the spent nuclear fuel. Instead of the fuel being considered as a resource, direct disposal was seen as the most reasonable alternative, that led to the idea that the fuel could be regarded as waste. The KBS-3 report (1983) presented the KBS-3 concept, involving encapsulation of the spent nuclear fuel in copper canisters and deposit them at a depth of about 500 meters below the ground surface, in crystalline rock. (SKB 1998.)

The long-term safety of KBS-3 repository has been measured up in a number of safety evaluations and safety assessments. They showed that a KBS-3 repository, built on the analyzed sites, can satisfy the requirements on safety, radiation protection and environmental protection that are made in laws and regulations. Other alternatives that have been evaluated and discussed for final disposal of spent nuclear fuel have been subjected to comprehensive studies and assessments, but have not been confirmed as completely safe alternatives. (SKB 2010.)

The KBS-3 disposal concept (Posiva 2010) consists of the following steps:

- The spent nuclear fuel is enclosed in water-tight and load canisters.
- The canisters are deposited at 400-700 meters depth in crystalline bedrock.
- The canisters are surrounded by a buffer preventing groundwater flow and protecting the canister.
- The rock cavities required to deposit the canisters are backfilled so that their functional characteristics are similar to those of the pristine bedrock.
- After the storage facility is full, the drill hole is sealed and the site marked.
- After 100,000 years of storage, the radioactivity level of the waste is at the same level as that uranium ore mined to make the fuel.

The KBS-3 concept involves encapsulating the spent fuel in copper canisters which are then deposited, in deposition holes in a tunnel system at a depth of 400–700 meters in the bedrock, and surrounded by a buffer of bentonite clays, see Figure 2-3. The purpose of the three barriers (canister, buffer and rock) is to isolate the radionuclides in the fuel from the surrounding environment. The KBS-3V concept means the deposition holes are drilled vertically into the bed rock. On the other hand, if the holes are drilled horizontally, then it is called KBS-3H, see Figure 2-4 (SKB 2010). This study is based on KBS-3V concept.

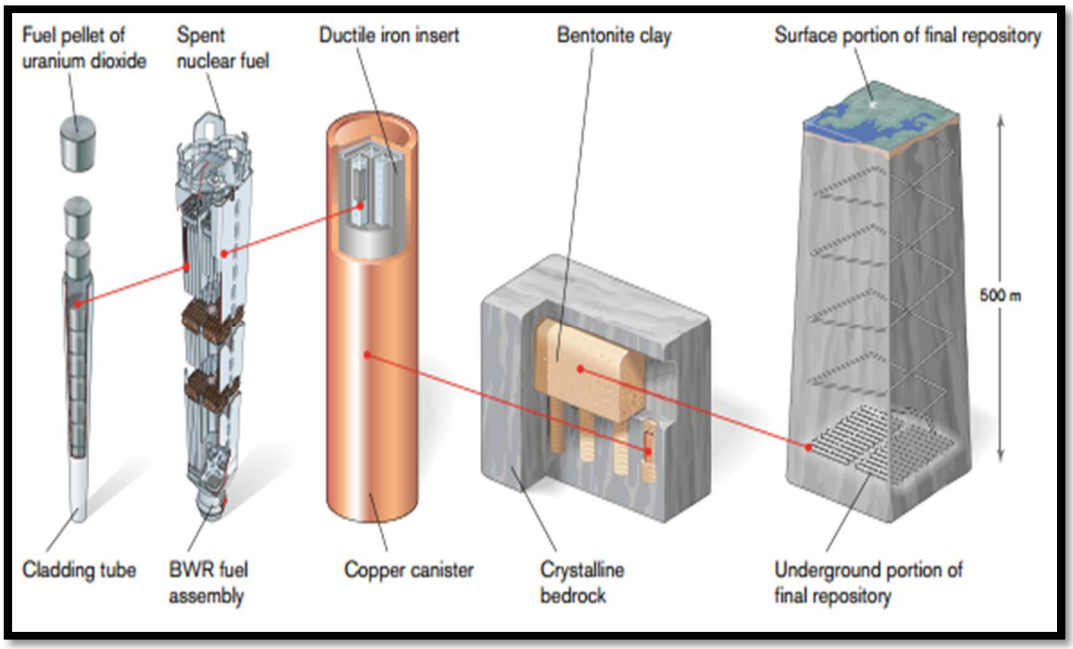

***Figure 2-3**. Principles of final disposal of spent nuclear fuel according to the KBS-3 concept (SKB 2010, p.33).*

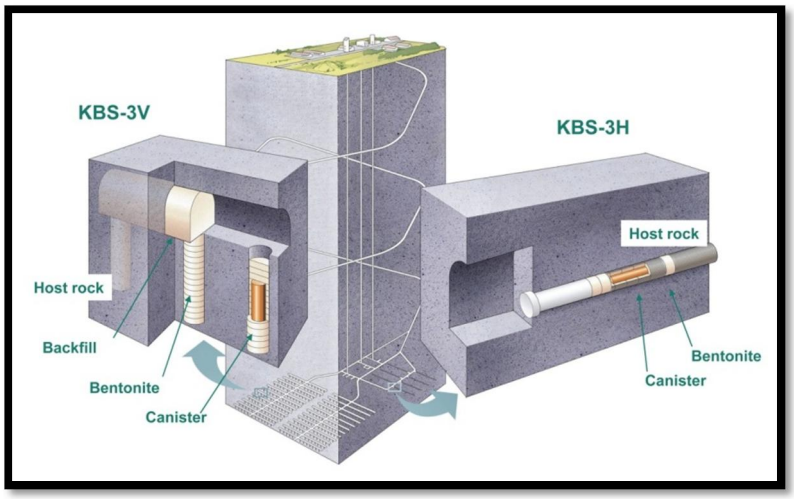

***Figure 2-4**. KBS-3V and KBS-3H concept (SKB 2010, p.35).*

In the multi-barrier principle, the safety of Finnish spent nuclear fuel repositories relies on natural and engineered barriers. The natural barrier component consists of the surrounding bedrock. The engineered barriers in a KBS-3 type repository are comprised of the, copper canister with cast iron insert, bentonite-based buffer and backfill, temporary and permanent plugs used for closure and sealing of the repository. The backfill component is placed above the canister which is vertically placed into the disposal holes drilled to the floor of the deposition tunnel in a KBS-3V concept. The main requirements of the backfill are: a) it should limit the upward expansion of the buffer into the deposition tunnel and b) prevent development of hydraulic transport pathways in the deposition tunnels so that the natural water flux at the repository level will not be affected. One of the most essential points is that the backfilling of deposition tunnels, because these excavations have the potential to affect the performance of the buffer, the canister and subsequently, radionuclide transport along the deposition tunnels. (Posiva 2010.)

2.3. Development of spent fuel disposal technology

2.3.1. Disposal technology components

Finnish repositories for spent nuclear fuel are planned to be excavated deep into crystalline bedrock. The radioactive materials will be isolated from the biosphere by a multi-barrier system consisting of natural and engineered barriers. See Figure 2-5. (Keto et al. 2009).

The disposal technology is divided into the following parts (Posiva 2010):

- Underground openings
- Buffer
- Canister
- Tunnel Backfilling
- Facility Closure and sealing

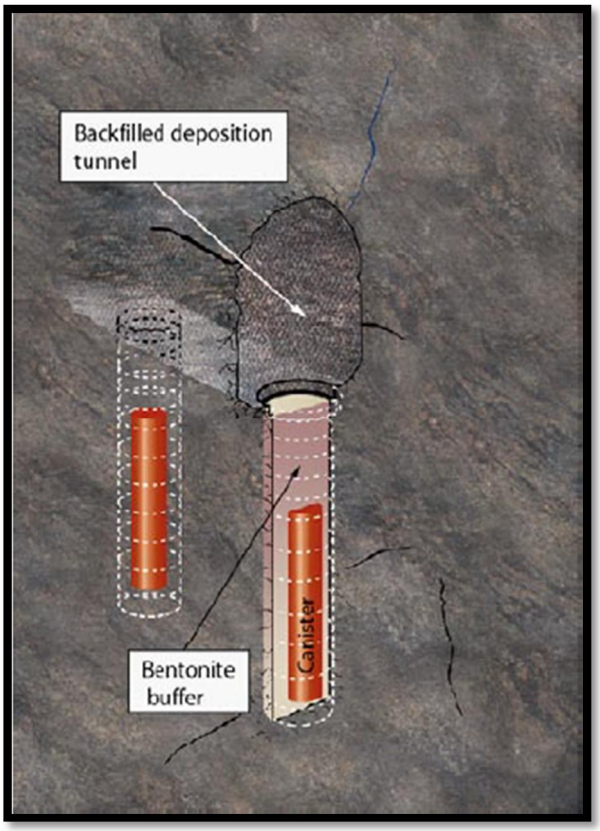

Figure 2-5*. The canister, a bentonite buffer surrounding the canister and the materials used for backfilling the deposition tunnels are all components of the engineered barrier system (Keto et al. 2009, p.7).*

2.3.2. Underground openings

The underground openings are referred to the spaces excavated into the rock which are necessary for the location of the disposal. These include the ONKALO research facility and associated auxiliary facilities, the vertical shafts, the central tunnels and the repository facilities. ONKALO is the underground rock characterization facility, and this is one of the elements of the site investigations conducted at Olkiluoto that will be extended to the final disposal depth of approximately 400m. The ONKALO research facilities are to be integrated with the disposal facility. (Posiva 2010.)

The main objective of these excavations is to plan and describe the different phase of construction of the underground facilities in order to determine and evaluate the long-term safety and to help in the implementation planning (Posiva 2010).

2.3.3. Buffer

The main function of the buffer is to protect the copper canisters in the deposition holes from any chemical and mechanical damages and, if canister damage occurs, to prevent

harmful substances migrating into the surroundings rocks. In order to fulfill to these requirements, the buffer must satisfy the following conditions (Posiva 2010):

1. Sufficiently low hydraulic conductivity in order to prevent any major advection.
2. Sufficient swelling pressure in order to ensure tightness and self-sealing ability as well as to prevent major microbiological activity and the sinking of the canister.
3. Sufficiently small pore structure in order to prevent migration of radionuclides with colloids.

In order to fulfill the above requirements, importance should be given to the density criteria of the buffer material. This is because the buffer density is related to the hydraulic conductivity and to the swelling pressure of the saturated buffer. Furthermore, the target density is in a very narrow range of values (1,950-2050 kg/m^3). It is also important to ensure that the density of the buffer is not jeopardized by the excess swelling into the deposition tunnel. (Juvankoski et al. 2010.)

The buffer must also guarantee the adequate protection of the canister against small rock dislocations, considering the canister properties, the selected buffer material and the rock conditions prevailing in the zone. The buffer properties themselves must not, as a consequence of the heat emitted from the canister, change to an extent that would be damaging. The buffer swelling pressure must be built sufficiently, so that it can prevent the spalling of surrounding rocks into the hole due to the increased temperature. (Posiva 2012.)

2.3.4. Canister

The disposal canister consists of two containers, one inside the other (Figure 2-6). The outer container is a copper shell and the inside container is made of cast iron insert. The spent nuclear fuel will be safety stored inside this assembly. Copper provides protection from corrosion and form a gas and watertight shell. The canister insert, which is made of graphite cast iron, guarantees the sufficient mechanical strength of the canister and ensures the tightness of the fuel. The canister insert is installed inside the copper canister before the canisters are delivered to the encapsulation facility. (Posiva 2010.)

Figure 2-6*. Different kinds of disposal canisters for spent fuel with both containers (Posiva 2010, p.25).*

2.3.5. Tunnel Backfilling

The main function of the backfill in the deposition tunnels is to sustain the multiple barrier principle by maintaining the safety functions of the individual barriers. To maintain this function the backfilling in deposition tunnels shall (Hansen et al. 2010):

1. Restrict advective transport.
2. Restrict upwards swelling/expansion of the buffer.
3. Not impair the safety functions of the barrier in any way.
4. Be long-term durable and its functions be preserved in the environmental expected in the repository.

The purposes of the tunnel backfill are to prevent the formation of flow paths along the excavated facilities, to contribute for keeping the buffer in place, to protect the canister and to support the surrounding rock. The sealing structure built at the mouth of the tunnel must prevent the loosening of the tunnel backfill from the tunnel when the facilities are open. In addition, the backfill material and sealing structure must not affect the other components of the engineered barrier system. (Posiva 2010.)

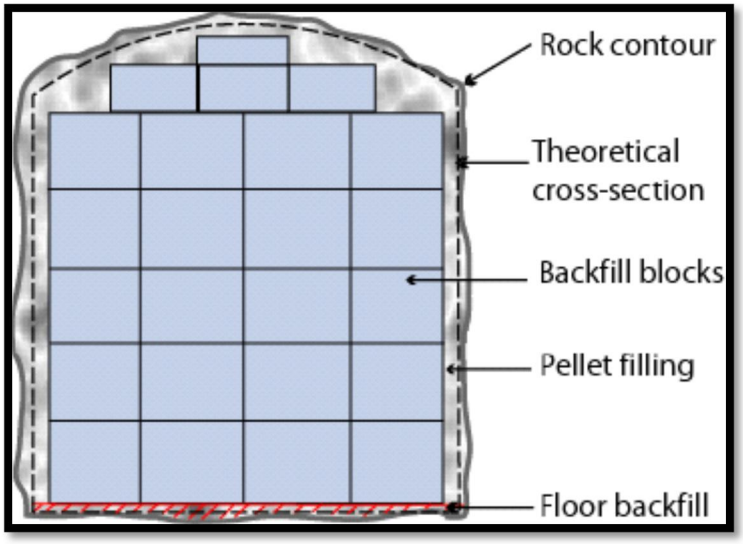

Figure 2-7*. Conceptual picture of a backfilled tunnel (Posiva 2010, p.253).*

According to the current basic design, the backfilling of the deposition tunnels will be conducted using blocks compacted from Friedland Clay, pellets filling up the space between the blocks and the rock and a filling for the foundation bed to be applied separately. The functioning and performance of the filling structure depends mostly on the composition of the backfilling materials, the densities of the backfilling components and the amount of empty space left in the tunnel. (Hansen et al. 2010.)

2.3.6. Facility Closure and sealing

At the end of the disposal construction phase, the facilities will be closed and sealed. A part of the repository panels will be sealed off during the operational phase so that the minimum number of facilities would be open at the same time. The auxiliary facilities and investigation holes followed by the other tunnels at the disposal depth and the access routes to the surface will be sealed when the construction phase ends. Finally, the access tunnel and shafts will be sealed. The most important functional requirements in the sealing process are to prevent the creation of flow paths between the surface and the repository as well as inadvertent entry to the facilities. (Posiva 2010.)

3. LITERATURE REVIEW

3.1. Related previous studies

Previous studies have been carried out at the University of Tampere in order to provide information on the strength and deformation properties of backfill formed by blocks and pellets. This information is useful to study the effect of interfaces on the strength parameters of the block backfill and also to model the backfill/buffer interaction. It belongs to the third phase of the joint SKB-Posiva programme "*Backfilling and Closure of the Deep Repository, BACLO*" (Keto et al. 2009). Tables 3-1 shows different types of triaxial and shear box tests that were carried out at University of Tampere.

***Table 3-1**. Test matrix of the study from University of Tampere (Kuula-Väisänen et al.2008).*

Method	Test material	Objective
Triaxial test CIDC Ø 50 mm	Asha 230b	Strength parameters of single compacted test material
	Friedland clay	
	Bentonite-ballast 30/70 mixture	
	Granules	
	Pellets	
Triaxial test CIDC Ø 100 mm	Pellets	
Shear box test 60x60 mm	Pellets	
	Friedland clay	
	Asha 230b	
	Bentonite-ballast 30/70 mixture	
Triaxial test CIDC Ø 300 mm	Friedland clay (Block)	Strength parameters of interface between blocks
Shear box test 60x60 mm	Friedland clay (Block)	
	Asha 230b (Block)	
	Bentonite-ballast 30/70 mixture (Block)	

Small scale triaxial tests were performed with unsaturated samples and samples were loaded under pressures of 100 kPa, 200 kPa and 400 kPa using a consolidated-undrained test procedure. Table 3-2 shows the initial properties of the tested materials and the values of apparent cohesion and friction angle using small scale triaxial test. The failure lines corresponding to the achieved peak strength values are shown in

Figure 3-1. A large scale triaxial test was also performed with samples consisting of a stack of Bjuv blocks cut into a circular shape. (Kuula-Väisänen et al. 2008.)

***Table 3-2**. Summary of initial properties of materials and apparent strength parameters in small triaxial tests (Kuula-Väisänen et al.2008).*

Material	Water content average (%)	Average dry density (kg/m^3)	Friction angle (°)	Cohesion (kPa)
Friedland-clay	9.10	1983	35.3	895
Asha 230	12.2	1659	47.9	343
Bentonite-ballast mixture (30/70)	7.80	2169	25.9	1031
Pellets	8.80	1045	21.9	52
Granules	18.2	1322	36.8	58

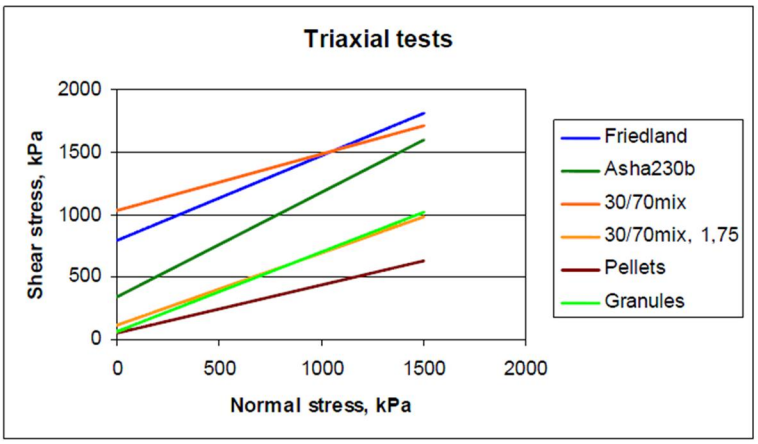

***Figure 3-1**. Failure lines of results in small scale triaxial tests (Kuula-Väisänen et al. 2008, p.14).*

A small shear box (60 x 60 mm) was used to perform the direct shear tests and the samples were applied under a normal stresses 100, 200, 400 and 800 kPa (Kuula-Väisänen et al. 2008). Single compacted samples and interfaces between blocks were tested. Tables 3-3 and 3-4 show the summary of initial data of the different tested materials and the respective apparent cohesion and friction angle.

The “lower” and “upper” concepts considered in the Table 3-3 means that the test was repeated by turning the sample upside down after the denser (upper) end of the sample had been shared first (lower). The sample is not homogeneous because of the way of manufacturing it. That explains, why the cohesion and friction angle have different values for the upper and for the lower in the same material. The results show that the

lower part of each one of the materials is given lower shear strengths than the respective values in the upper part. The pellets have the lowest shear strength as expected, due to the granular behaviour of pellets and not as a continuous material. (Kuula-Väisänen et al. 2008.)

***Table 3-3**. Summary of initial properties of materials and apparent strength parameters in single sample direct shear tests (Kuula-Väisänen et al. 2008).*

Material	Water content average (%)	Average dry density (kg/m^3)	Friction angle (°)	Cohesion (kPa)
Friedland-clay, lower	8.30	2010	37.7	1334
Friedland-clay, upper	8.30	2010	49.8	1157
Asha 230, lower	12.7	1680	49.4	338
Asha 230, upper	12.7	1680	46.3	484
Bentonite-ballast mixture (30/70), upper	6.70	2200	34.2	1083
Bentonite-ballast mixture (30/70), lower	6.70	2200	49.6	1124
Pellets	8.70	1035	26.9	40

***Table 3-4**. Obtained apparent strength parameters in interface direct shear test (Kuula-Väisänen et al. 2008).*

Material	Interface wetting	Friction angle (°)	Cohesion (kPa)
Friedland-clay blocks	Dry	24.4	0.7
	Tapwater 2g	18.4	16.0
	Saltwater 2g	12.3	66.3
	Saltwater 4g	18.5	13.0
Asha 230b blocks	Dry	23.5	7.4
	Saltwater 4g	15.7	48.3
Bentonite-ballast mixture (30/70) blocks	Dry	24.7	8.3
	Saltwater 2g	3.7	39.4
	Saltwater 4g	4.9	21.6

3.2. Interaction between buffer and backfill

The sufficient rigidity of the backfill in unsaturated state is one of the main requirements of the deposition tunnels (Korkiala-Tanttu 2009). For that reason, many studies have been performed to study the effectiveness of the buffer/backfill interactions. Finite element modelling was carried out to study the interaction between buffer and backfill and to find the dominating forces and their ratios. It was also needed for the long-term safety evaluations concerning the performance of backfill and buffer (Korkiala-Tanttu 2009). Several modelling studies including interactions between buffer and backfill have been reported (Korkiala-Tanttu 2009, Börgesson & Hernelind 2009).

Buffer bentonite was assumed in fully saturated state and backfill in dry state and it was modeled as discrete blocks system. The geometry of the problem is the reference solution adopted for Olkiluoto deposition hole, canister and buffer (Figure 3-2). An axisymmetric modelling case was used to represent the studied geometry (Figure 3-3). It was modeled in PLAXIS 2D 2010/2011 (Leoni 2012).

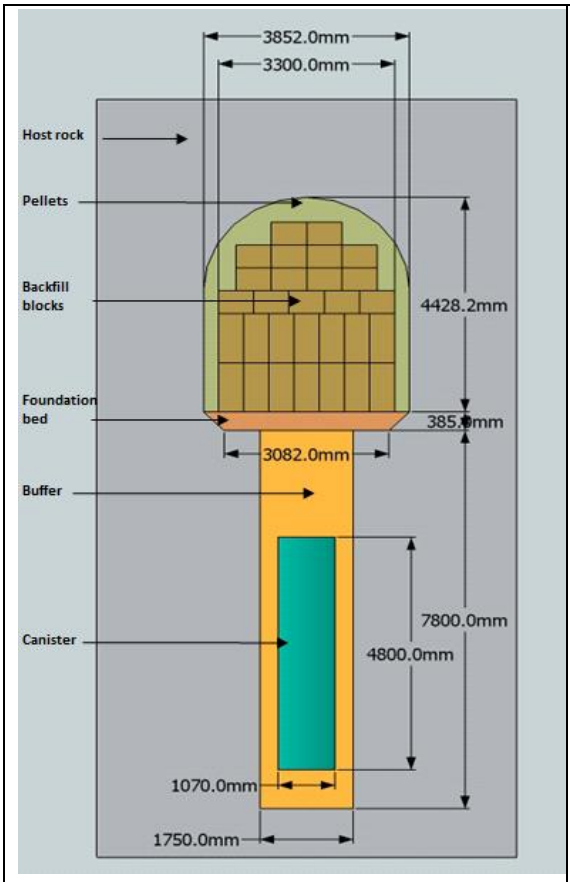

***Figure 3-2**. Geometry of OL1-2 section (Leoni 2012, p.4).*

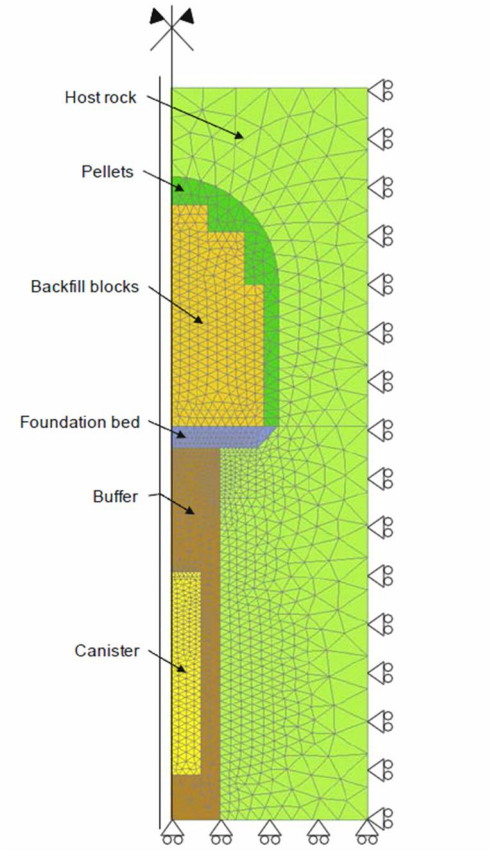

***Figure 3-3**. Mesh for axisymmetric calculations, case AX-01 (Leoni 2012, p.7).*

In Leoni´s model (Leoni 2012) the interface elements were according to Mohr-Coulomb constitutive behavior and the parameters were the interface cohesion, friction angle, dilatancy angle, Poisson´s ratio and elastic stiffness. Due to the lack of data from tests to calibrate interface behavior, some assumptions were taken. In this case a linear elastic constitutive law was chosen. The soil strength parameters used in the modeling coming from available laboratory tests are given in Table 3-5. (Leoni 2012.) These laboratory tests were taken of the reported data from Korkiala-Tanttu et al. (2007) and Johannesson et al. (2010).

Table 3-5*.Interface input strength parameters (Leoni 2012).*

Interfaces	φ´ (°)	c´ (kPa)
Block/block	24.0	0.0
Buffer/rock	8.69	0.0
Pellet/rock	10.0	0.0
Pellet/buffer	5.0	0.0
Foundation/rock	10.0	0.0
Foundation/blocks	5.0	0.0
Foundation/buffer	5.0	0.0
Foundation/pellet	27.0	10.0
Canister/buffer	5.0	0.0

The accuracy of data obtained from laboratory tests is an important factor in order to model the corresponding scenarios. Mechanical models would be more reliable and would represent better the reality if the used parameters came from laboratory tests instead of taking theoretical assumptions. Furthermore, strength parameters are becoming more important since the models that are required for calculating the buffer/backfill interactions in the deposition tunnels can represent and prevent future problems in the waste disposal system.

4. MATERIALS

4.1. General

The materials that were tested in this study can be divided into two different groups: clay materials and granite stones. The tested clay materials were Friedland-clay blocks, Cebogel QSE pellets, granulated bentonite and foundation material. Clay materials were collected from Riihimäki and delivered by Ekokem Oy in two different shipments, one was in August 2011 and the last one was in April 2012. Pellets, bentonite granulated and foundation material were received in airtight buckets and they were placed directly inside the cold room without any modification. The humidity of the received material was controlled in cold room with an average temperature of 7°C. Granite stones were bought from a hardware shop.

Figure 4-1*. Granular materials are stored in air-tight buckets inside the cold room.*

The Friedland-clay blocks and the granite stones were transported separately. After the shipment, the blocks were covered directly with a plastic sheet in the laboratory to minimize moisture loss, and the granite stones were left on a table in the laboratory.

4.2. Clay materials

Bentonite is an expansive clay material consisting mostly of montmorillonite and other smectites. It is chemically and mechanically stable and allows plastic deformations. Circulation of water is restricted in bentonite; however, it is permeable to gases. Another important property of some clays like bentonite is that they swell when they come into contact with water. If bentonite is compacted before or during placement,

then it becomes very dense, fills the voids and shows very low hydraulic conductivity and high swelling pressure. Additionally, bentonite can be considered as a very effective sorbent, which implies further retarding on transport. The most important variables that affect these processes are the effective porosity and surface area, as well as the cation exchange capacity of bentonite. Due to its expansion, upon wetting and associated extremely low hydraulic conductivity, bentonite and other swelling clays were selected to be used for backfilling, sealing of deposition tunnels and other underground facilities in the repository for high level spent nuclear fuel. (Rautioaho & Korkiala-Tanttu 2009.)

4.2.1. Friedland blocks

Friedland clay is smectite-rich clay from north-eastern Germany, near the town of Neubrandenburg. The clay is of tertiary origin and was formed by a complex process including sedimentation, weathering, erosion and hydrothermal alteration. The swelling component of the clay consists of mixed-layer of mica and montmorillonite (Riikonen 2009). The Friedland clay tested in this study was in block shape, with dimensions of 300 mm x 147 mm x 75 mm (Figure 4-2). The initial water content of these blocks was an average of 6.00 %.

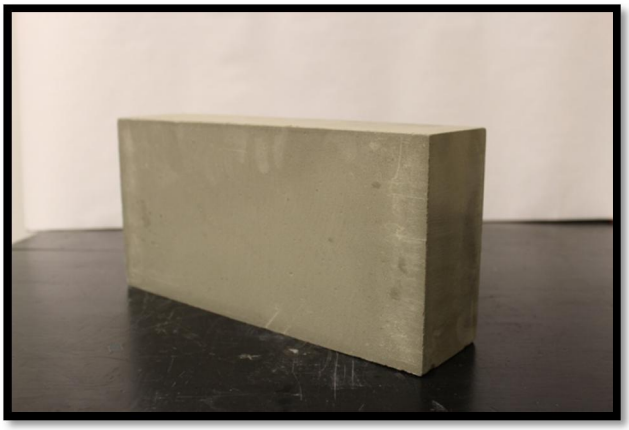

Figure 4-2*. Friedland-clay block.*

4.2.2. Cebogel QSE pellets

This material consists of high quality activated sodium bentonite from the Isle of Milos (Greece). The montmorillonite content of high-grade Milos Ca-bentonite is 80%. Cebogel QSE pellets are cylindrical bentonite granules with diameters about 6.5 millimeters and lengths from 5 to 20 mm (Figure 4-3) (Riikonen 2009). Grain size

distribution of Cebogel QSE pellets is given in Figure 4-5. The measured initial water content for these pellets was an average of 10.4 %.

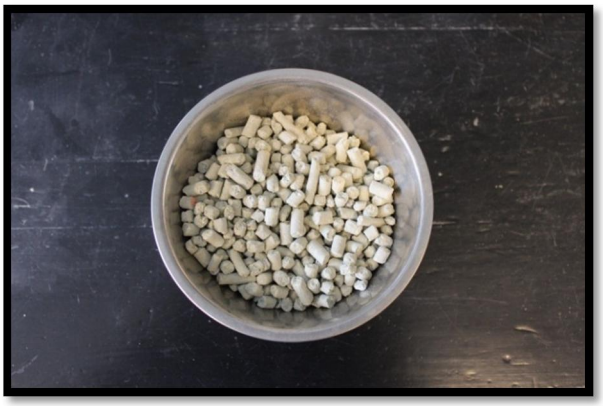

Figure 4-3*. Cebogel QSE pellets.*

4.2.3. Granulated bentonite

Granulated bentonite consists of crushed raw clay. Crushed materials can be selected depending on the size in order to provide graded products that can be used to fill the voids between pellets as backfilling material. The other point to take into account is related with the densification of the granular materials during the placement. This material tends to obstruct the installation equipment where water is added to the material during placement. Then, the contact with the water should be avoided to ensure the correct placement of the granulated material in the desired location. (Dixon 2011.)

Two batches of granulated bentonite were received to the laboratory in order to be tested. However, due to the similarity in their chemical and physical properties (for example, grain size distribution) (see Figure 4-5), they were mixed manually to form a unique granulated bentonite mixture. The tests were then carried out with this unique granulated bentonite. The average initial water content of the granulated bentonite was around 20.5 %.

Figure 4-4. *Granulated bentonite.*

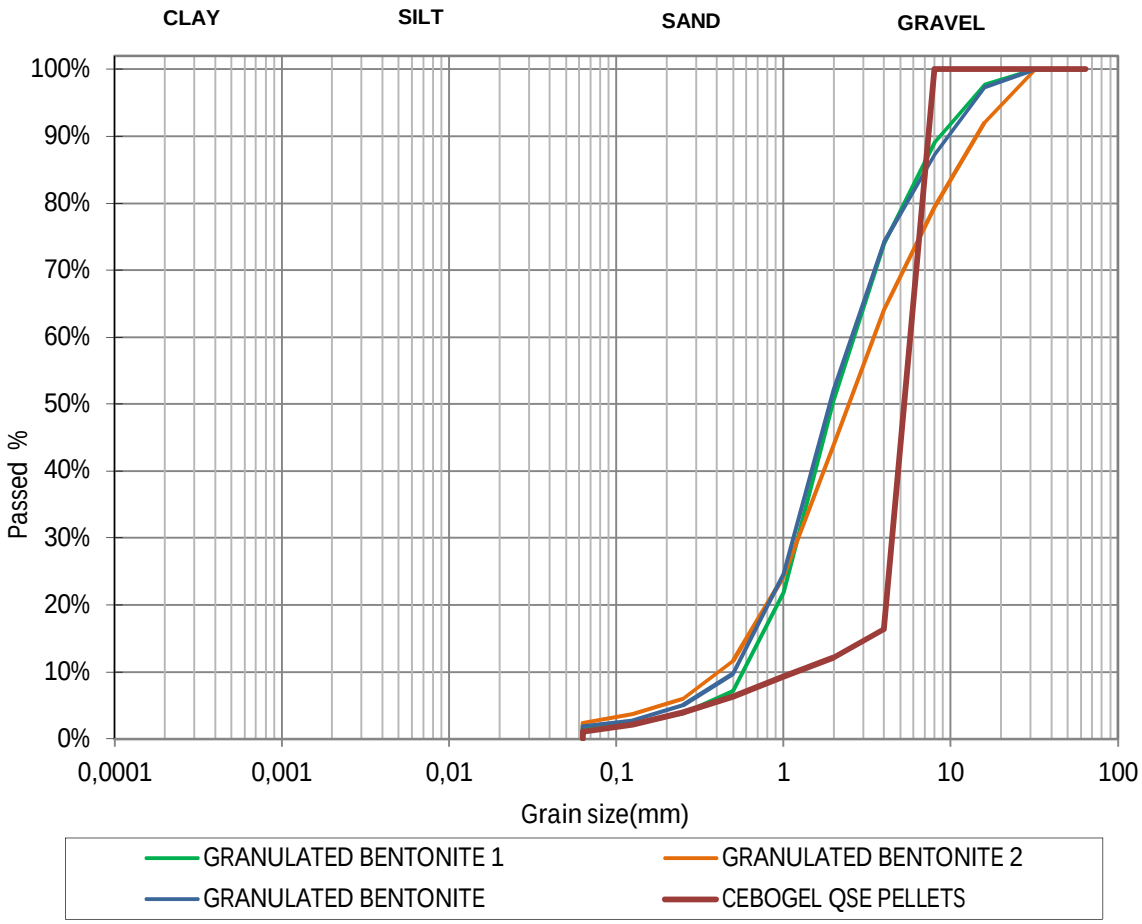

Figure 4-5. *Grain size distribution of CEBOGEL QSE pellets and granulated bentonites. Granulated bentonite 1 and granulated bentonite 2 were the received materials and granulated bentonite was the resultant mixture.*

4.2.4. Foundation bed material

The most important properties of the foundation bed material are the self-sealing capacity and low hydraulic conductivity, which should be below 1×10^{-10} m/s (Hansen et al. 2010). A mixture of AC-200 bentonite and crushed rock (50/50) was selected as the foundation material in this study (Figure 4-6). This foundation bed material was mixed by Ekokem Oy in Riihimäki and it was well compacted by a roller in the test tunnel base (Nemlander & Keski-Kuha 2012). The AC-200 is a montmorillonite based activated Ca-bentonite from the Isle of Milos (Greece). It is a fine material with the most of the particles size below 0.0063 mm. The crushed rock was produced from blasted stones excavated from the research repository in ONKALO. The maximum grain size of the crushed rock should be 0-10 mm in order to produce good homogeneity for the mixture (Riikonen 2009). The initial water content of the foundation bed mixture was an average of 15.9 % and the grain size distribution for this mixture and for the crushed rock is shown in Figure 4-7.

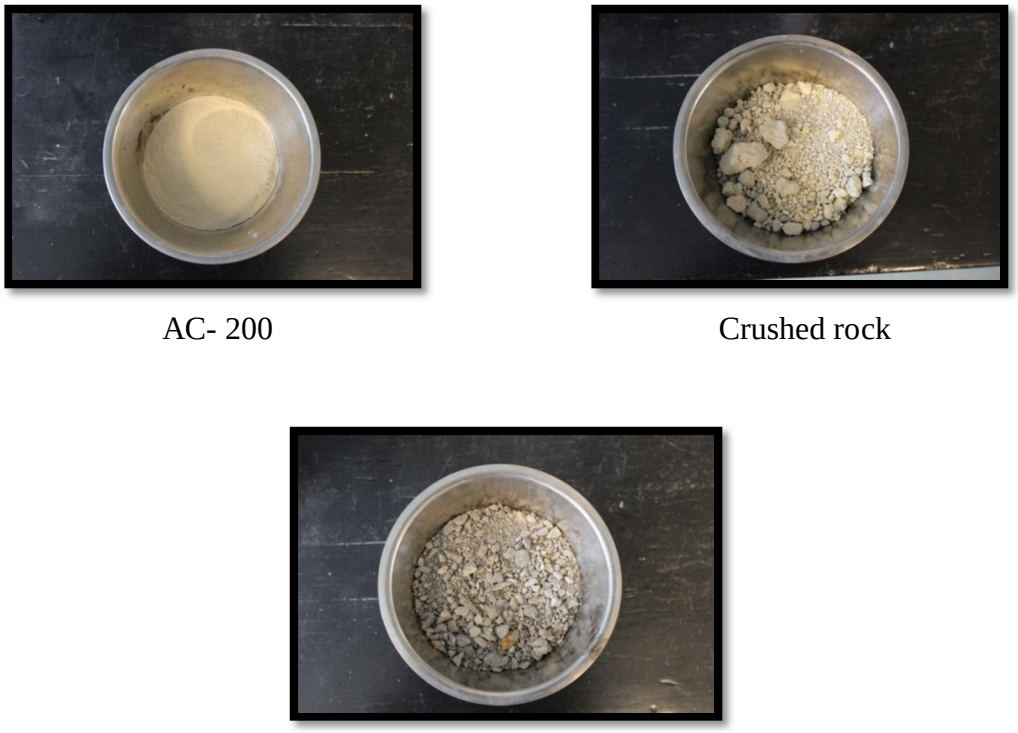

Figure 4-6*. AC-200, crushed rock and the mixture (50/50) of these two materials to form the foundation bed mixture.*

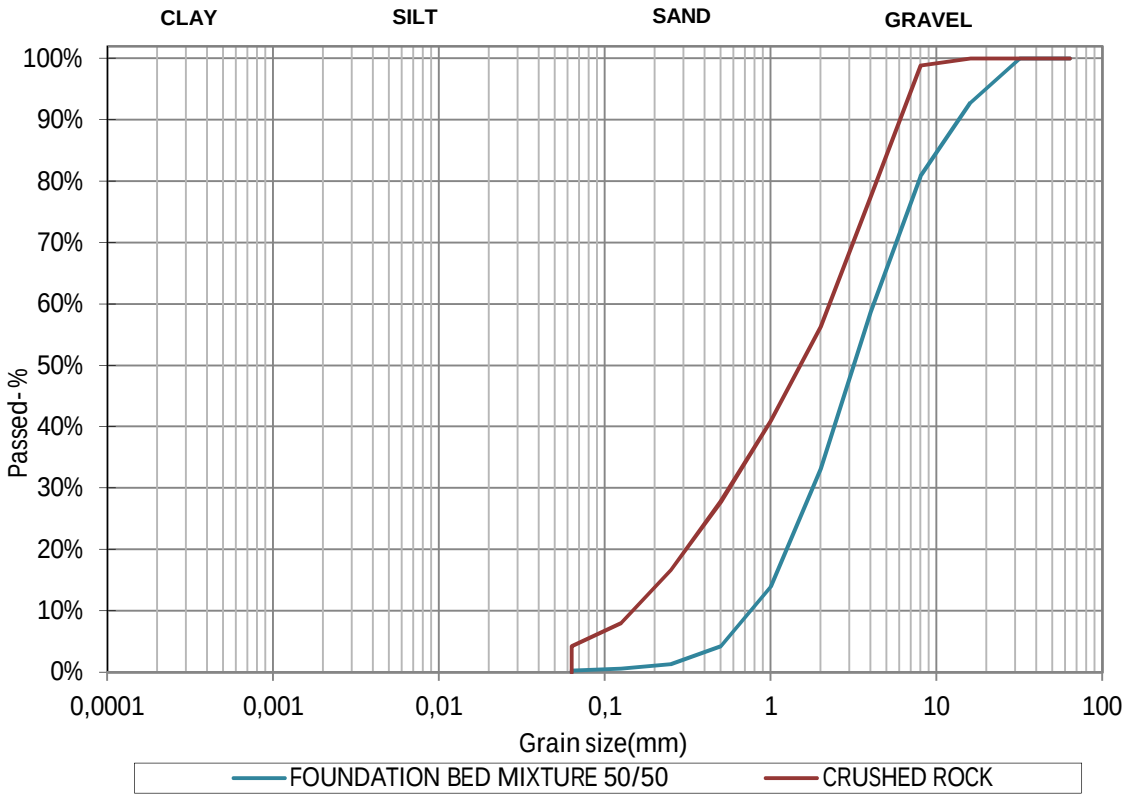

Figure 4-7*. Grain size distribution of foundation bed mixture 50/50 and crushed rock.*

4.3. Granite stone

The granite stone is one of the most durable stones and has a coarse-grained structure. It is composed of quartz, feldspars and micas, as well as a variety of other minerals, which contribute to the color and texture of natural granite stones. The principal properties of the granite are very low porosity and weather resistant (Alden n.d.). The main purpose of using granite stones in this study was to test the interface shearing between the stone and other materials. Hence, the strength of the material itself was not of interest, only the surface roughness was important. Therefore the basic granite stone material was chosen and the stones were bought from a local hardware shop.

The dimensions of the tested granite stone plates were 300 mm x 300 mm x 30 mm (Figure 4-9). The approximate weight of the stones was ranging from 7100 to 7400 kg. Three types of granite stone plates were tested with different surface roughness. Depending on the surface roughness, they were identified as smooth granite stone, intermediate roughness granite stone and rough granite stone.

Figure 4-9*. Granite stone.*

In order to distinguish the different surface roughness of the tested granites stones, the average roughness parameter (R_a) was determined. The average roughness is the most commonly used parameter for general quality control and it can be calculated using the equation 1 (Gadelmawla et al. 2002):

$$R_a = \frac{1}{n} * \sum_{i=1}^{n} |y_i| \qquad (1)$$

Where:

n - Number of sample points evaluated

y_i - Absolute value of the profile from the mean line

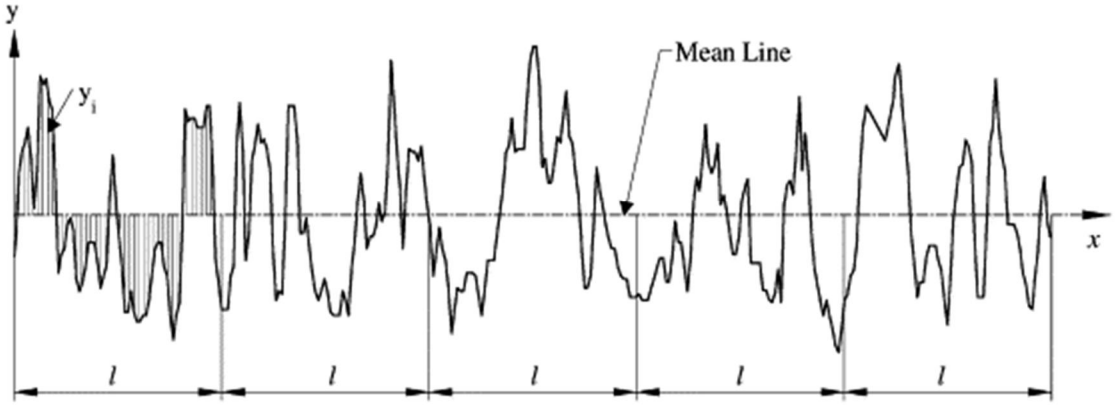

Figure 4-10*. Definition of the average roughness parameter (Gadelmawla et al. 2002).*

In order to determine the average surface roughness, the vertical and horizontal displacement measurements were needed and they were measured by using the direct shear box equipment as it is shown in Figure 4-11. A transducer was placed vertically in

contact with the granite stone surface to measure the vertical displacement and another displacement transducer was placed horizontally to measure the horizontal displacement and the displacement data was logged into a computer. Figure 4-12 to Figure 4-14 show the plots of the horizontal and vertical displacements for each one of the granite stones. The obtained results for the average roughness parameter are shown in Table 4-1.

***Figure 4-11**. Displacement transducers measuring vertical and horizontal displacements.*

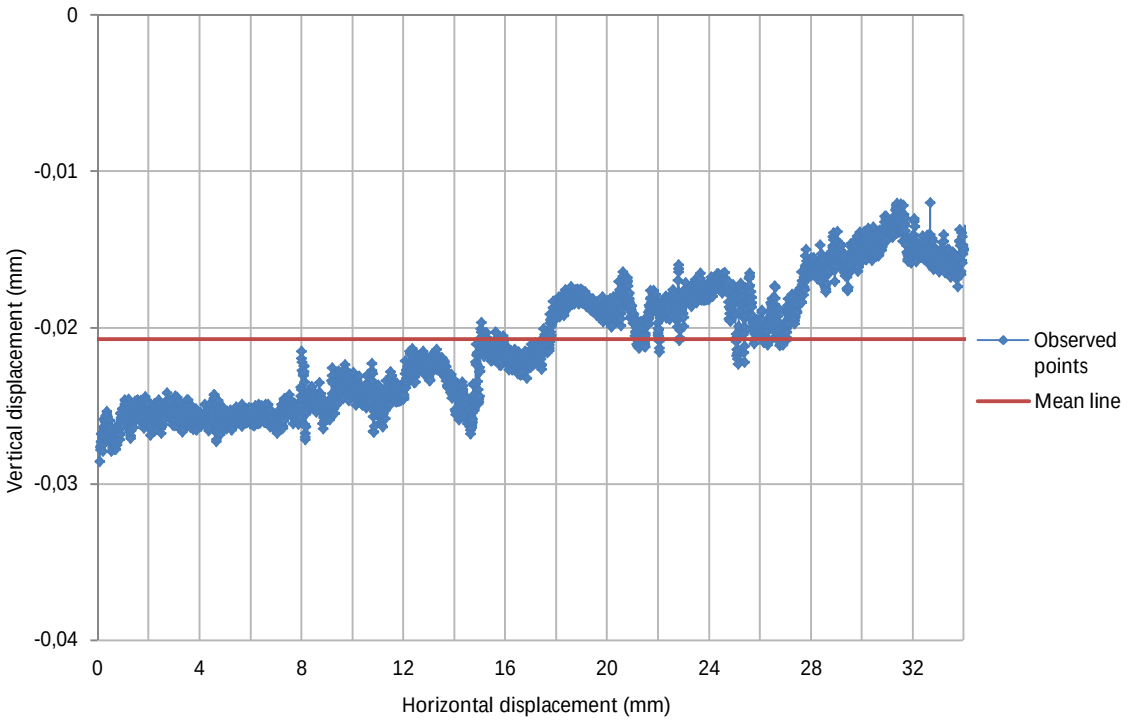

***Figure 4-12**. Horizontal displacement against vertical displacement in smooth granite stone.*

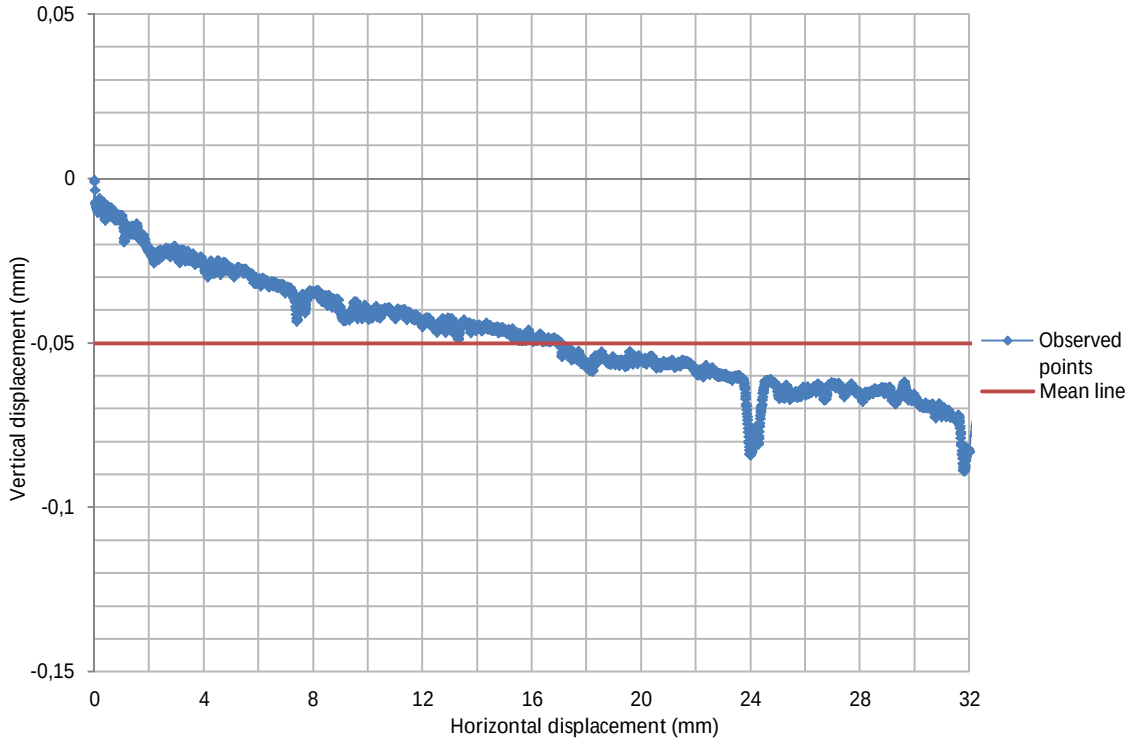

***Figure 4-13**. Horizontal displacement against vertical displacement in intermediate roughness granite stone.*

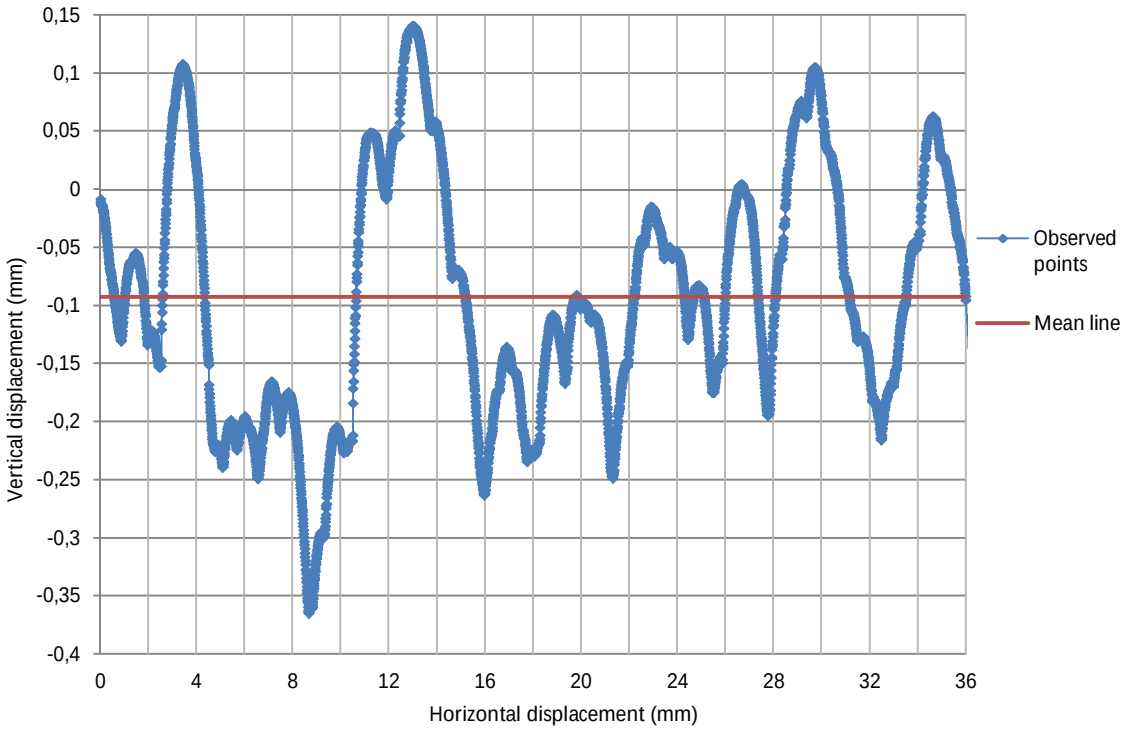

***Figure 4-14**. Horizontal displacement against vertical displacement in rough granite stone.*

***Table 4-1**. Average roughness parameter values every kind of granite stones.*

Roughness	Average roughness parameter R_a (μm)
Smooth	3.678
Intermediate	14.776
Rough	87.754

A significant difference in R_a can be observed between the rough stone and the other two. Nevertheless, no considerable difference appeared between the values from the intermediate and the smooth granite stone, so, similar shear strengths were expected in both cases.

5. TEST METHOD

5.1. Equipment

Shear box tests were carried out in a large 300 mm x 300 mm square Farnell shear box apparatus. The equipment consists of an apparatus structure, a shear box, a load plate, a load hanger, transducers and a computer to log the data automatically.

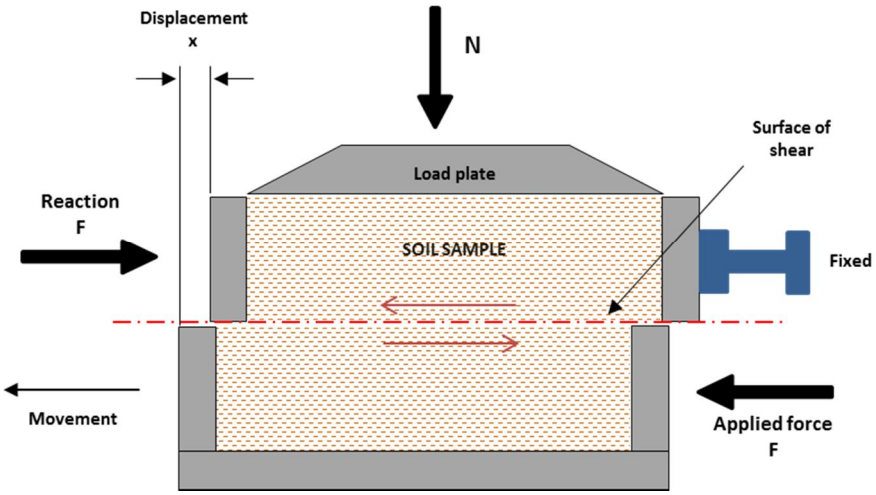

***Figure 5-1**. Principle of shear box apparatus.*

5.1.1. Apparatus structure

The structure of the shear box apparatus is formed by an electric motor, a load beam, a loading system and a hydraulic system. The electric motor is responsible for the implementation of the shear force. It allows the user to set different speeds which control the rate of the shearing. The table attached to the apparatus gives different combinations to achieve the desired speed (Figure 5-2). This motor is connected to a piston that transmits the horizontal movement to the shear box. The speed combination C2 which corresponds to a speed of 0.5 mm/s was used in this study (Figure 5-2). Furthermore, the corresponding loads were supported by the load beam which was also needed to transmit the forces to the shear box as a normal stress (Figure 5-3).

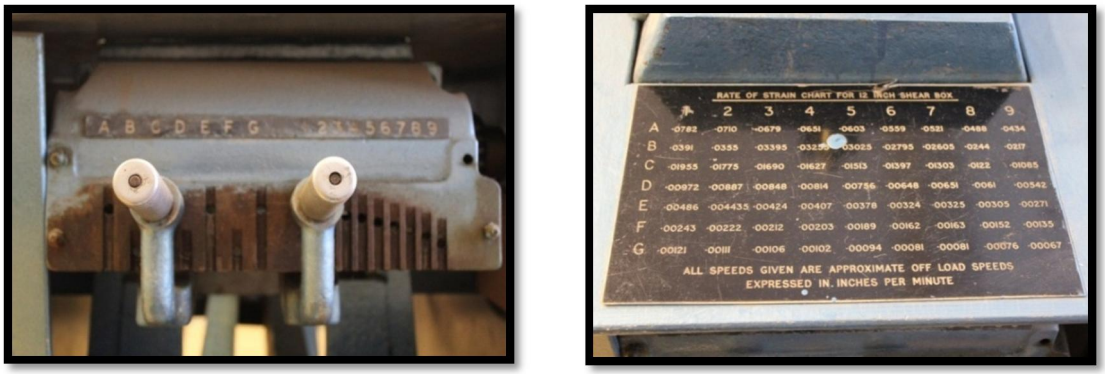

***Figure 5-2**. Combinations for the speed of the motor*

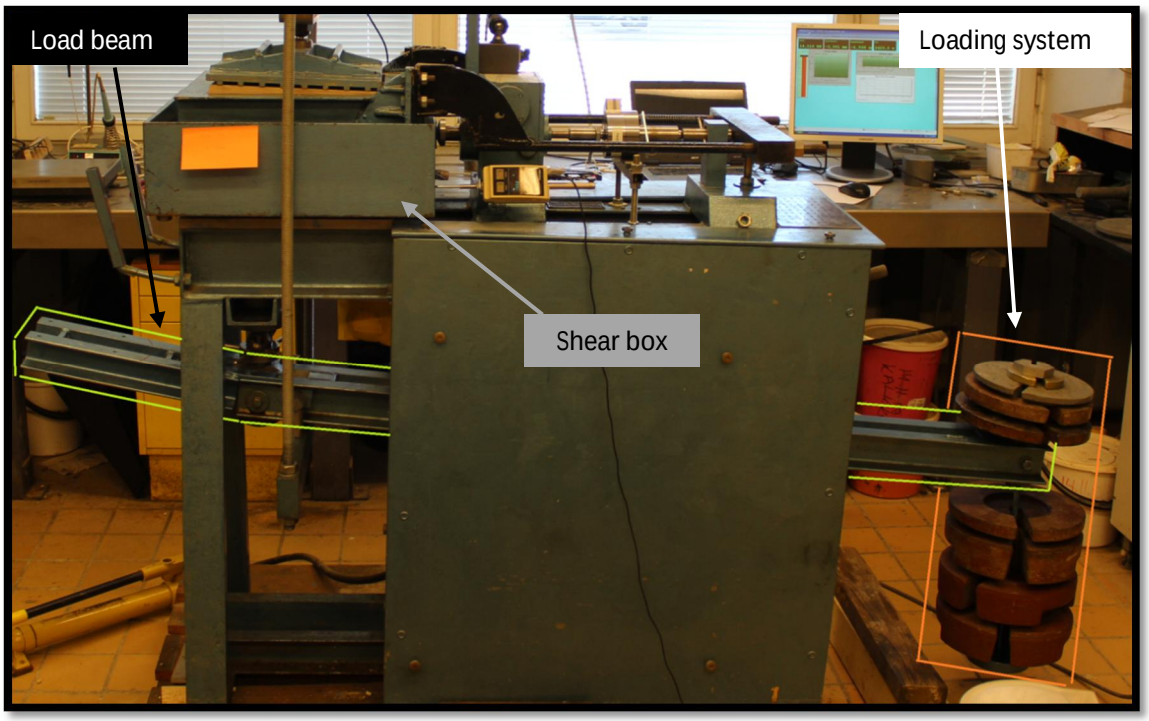

***Figure 5-3**. Load beam and loading system.*

The required loads were selected from a pool of 0.125, 0.25, 0.5, 1.0, 2.0, 6.0, 10.0 and 25 kilograms weights. A combination of these weights was used to obtain the required loading for each shear box test (Figure 5-3). Besides this, a hydraulic system was installed in this apparatus to facilitate the placement of the load beam in the correct alignment in order to transmit the normal force to the sample placed inside the shear box (Figure 5-4).

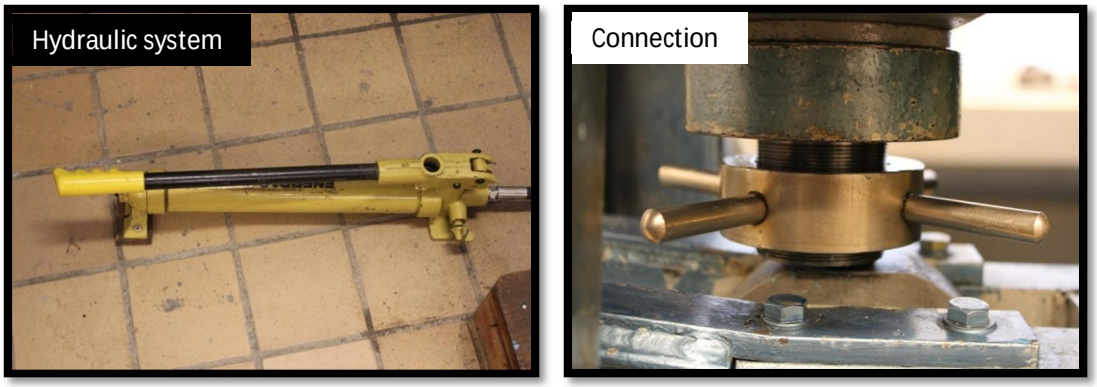

***Figure 5-4**. Hydraulic system and connection between shear box and load beam.*

5.1.2. Shear box

The shear box is the most important component of this set-up since it is the place where the sample is located and where the shearing takes place. In this Farnell Model, the shear box is square in plan and divided horizontally into two equal halves which create the shearing surface while moving horizontally. The dimensions of this box are 300 mm x 300 mm and it was assembled on the apparatus structure as shown in Figure 5-3. The lower part of the shear box is a moving part while the upper part is fixed. Both have the same thickness of 87 mm. The geometry and different parts of the shear box are given in figures from 5-5 to 5-7.

In order to keep the two halves of the shear box securely connected during the consolidation phase, two bolts were positioned to fix them. The consolidation phase was carried out before starting the shearing, when the vertical load was applied and there was no horizontal displacement. After the consolidation, bolts were removed in order to allow the lower half of the shear box to move freely against the upper half during the shearing.

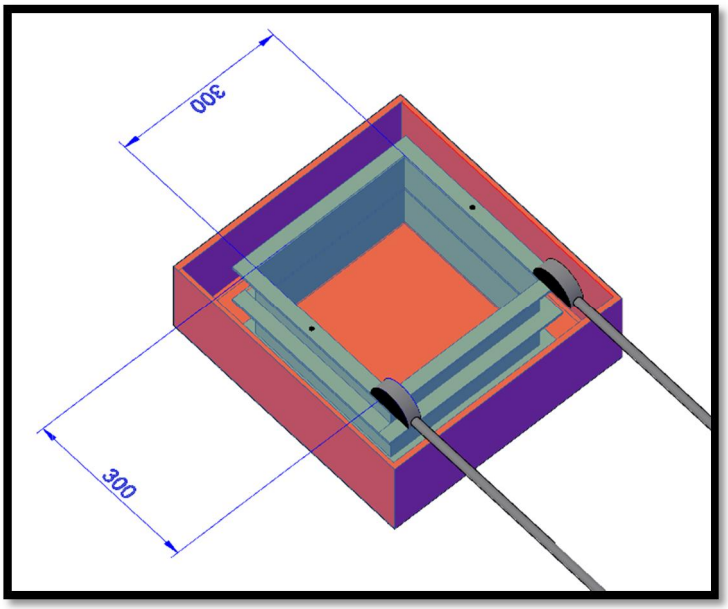

***Figure 5-5**. Geometry of the shear box (measures in mm).*

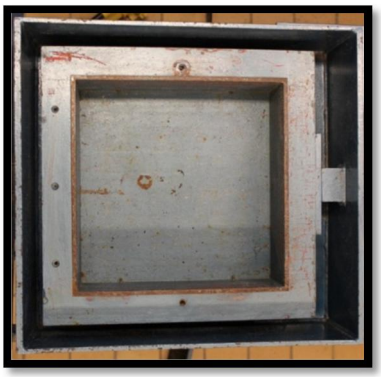

***Figure 5-6**. Moving lower half.*

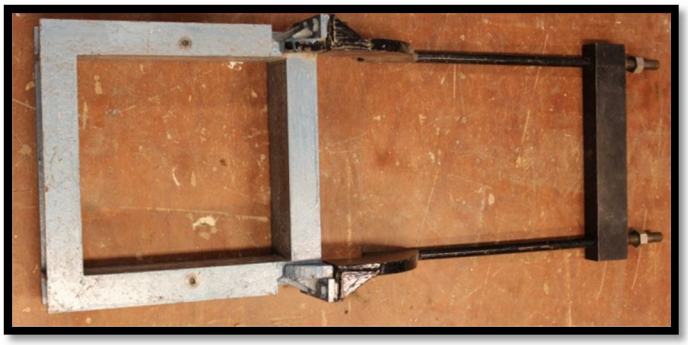

***Figure 5-7**. Fixed upper half.*

5.1.3. Load plate

The load plate was placed on the sample and the weight of the load plate was 13.792 kg. This plate was designed to distribute the vertical load on the surface of the sample evenly. The load plate had a gridded internal surface which is formed by 8 longitudinal strips with dimensions of 7 mm in depth and 10 mm in width. These longitudinal strips are evenly distributed over the width of the load plate. Also an extra smooth wooden plate with an average thickness of 20.65 mm was placed under the load plate to ensure the transmission of the normal force on to the granular material which was placed in the upper half of the shear box (Figure 5-8).

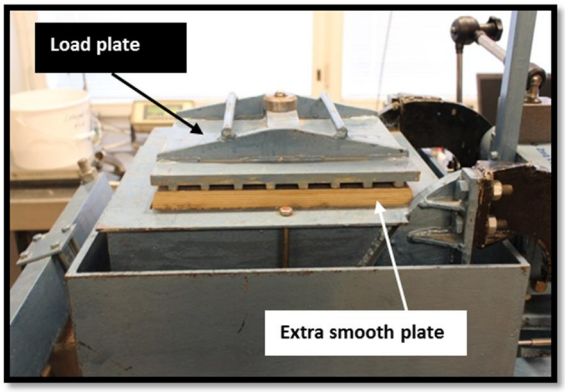

Figure 5-8*. Load plate and extra smooth plate*

5.1.4. Load hanger

The load hanger drives the entire compressive load to the load plate. The hanger is also connected to the load beam, so all the loads are transmitted. The weight of the load hanger is 32.703 kg without any extra load on it. A dial gauge is located in the hanger and it measures the compression that is experienced by the sample. The measurement in the dial gauge keeps changing depending on the load on the loading system.

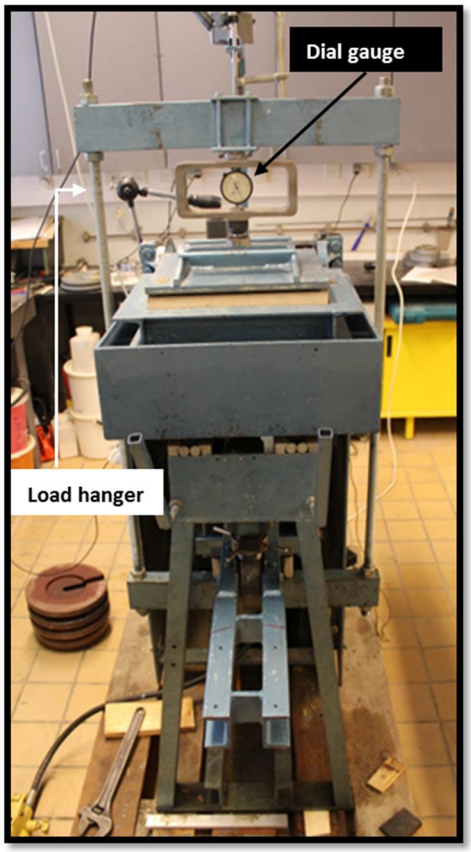

Figure 5-9*. Load hanger and dial gauge.*

5.1.5. Transducers

Transducers were used to measure the displacement and force measurements and they were positioned as required. There were four transducers in each test, three of them were measuring displacement and one of them was used to measure the horizontal force. One of the displacement transducers was used to measure the vertical displacement and it was placed vertically in contact with the load hanger. Another transducer was placed horizontally in contact with the moving lower half of the shear box and it was measuring the horizontal displacement. The third displacement transducer was also measuring horizontal displacement and it was located as the other horizontal one in contact with the moving lower half and it measured the horizontal displacement during each test, but this data was not collected automatically.

The transducer used to measure the horizontal force has been designed to stand a maximum force of 20 kN. This force transducer was connected to the piston responsible to move the lower half of the shear box. Horizontal force measurements data was logged by this transducer.

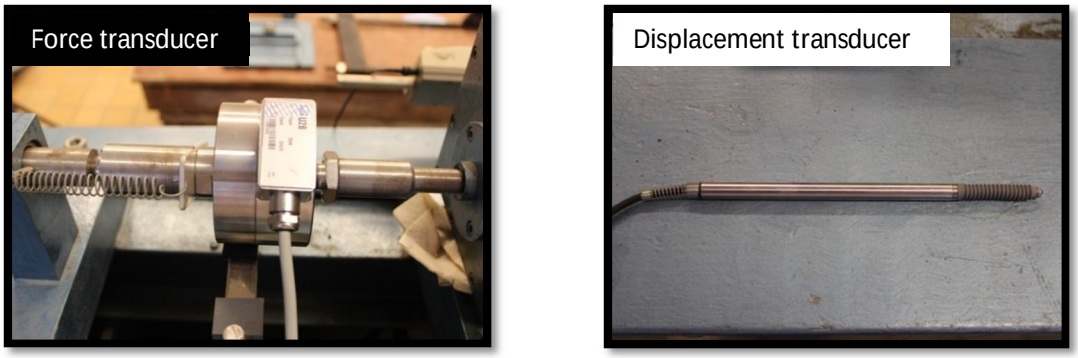

***Figure 5-10**. Force transducer and displacement transducer*

5.1.6. Computer and software

A computer was linked to the apparatus through a hub where the transducers were connected. These transducers were able to measure the displacement and software was installed in the computer to collect the data. Data was continuously stored in Microsoft Excel files for each one test.

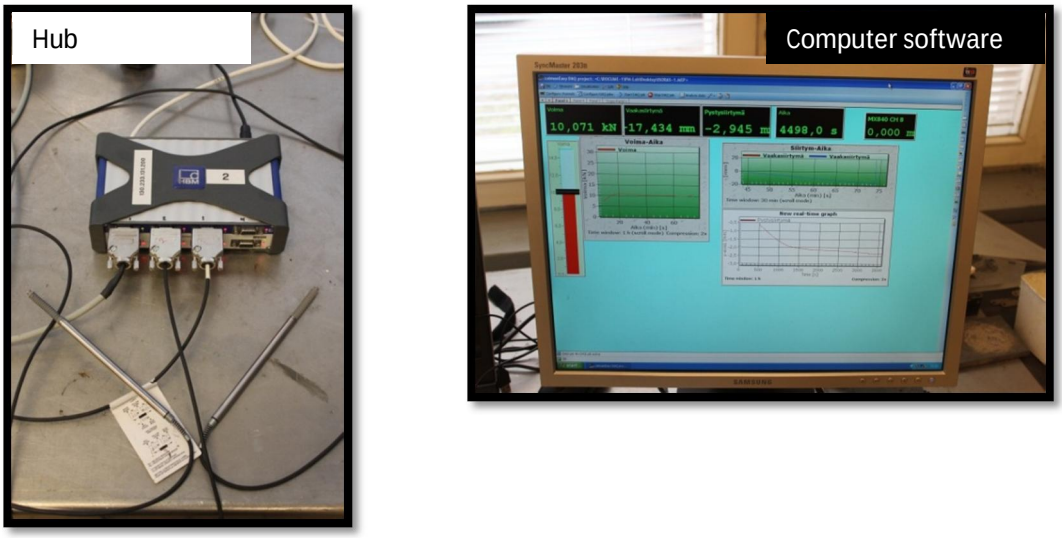

***Figure 5-11**. Hub and computer software*

5.2. Methodology

Direct shear box tests were carried out according to the technical specifications given in CEN ISO/TS 17892-10:2004. As per these specifications, the test method consists of:

- Placing the test sample inside the direct shear box,
- applying a pre-determined normal stress,
- providing for draining of the test sample,

- consolidating the specimen under compression stress,
- unlocking the frames that hold the sample,
- displacing one frame horizontally with respect to the other at a constant rate of shear-deformation,
- and measuring the shearing force and horizontal displacements as the sample sheared. Shearing load is applied slowly enough to allow excess pore pressure to dissipate by drainage so that effective stresses will be equal to total stresses.

In this study, samples were tested in their original water content. The general test procedure which was carried out in this study as follows:

1- First of all, blocks or granite stone (depending on the test) were placed in the lower half of the shear box. As the blocks did not fit exactly into the shear box, extra thin wooden and steel pieces were placed in three of the four sides of the blocks to bridge the gap between the shear box and the sample as illustrated in Figure 5-12.

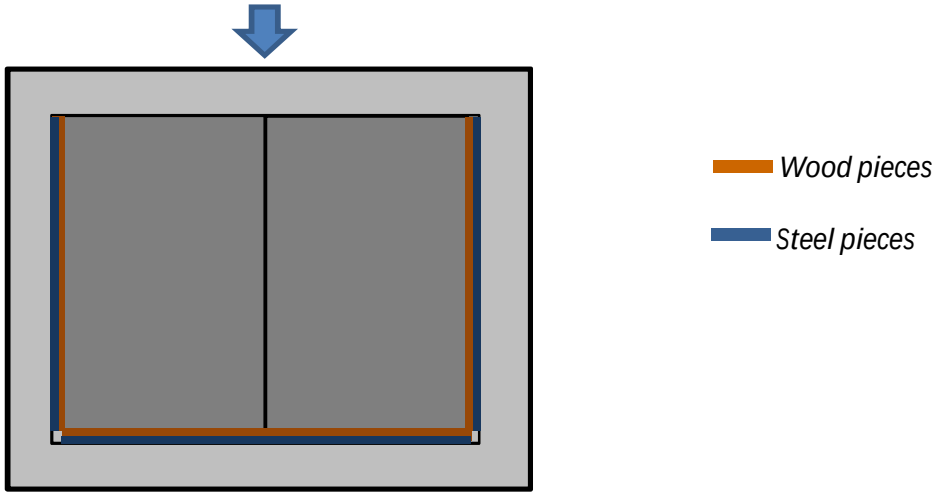

Figure 5-12*. Distribution of additional wooden and steel plates around the blocks.*

2- Small samples of the granular materials were taken prior to the test to determine the dry density (ρ_d) and the water content (w) of each material.

3- After the material was placed in the lower half of the shear box and well-positioned, the upper half was put on top it. The upper half was fixed with two bolts and the granular material (pellets, granulated bentonite or foundation bed

material) was placed into it. Granulated bentonite and foundation bed material were manually compacted before the load plate was placed as shown in Figure 5-13. In case of block/block interface, two blocks were placed in the upper half.

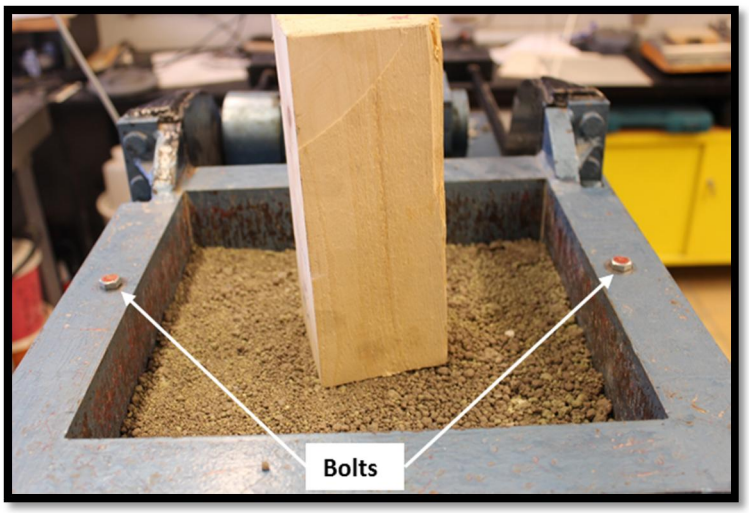

Figure 5-13*. Manual compaction of foundation bed material placed into the upper half of the shear box.*

4- Once tested for ρ_d and w, samples were placed inside the shear box and the load plate and the load hanger were positioned on the sample as it was explained before. The test was continued with the consolidation phase in which, the settlement due to normal stress occurs. After the settlement phase, the shearing test was started in a constant rate of 0.5 mm/min.

5- The shear box test was carried out until the measured shearing force started to decrease or when the tilt of the load plate became significantly higher.

The importance of the tilt is related with the verticality of the normal force transmitted to the load plate. When the load plate was absolutely horizontal, then the applied normal force was completely perpendicular to the sample surface and hence the shear test data was more reliable. When the load plate starts to tilt, the transmission of the compression pressure is no longer perpendicular to the sample surface which could eventually affect the accuracy of the results.

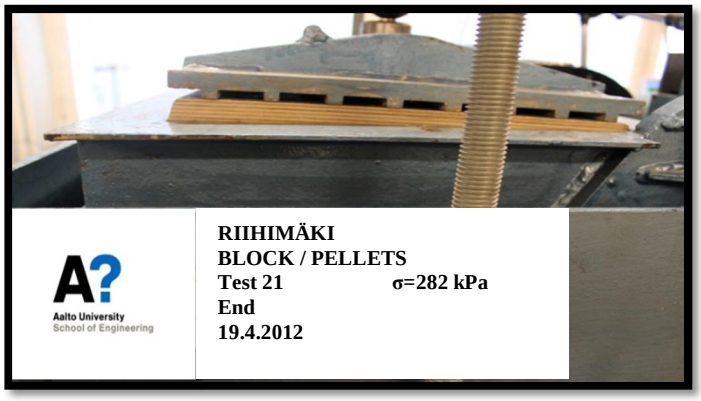

***Figure 5-14**. Tilting of load plate in test 21(Block/ pellets interface).*

After the test, specimens from the tested granular materials were taken to determine the dry density (ρ_d) and water content (w). This was done to compare these properties before and after testing. It was observed that they did not vary significantly due to the testing as the granular material was always in dry state.

Moreover, sieve tests were carried out in the same samples that were taken to determine the dry density and water content according the technical specifications in CEN ISO/TS 17892-4:2004. This sieving was useful in order to know which grain size had each one of the granular material. A sieve shaker was used to carry out this task. The following sieves openings were used in the sieving: 16, 8, 4, 2, 1, 0.5, 0.25, 0.125 and 0.063 mm, see Figure 5-15. Sieves accomplish the requirements of ISO 565:1990 and ISO 3310-1.

***Figure 5-15**. Sieve shaker machine.*

6. SHEAR BOX TESTS

6.1. Test program

Seven different types of interfaces were considered in this study. Those are:

- Block / block,
- Block / pellets,
- Block / granulated bentonite,
- Block / foundation material,
- Smooth granite stone / pellets,
- Intermediate roughness granite stone / pellets, and
- Rough granite stone / pellets.

The tested interfaces were horizontal and the material was almost dry with the only water coming from the original water content of the material. A total of 26 tests were carried out as shown in Table 6-1.

***Table 6-1**. Testing program of performed shear box tests.*

TEST	DATE	MATERIAL 1 (LOWER HALF)	MATERIAL 2 (UPPER HALF)
Test 1	May-2011	Friedland-clay Block	Friedland-clay Block
Test 2	May-2011	Friedland-clay Block	Friedland-clay Block
Test 3	May-2011	Friedland-clay Block	Friedland-clay Block
Test 4	May-2011	Friedland-clay Block	Friedland-clay Block
Test 10	May-2011	Friedland-clay Block	Cebogel QSE Pellets
Test 11	May-2011	Friedland-clay Block	Cebogel QSE Pellets
Test 12	May-2011	Friedland-clay Block	Cebogel QSE Pellets
Test 13	May-2011	Friedland-clay Block	Cebogel QSE Pellets
Test 14	May-2011	Friedland-clay Block	Cebogel QSE Pellets
Test 15	May-2011	Friedland-clay Block	Cebogel QSE Pellets
Test 21	April-2012	Friedland-clay Block	Cebogel QSE Pellets
Test 22	April-2012	Friedland-clay Block	Foundation bed material
Test 23	May-2012	Friedland-clay Block	Foundation bed material
Test 24	May-2012	Friedland-clay Block	Foundation bed material
Test 25	May-2012	Friedland-clay Block	Granulated Bentonite
Test 26	May-2012	Friedland-clay Block	Granulated Bentonite
Test 27	May-2012	Friedland-clay Block	Granulated Bentonite
Test 28	June-2012	Intermediate roughness granite stone	Cebogel QSE Pellets
Test 29	June-2012	Smooth granite stone	Cebogel QSE Pellets
Test 30	June-2012	Rough granite stone	Cebogel QSE Pellets
Test 31	June-2012	Intermediate roughness granite stone	Cebogel QSE Pellets
Test 32	June-2012	Smooth granite stone	Cebogel QSE Pellets
Test 33	June-2012	Rough granite stone	Cebogel QSE Pellets
Test 34	June-2012	Intermediate roughness granite stone	Cebogel QSE Pellets
Test 35	June-2012	Smooth granite stone	Cebogel QSE Pellets
Test 37	June-2012	Rough granite stone	Cebogel QSE Pellets

Every test was performed in dry state. The room temperature during the tests was always kept at 22 °C and the density of water was ρ_w = 997.80 kg/m^3 (Snelling 2008). It is important to notice that the height of sample that was considered in the calculations was from the part of the sample placed into the upper half of the shear box and, this was considered as the effective height of the sample. In the tests including blocks, they were placed in the lower half of the shear box and were aligned with the longest side parallel to the shearing direction (Figure 6-1). The tests with granite stones were performed with the stone in the lower half.

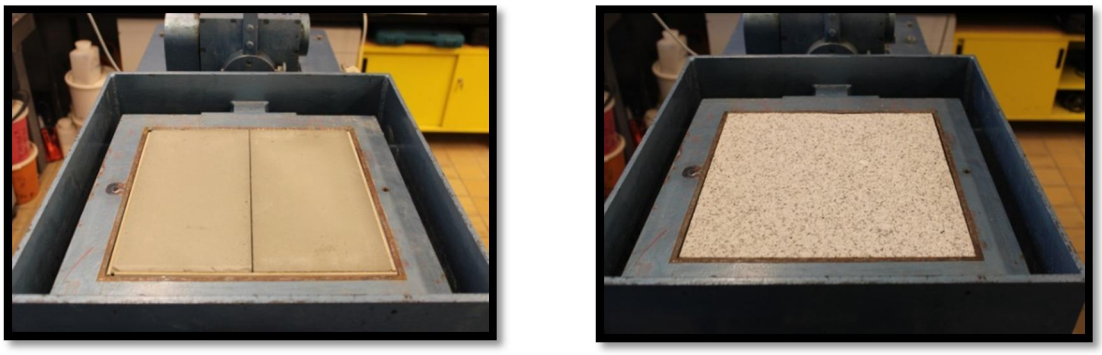

***Figure 6-1**. Lower half of shear box with blocks and granite stone in the correct position.*

6.2. Block/block

In each block/block test, four Friedland-clay blocks: two of them were placed in the upper half of the shear box and two in the lower half (Figure 6-2). Initial dimensions of the effective sample are shown in Table 6-2. The measured grain density in the pycnometer was ρ_s = 2790 kg/m^3 and this was used in the calculations to obtain the initial data (bulk density, dry density, water content, void ratio, degree of saturation) from the upper blocks (Table 6-3).

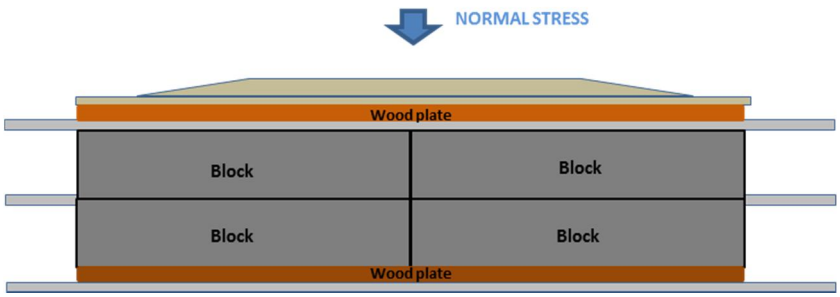

***Figure 6-2**. Cross section of block/block shear box test.*

***Table 6-2**. Dimensions of block/block upper half.*

Height (mm)	Area (mm^2)	Volume (mm^3)
74.7	$9 \cdot 10^4$	$6.726 \cdot 10^6$

***Table 6-3**. Initial data from block/block upper half.*

TEST	ρ (kg/m^3)	ρ_d (kg/m^3)	w (%)	$e_0 = \frac{\rho_s}{\rho_d} - 1$	$S_R = \frac{w_0 \times \rho_s}{e_0 \times \rho_w}$
				e_0	S_R (%)
Test 1	2000	1880	6.24	0.484	37
Test 2	2000	1880	6.24	0.484	37
Test 3	2000	1880	6.24	0.484	37
Test 4	2000	1880	6.24	0.484	37

6.3. Block/pellets

In block/pellets tests, pellets were weighed and placed without any compaction (Figures 6-4 and 6-5). Initial dimensions of the effective sample (pellets) are shown in Table 6-4 and initial properties of pellets are given in Table 6-5. In the initial data, it was assumed that the grain density of the pellets is ρ_s = 2780 kg/m^3 (Kumpulainen & Kiviranta 2011).

***Figure 6-3**.Pellets in the upper half of the shear box.*

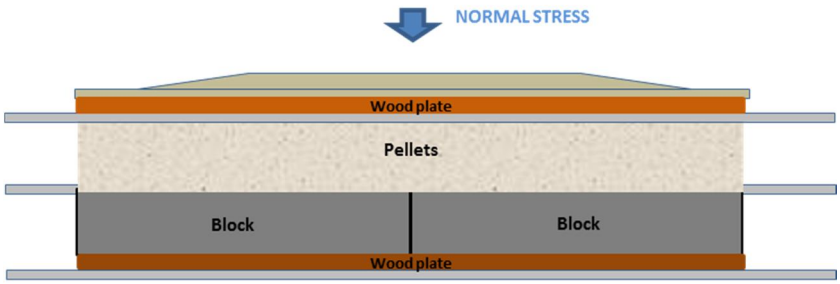

***Figure 6-4**.Cross section of block/pellets shear box test.*

***Table 6-4**. Dimensions of block/pellets upper half.*

Height (mm)	Area (mm^2)	Volume (mm^3)
87	$9 \cdot 10^4$	$7.830 \cdot 10^6$

***Table 6-5**. Initial data from pellets in block/pellets tests.*

TEST*	ρ (kg/m^3)	ρ_d (kg/m^3)	w (%)	$e_0 = \frac{\rho_s}{\rho_d} - 1$	$S_R = \frac{w_0 \times \rho_s}{e_0 \times \rho_w}$
				e_0	S_R (%)
Test 10	1140	970	17.4	1.866	26
Test 11	1260	1080	17.4	1.574	31
Test 12	1170	1000	17.4	1.780	27
Test 13	1220	1040	17.4	1.673	29
Test 14	1170	1000	17.4	1.780	27
Test 15	1320	1130	17.4	1.460	33
Test 21	1140	1050	9.55	1.648	16

**Note: It should be noted that some of these block/pellets tests were performed with the same sample that was used in previous tests. This is the case of Test 11, Test 13 and Test 15 where the tested samples were the tested samples coming from Test 10, Test 12 and Test 14 respectively. The procedure was to perform the direct shear box test in one sample and after that, the normal stress were incremented and then sheared again.*

6.4. Block/granulated bentonite

In block/granulated bentonite tests; the effective sample height was the height of the granulated bentonite placed in the upper half of the shear box. This bentonite was previously manually compacted in layers. Initial data from this granulated bentonite is shown in Table 6-6 and 6-7. A grain density value of ρ_s = 2750 kg/m^3 was assumed for initial calculations (Karnland 2010).

***Table 6-6**. Dimensions of block/granulated bentonite upper half.*

Height (mm)	Area (mm^2)	Volume (mm^3)
87	$9 \cdot 10^4$	$7.830 \cdot 10^6$

***Table 6-7**. Initial data from granulated bentonite in block/granulated bentonite tests.*

TEST	ρ (kg/m^3)	ρ_d (kg/m^3)	w (%)	$e_0 = \frac{\rho_s}{\rho_d} - 1$	$S_R = \frac{w_0 \times \rho_s}{e_0 \times \rho_w}$
				e_0	S_R (%)
Test 25	1320	1090	20.8	1.523	38
Test 26	1300	1090	19.3	1.523	35
Test 27	1290	1080	20.6	1.546	37

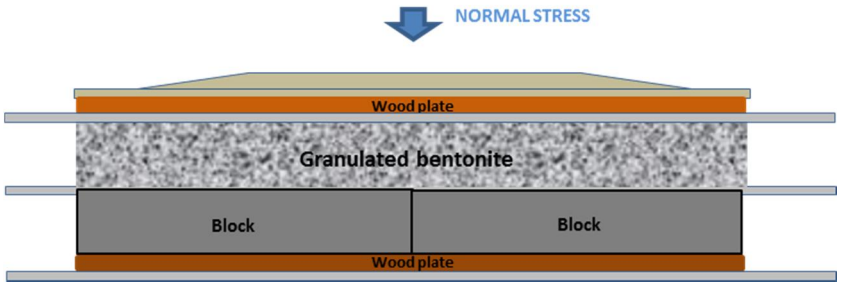

***Figure 6-5**. Cross section of block/granulated bentonite shear box test.*

6.5. Block/foundation bed material

The sample was foundation bed material and it was in contact with the Friedland-clay blocks which were placed at the lower half of the shear box. Foundation bed material was placed and manually compacted in the upper half of the shear box. Initial data from foundation bed material is given in Table 6-8 and 6-9. A grain density value of ρ_s = 2700 kg/m^3 was assumed for initial calculations (Keto et al. 2006).

***Table 6-8**. Dimensions of block/foundation bed material upper half.*

Height (mm)	Area (mm^2)	Volume (mm^3)
87	$9 \cdot 10^4$	$7.830 \cdot 10^6$

***Table 6-9**. Initial data from foundation material in block/foundation bed material tests.*

TEST	ρ (kg/m^3)	ρ_d (kg/m^3)	w (%)	$e_0 = \frac{\rho_s}{\rho_d} - 1$	$S_R = \frac{w_0 \times \rho_s}{e_0 \times \rho_w}$
				e_0	S_R (%)
Test 22	1380	1220	13.7	1.217	33
Test 23	1380	1230	12.7	1.200	29
Test 24	1370	1190	15.5	1,271	33

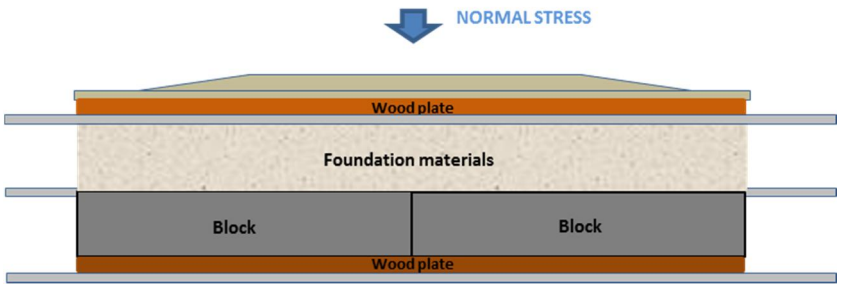

***Figure 6-6**. Cross section of block/foundation bed material shear box test.*

6.6. Granite stone/pellets

The granite stone/pellets interface was similar to the block/pellets interfaces but replacing the Friedland-clay blocks in the lower half of the shear box was replaced with a granite stone plate. According to the surface roughness, the granite stones were classified into three: smooth, intermediate roughness and rough. Granite stones were washed with pressurized water before testing to ensure the surface is clean (Figure 6-7). Initial data for pellets in these tests with granite stone are shown in Table 6-10 and 6-11.

Figure 6-7*. Cleaning the granite stone.*

Table 6-10*. Dimensions of granite stone/pellets upper half.*

Height (mm)	Area (mm^2)	Volume (mm^3)
87	$9 \cdot 10^4$	$7.830 \cdot 10^6$

***Table 6-11**. Initial data from pellets in granite stone/pellets tests.*

TEST	TYPE OF GRANITE STONE	ρ (kg/m^3)	ρ_d (kg/m^3)	w (%)	$e_0 = \frac{\rho_s}{\rho_d} - 1$	$S_R = \frac{w_0 \times \rho_s}{e_0 \times \rho_w}$
					e_0	S_R (%)
Test 28	Intermediate roughness	1160	1050	10.3	1.648	29
Test 29	Smooth	1180	1080	10.0	1.574	31
Test 30	Rough	1180	1070	10.4	1.598	30
Test 31	Intermediate roughness	1210	1100	9.73	1.527	32
Test 32	Smooth	1250	1140	9.71	1.439	34
Test 33	Rough	1180	1070	9.84	1.598	30
Test 34	Intermediate roughness	1170	1070	9.66	1.598	30
Test 35	Smooth	1150	1050	9.90	1.648	29
Test 37	Rough	1140	1040	9.77	1.673	29

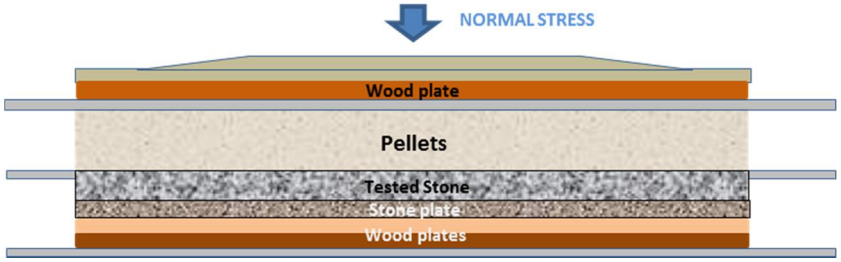

***Figure 6-8**. Cross section of granite stone/pellets shear box test.*

7. RESULTS

7.1. Block/block

Table 7-1 and Figures 7-1 and 7-2 present the block/block shear test results. No significant tilting of the load plate was observed due to the absence of loose materials in these tests.

***Table 7-1**. Applied normal stress, maximum shear stress and corresponding horizontal displacement in block/block tests.*

TEST	Applied normal stress σ (kPa)	Maximum shear stress * τ (kPa)	Horizontal displacement Δx (mm)
Test 1	55	23.21	11.00
Test 2	90	35.56	30.00
Test 3	20	10.66	9.00
Test 4	35	16.20	28.00

**Note: These maximums shear stresses are the residual shear stresses due to only few points are reaching the peak stress as it can be observed in Figure 7-1.*

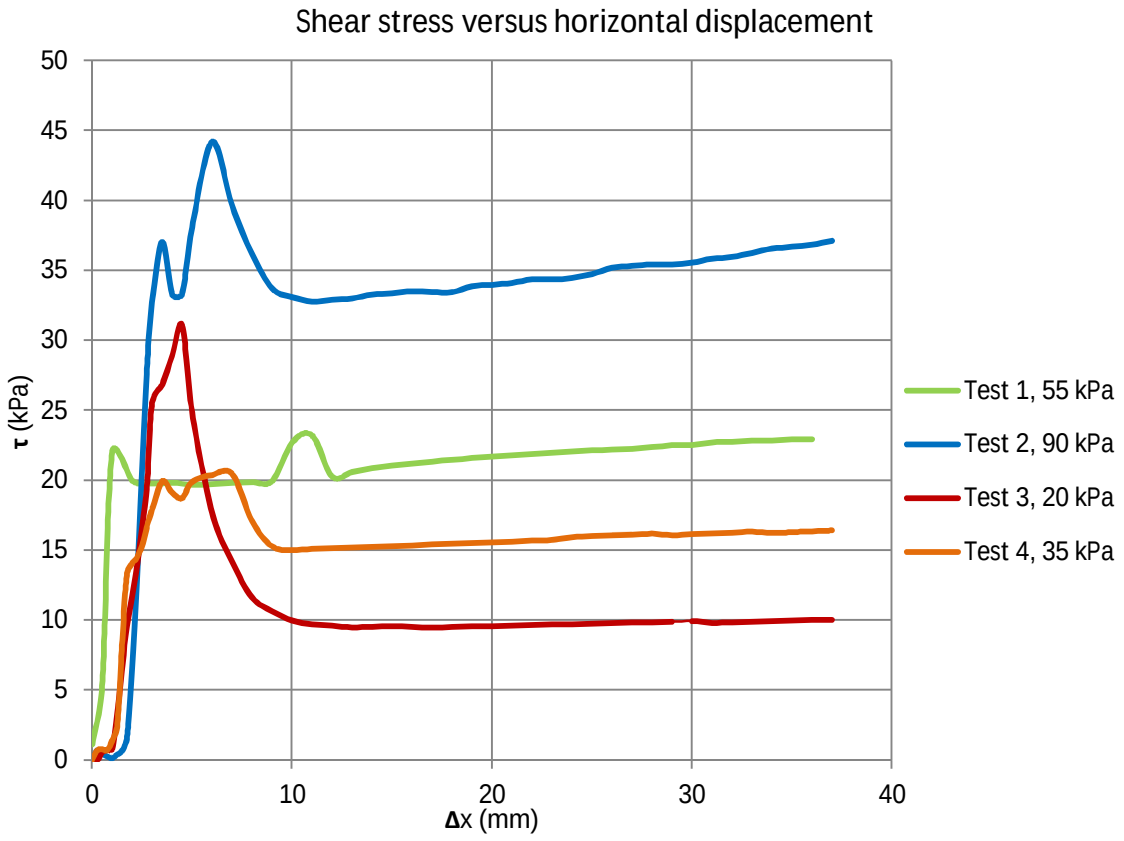

***Figure 7-1**. Shear stress against horizontal displacement in block/block tests.*

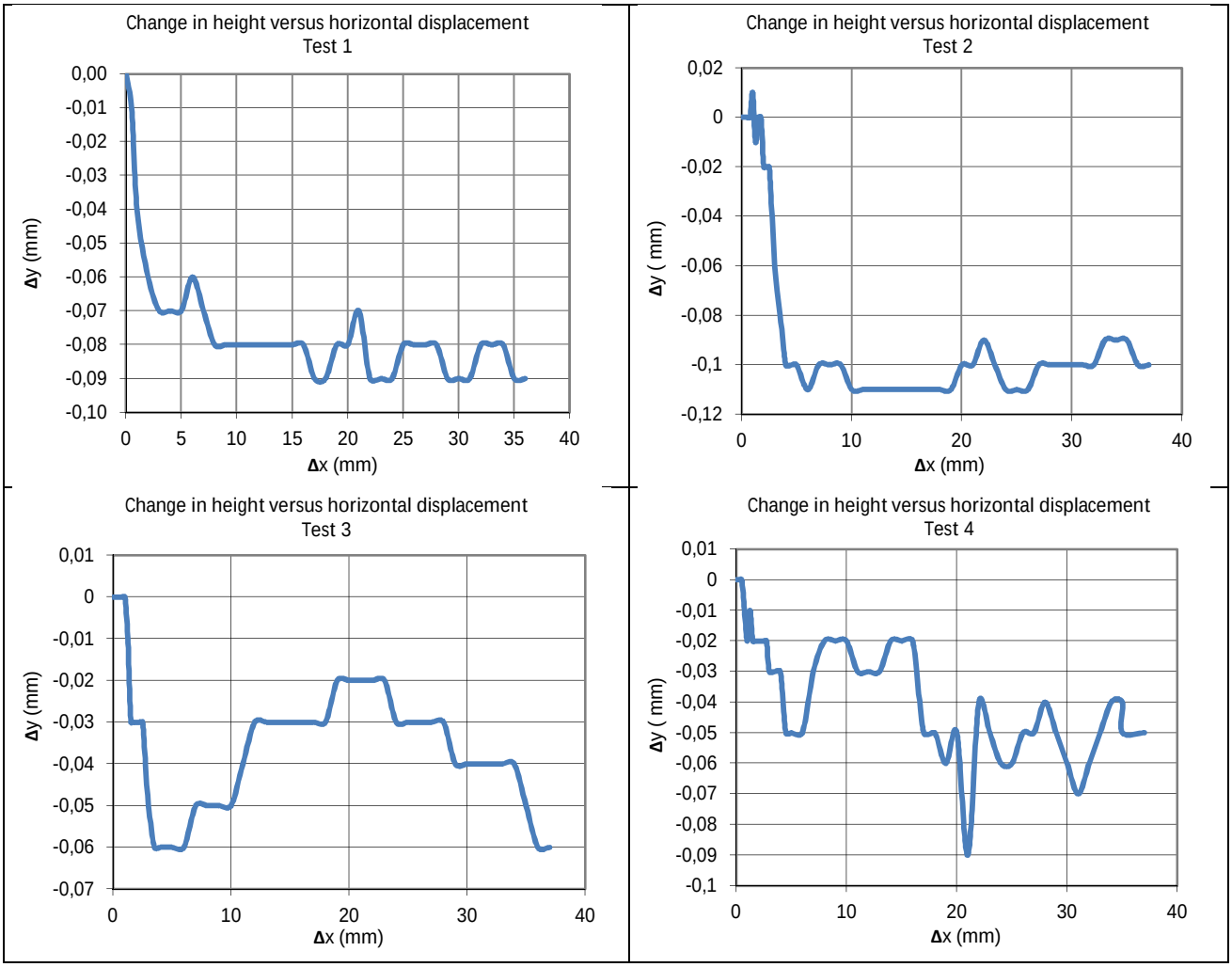

Figure 7-2*. Change in height versus horizontal displacement in block/block shear tests.*

7.2. Block/pellets

The results from block/pellets tests can be observed in Table 7-2 and Figures 7-4 to 7-6. These tests were terminated due to the tilting of the loading plate as it can be seen in Figure 7-3. Only 5 tests (Test 12, 13, 14, 15, 21) can be considered as a good representation because test 10 and test 11 had very low normal stress and consequently a very small change in height.

As it is shown in the Figure 7-6, the initial horizontal displacements of test 13 and test 15 are not zero; this is because these two tests were continued with the same sample which was used in the previous test with a different normal stress. The sample used for test 13 was the same sample that was tested before in test 12 and the likewise in test 15 with the sample from test 14. This explains why the initial horizontal displacements from test 13 and 15 are same as the final horizontal displacements from test 12 and 14 respectively.

***Table 7-2**. Applied normal stress, maximum shear stress and corresponding horizontal displacement in block/pellets tests.*

TEST	Applied normal stress σ (kPa)	Maximum shear stress τ (kPa)	Horizontal displacement Δx (mm)
Test 10	20	9.5	4.50
Test 11	40	17.9	9.50
Test 12	60	26.5	10.00
Test 13	115	50.5	11.60
Test 14	149	62.4	9.00
Test 15	205	86.5	15.00
Test 21	283	139.3	21.80

***Figure 7-3**. Tilting of the upper part in Test 21*

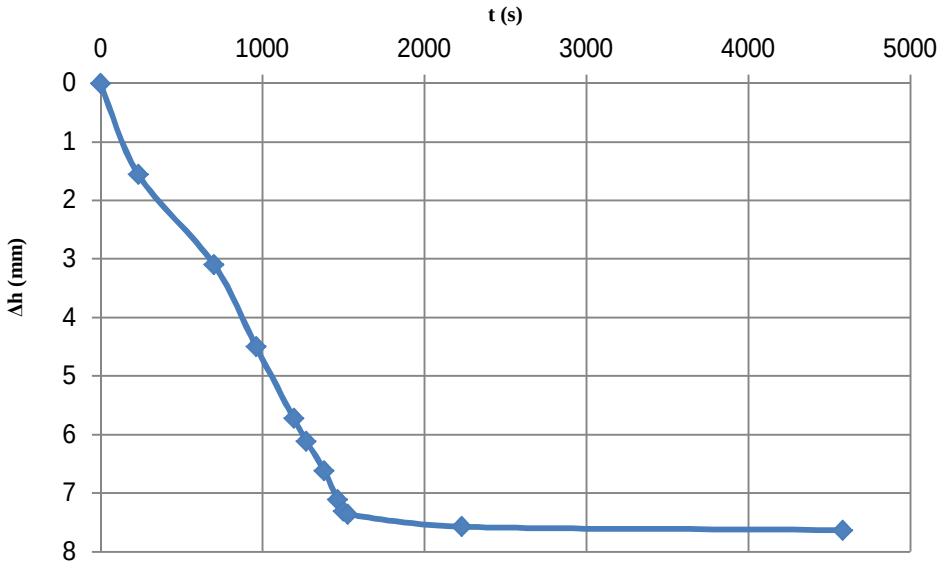

***Figure 7-4**. Settlement against time for Test 21 in consolidation phase.*

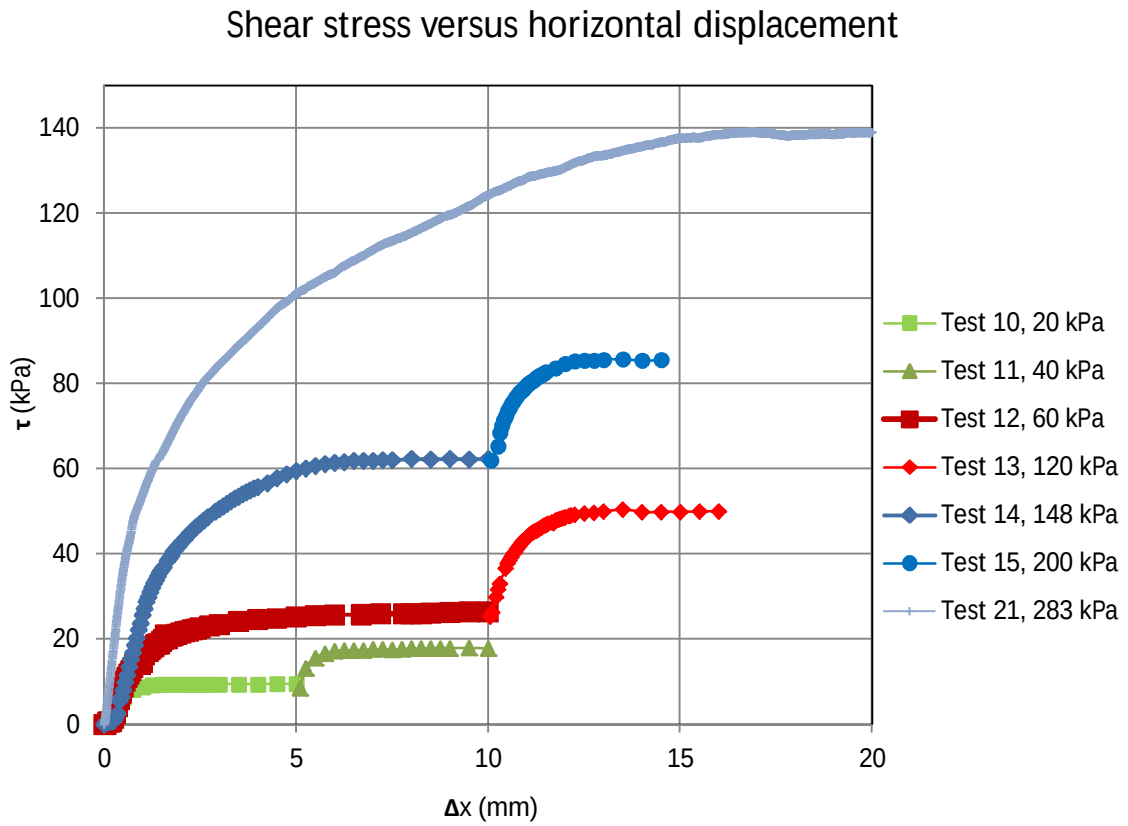

***Figure 7-5**. Shear stress against horizontal displacement in block/pellets tests.*

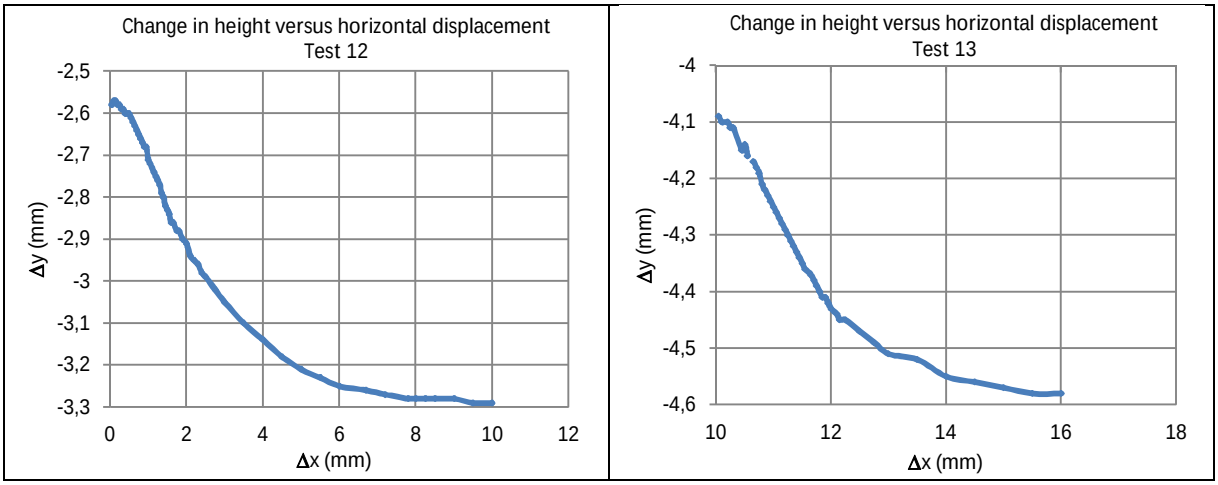

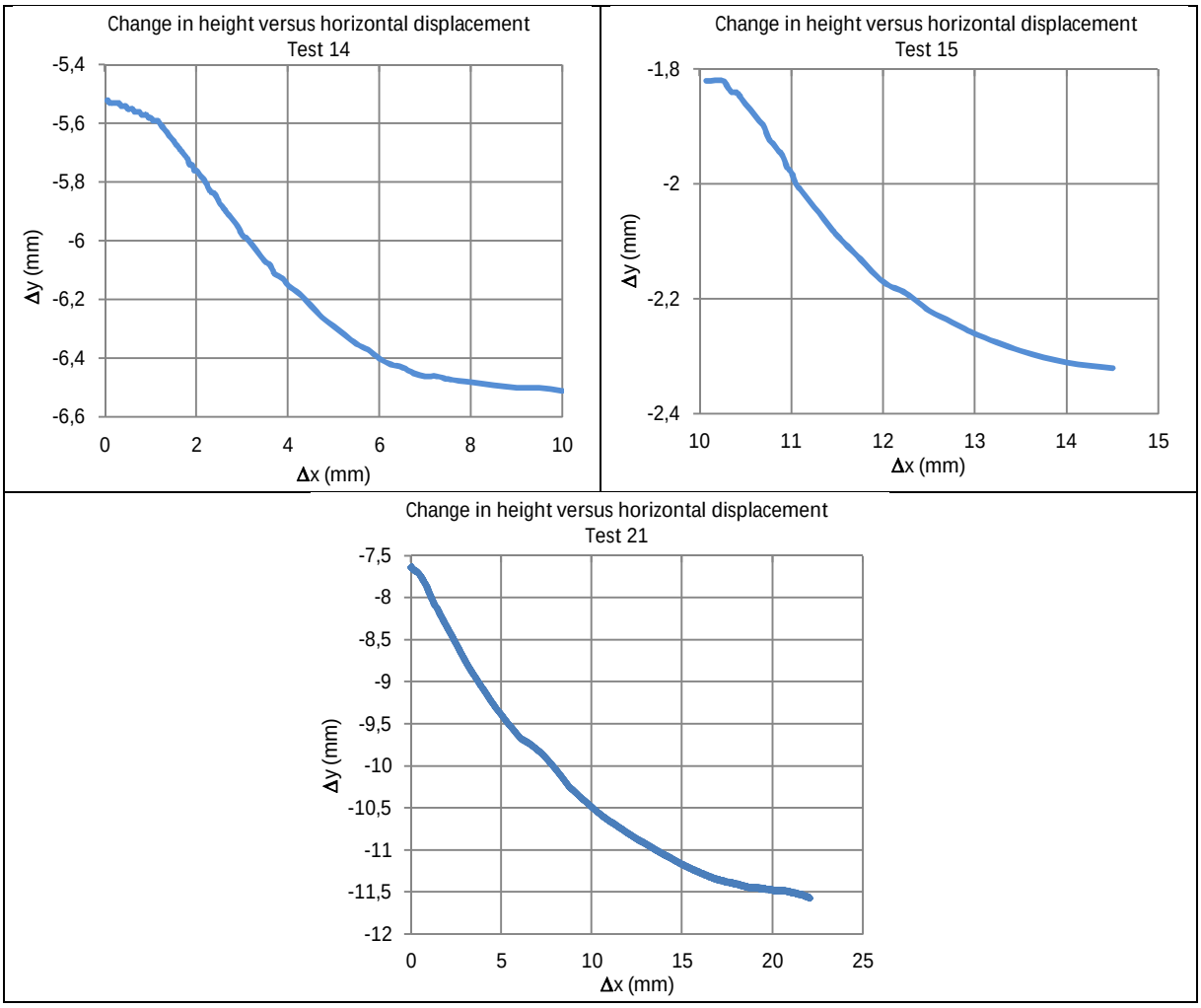

Figure 7-6*. Change in height versus horizontal displacement in block/pellets tests.*

7.3. Block/granulated bentonite

Table 7-3 shows the obtained results for block/granulated bentonite tests. Graphs representing the results are shown in Figures 7-8 and 7-9. No visible tilting was observed in this interface (Figure 7-7).

Table 7-3*. Applied normal stress, maximum shear stress and corresponding horizontal displacement in block/granulated bentonite tests.*

TEST	Applied normal stress σ (kPa)	Maximum shear stress * τ (kPa)	Horizontal displacement Δx (mm)
Test 25	282	122.9	8.90
Test 26	143	65.2	8.60
Test 27	72	33.0	8.90

**Note: These maximums shear stresses are the residual shear stresses due to only few points are reaching the peak stress as it can be seen in Figure 7-8.*

***Figure 7-7**. No significant tilting of the upper part in Test 26.*

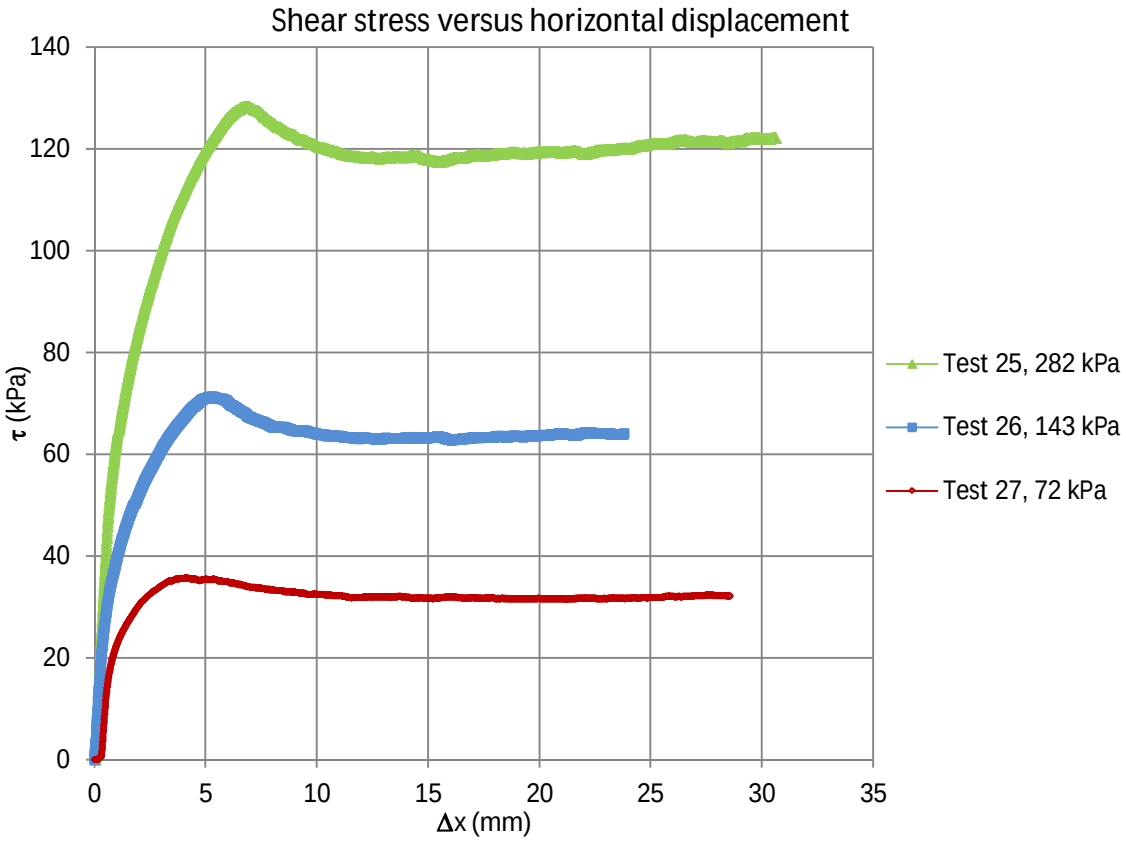

***Figure 7-8**. Shear stress against horizontal displacement in block/granulated bentonite tests.*

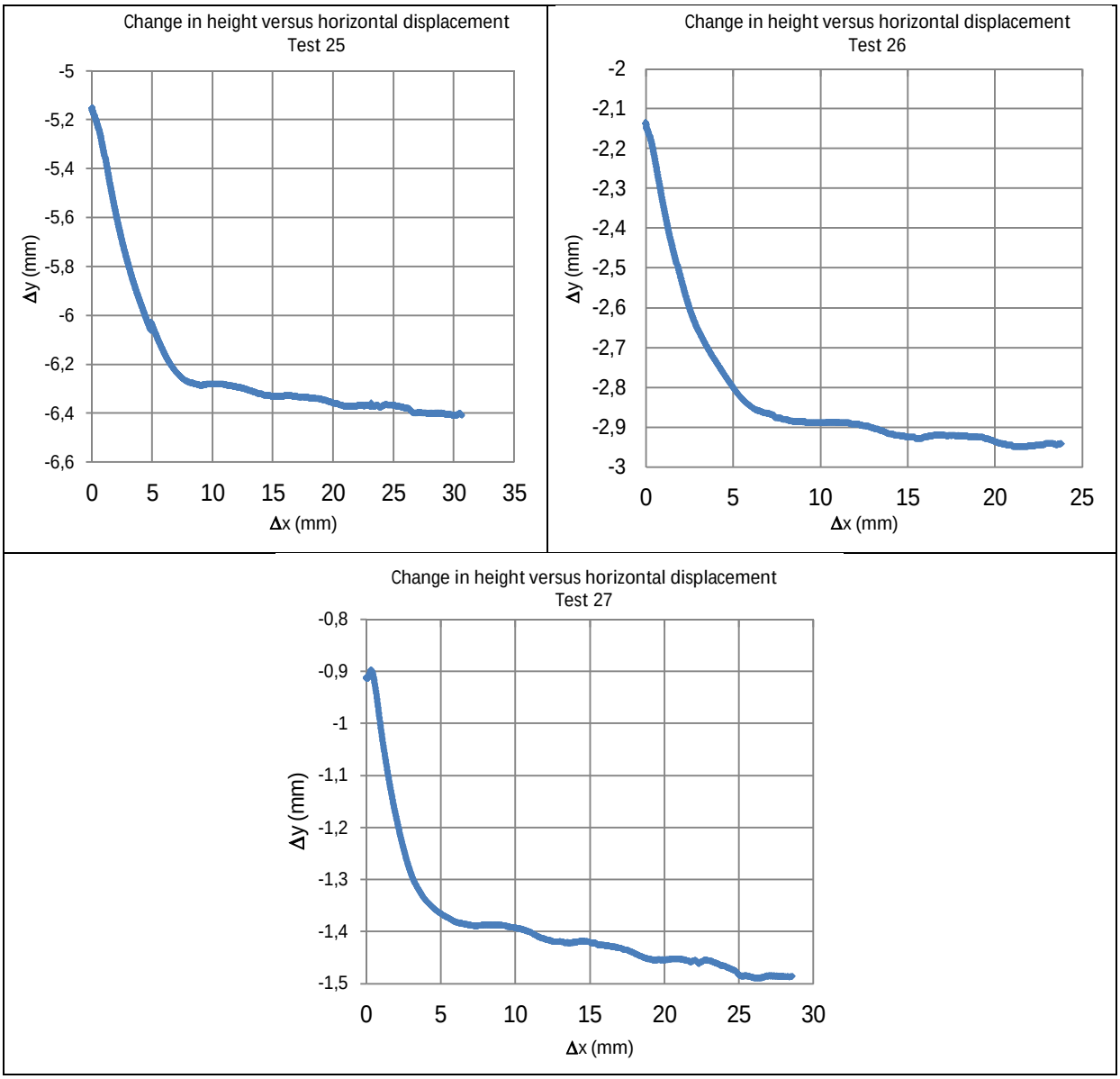

***Figure 7-9**. Change in height versus horizontal displacement in block/granulated bentonite tests.*

7.4. Block/foundation bed material

The test results from block / foundation bed material are given in Table 7-4 and Figures 7-10 and 7-11. A slight tilt occurred during the shearing as it is shown in Figure 7-12.

***Table 7-4**. Applied normal stress, maximum shear stress and corresponding horizontal displacement in block/foundation bed material tests.*

TEST	Applied normal stress σ (kPa)	Maximum shear stress τ (kPa)	Horizontal displacement Δx (mm)
Test 22	282	128.0	9.10
Test 23	143	69.5	25.00
Test 24	72	36.8	14.00

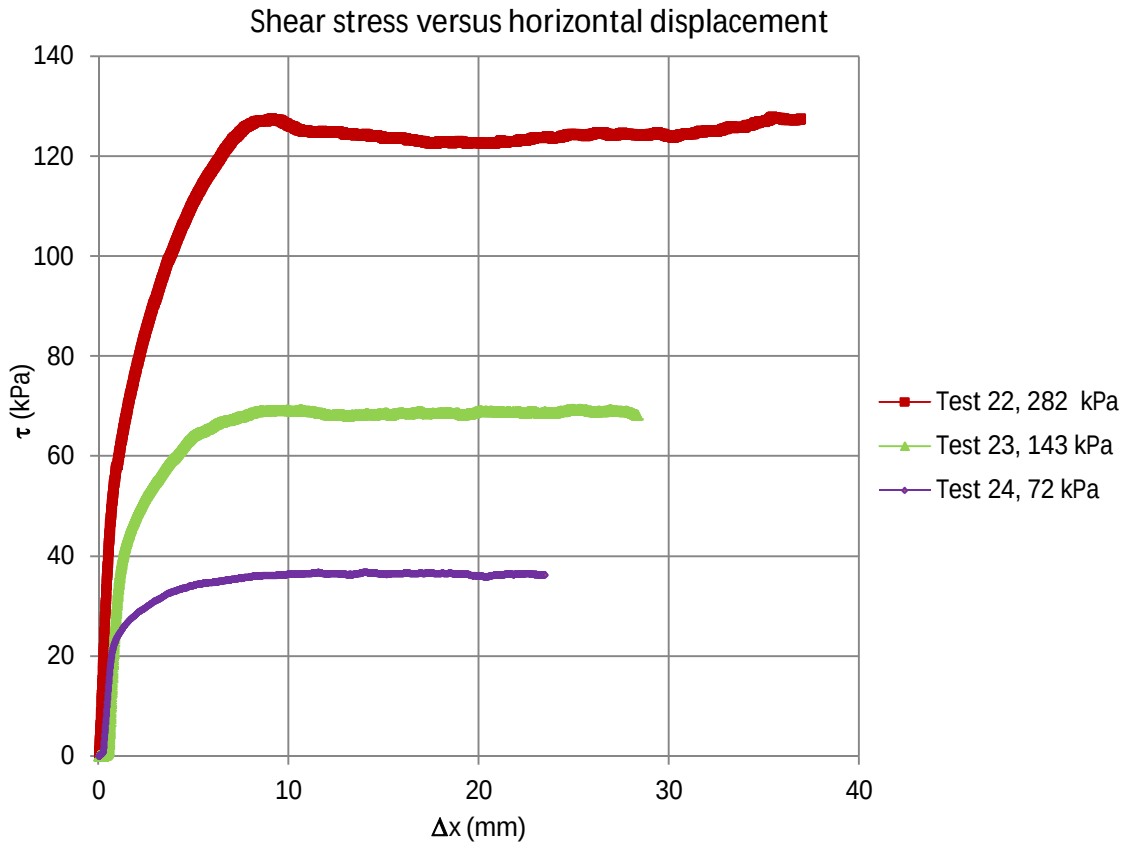

***Figure 7-10**. Shear stress against horizontal displacement in block/foundation bed material tests.*

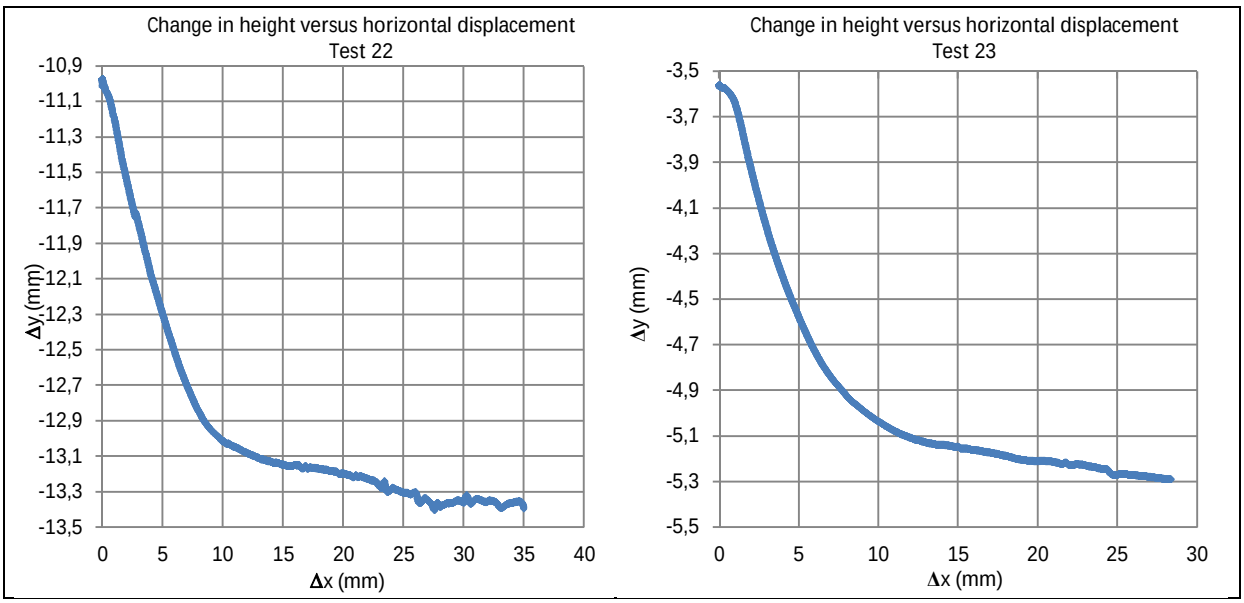

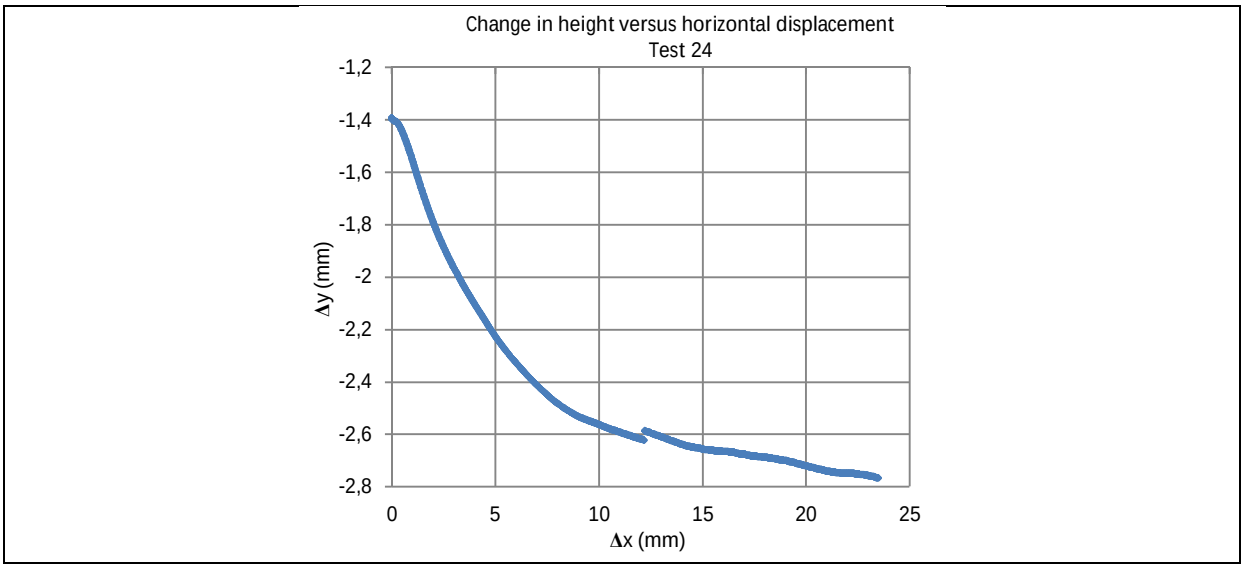

***Figure 7-11**. Change in height versus horizontal displacement in block/foundation bed material tests.*

***Figure 7-12**. Tilting of the upper part in Test 22.*

7.5. Granite stone/pellets

7.5.1. Smooth stone

Smooth granite stone/pellets interface results can be observed in Table 7-5, Figure 7-13 and Figure 7-14. Tilting during shearing in Test 35 can be observed in Figure 7-15.

***Table 7-5**. Applied normal stress, maximum shear stress and corresponding horizontal displacement in smooth granite stone/pellets tests.*

TEST	Applied normal stress σ (kPa)	Maximum shear stress τ (kPa)	Horizontal displacement Δx (mm)
Test 29	72	40.3	24.00
Test 32	143	74.4	23.10
Test 35	284	144.0	23.30

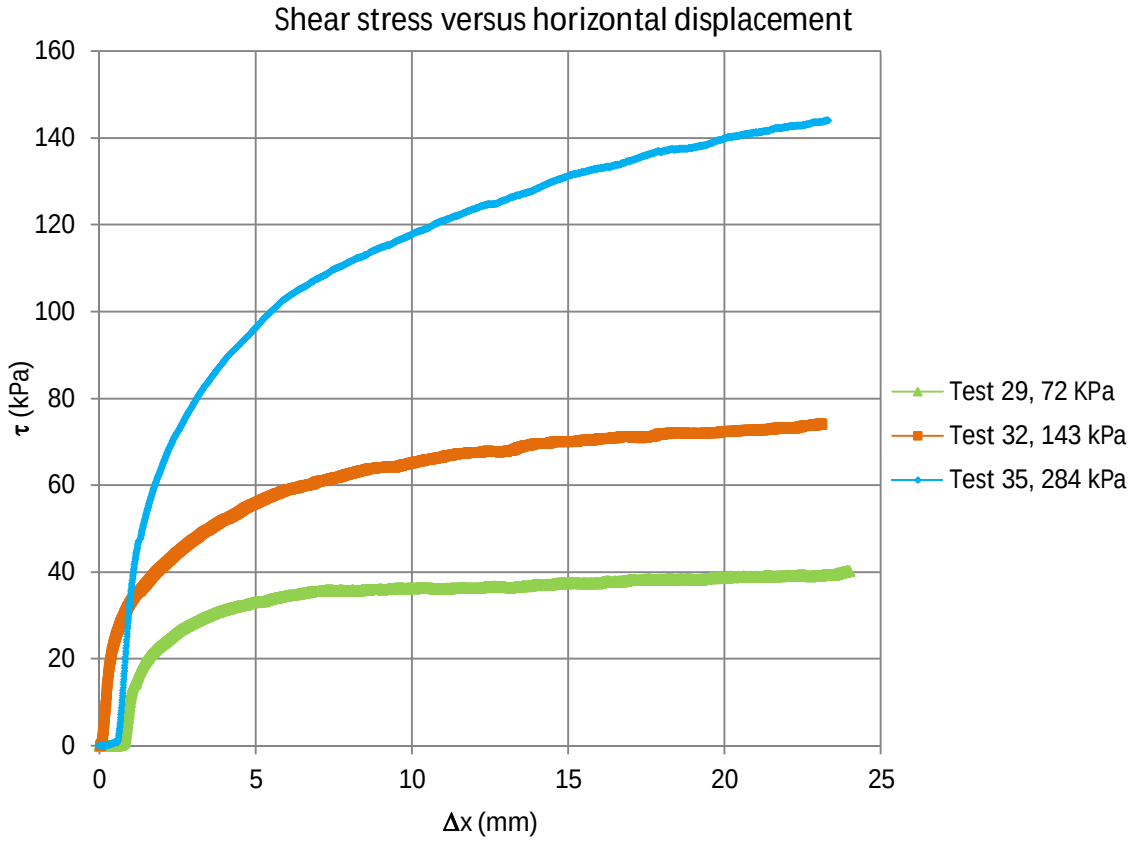

***Figure 7-13**. Shear stress against horizontal displacement in smooth granite stone/pellets tests.*

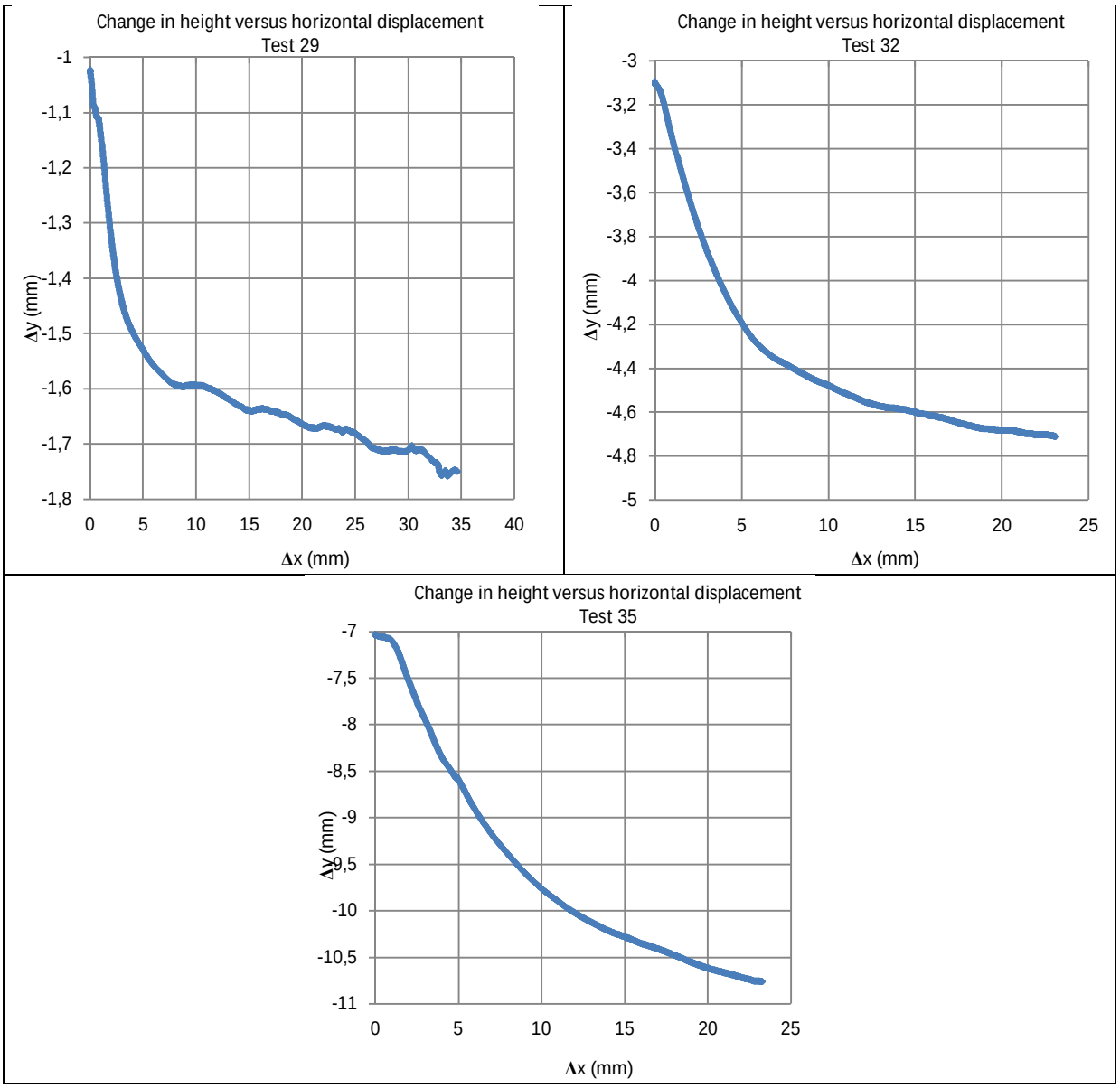

Figure 7-14*. Change in height versus horizontal displacement in smooth granite stone/pellets tests.*

Figure 7-15*. Tilting of the upper part in Test 35.*

7.5.2. Intermediate roughness stone/pellets

As in the smooth granite stone, only a small tilt was appeared with the maximum normal stress. The test results are given in Table 7-6, Figure 7-16 and 7-17.

***Table 7-6**. Applied normal stress, maximum shear stress and corresponding horizontal displacement in intermediate roughness granite stone/pellets tests.*

TEST	Applied normal stress σ (kPa)	Maximum shear stress τ (kPa)	Horizontal displacement Δx (mm)
Test 28	72	36.4	24.60
Test 31	143	69.1	22.80
Test 34	284	128.2	28.90

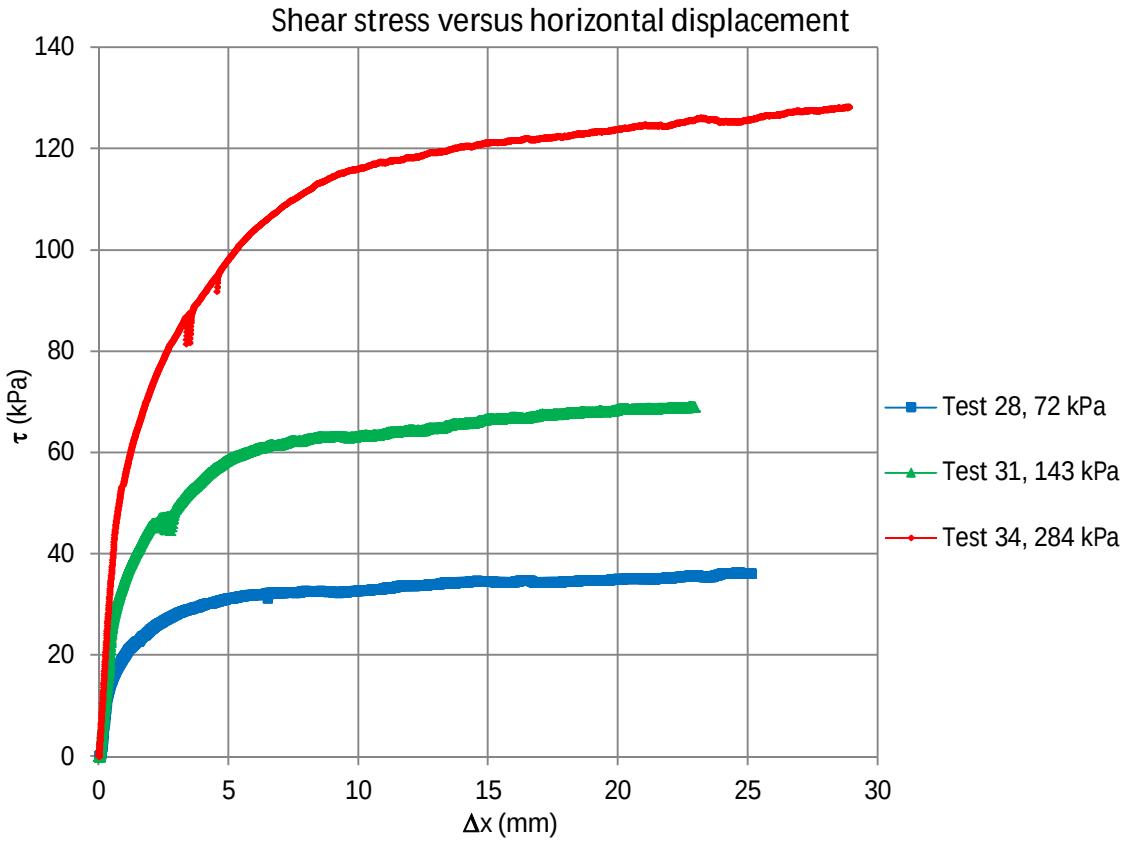

***Figure 7-16**. Shear stress against horizontal displacement in intermediate roughness granite stone/pellets tests.*

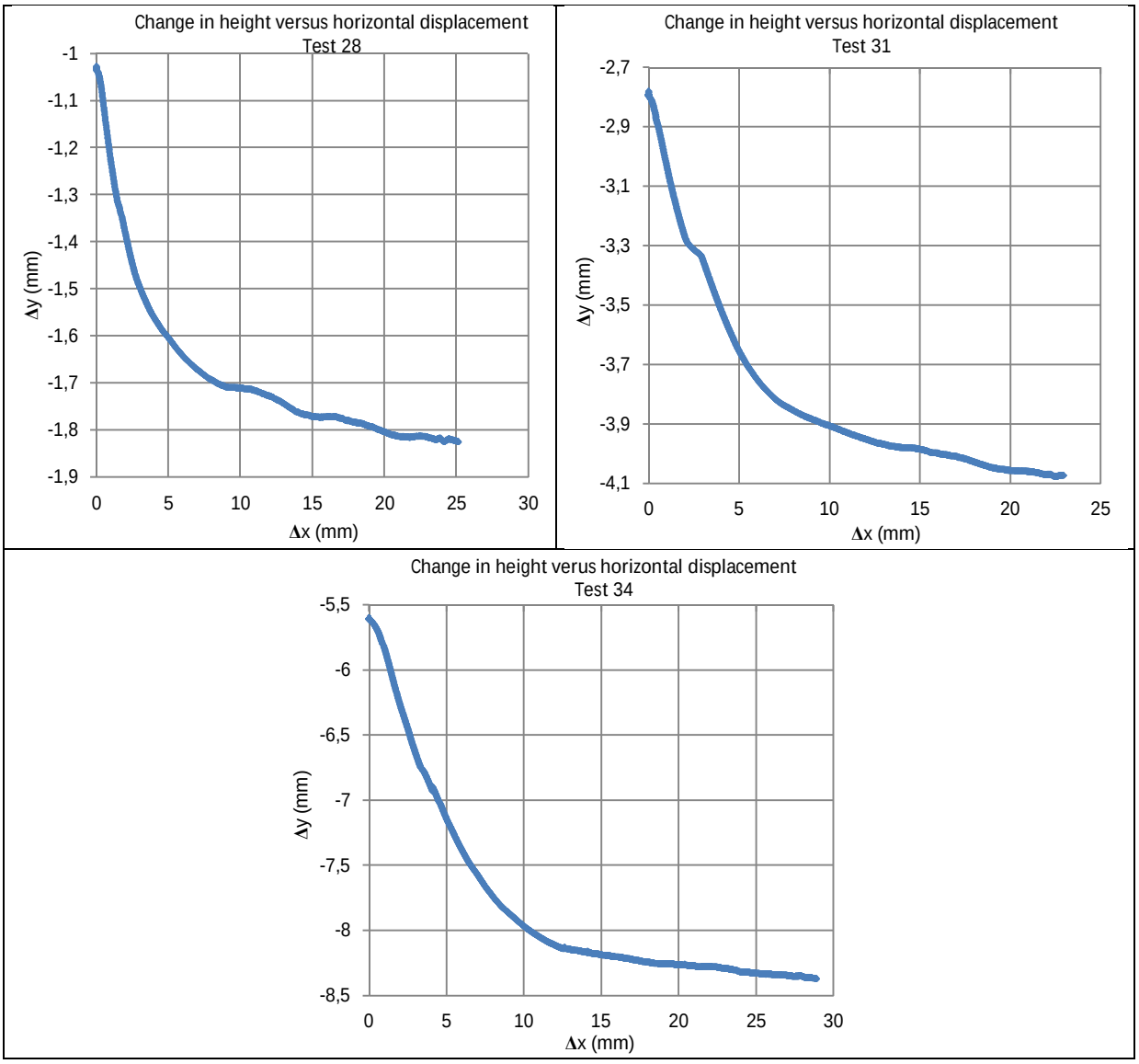

Figure 7-17*. Change in height versus horizontal displacement in intermediate roughness granite stone/pellets tests.*

7.5.3. Rough stone / pellets

Test results for the rough stone/pellets interface are shown in Table 7-7 and Figure 7-18 to 7-19. No significant tilting was observed in these tests.

***Table 7-7**. Applied normal stress, maximum shear stress and corresponding horizontal displacement in rough granite stone/pellets tests.*

TEST	Applied normal stress σ (kPa)	Maximum shear stress τ (kPa)	Horizontal displacement Δx (mm)
Test 30	72	47.3	23.10
Test 33	143	94.4	22.80
Test 37	284	177.9	23.40

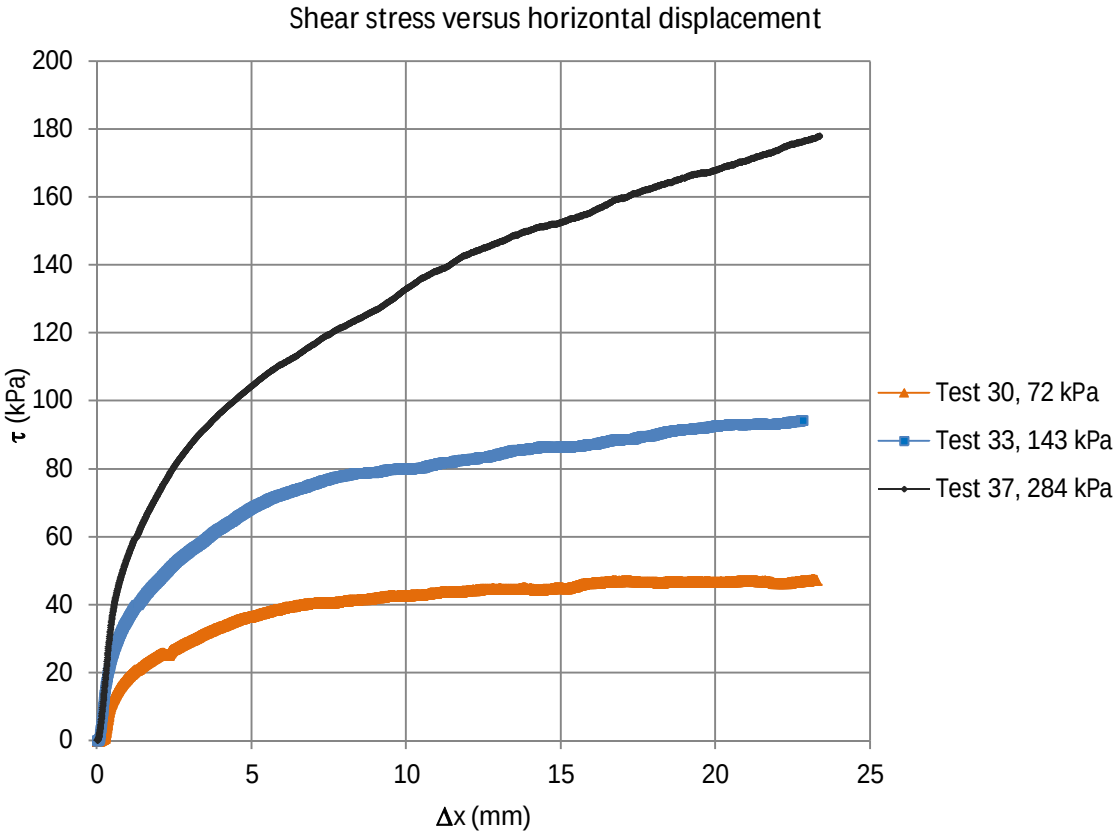

***Figure 7-18**. Shear stress against horizontal displacement in rough granite stone/pellets tests.*

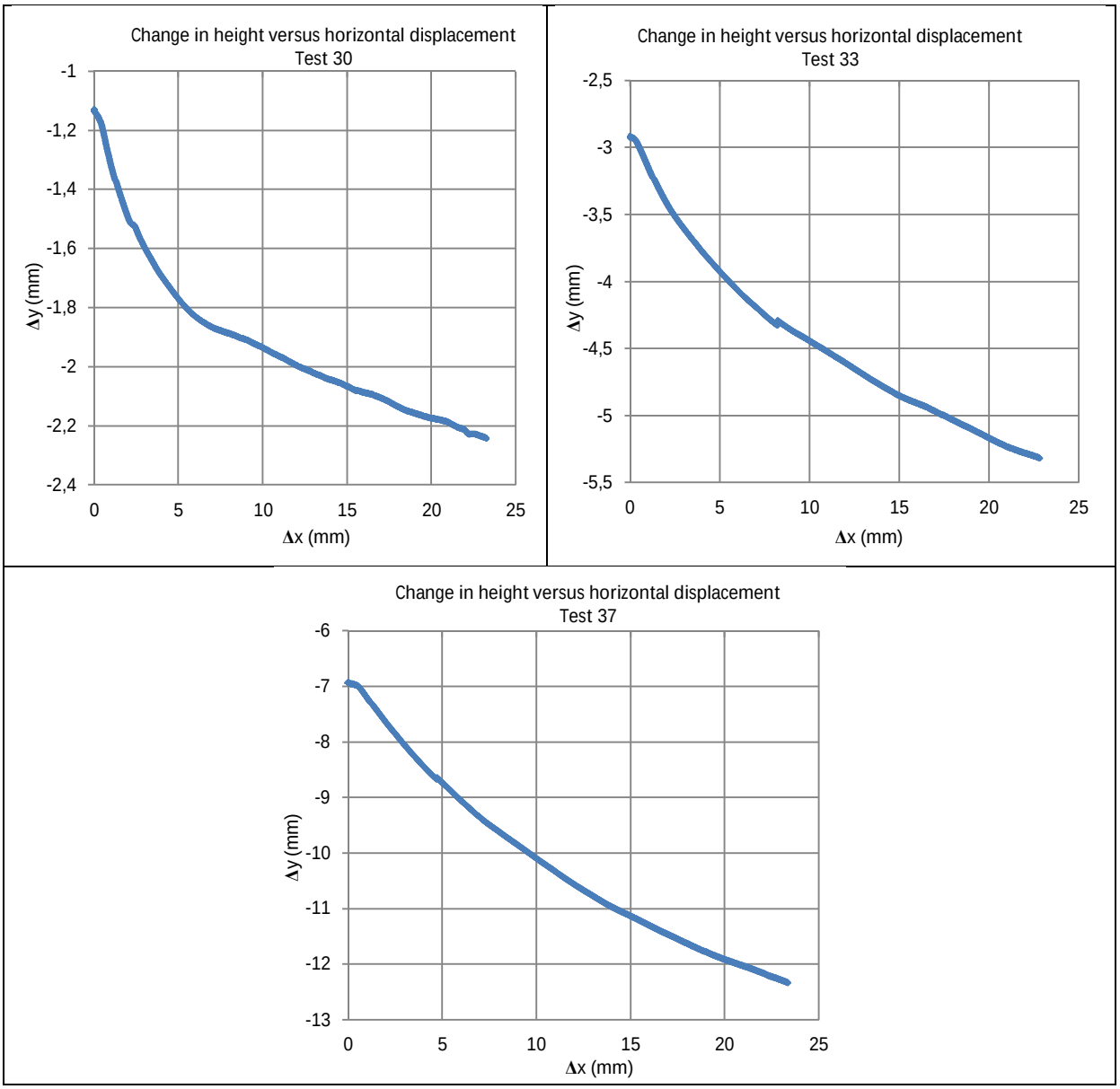

Figure 7-19*. Change in height versus horizontal displacement in rough granite stone/pellets tests.*

8. ANALYSIS OF THE RESULTS

8.1. Applied theory

As the objective of this project is to study the shear behavior of different interfaces, test results lead to analyze the friction angle (φ) and the cohesion (c) of the corresponding interfaces. Each one of the interfaces has different values of shear stress for the applied normal stress. Represented points in the graphs below are a pair of normal stress and shear stress (σ, τ), for every interface there is more than one test and for each test there are three points. The distribution of the points is approximately linear which is called the "failure line" according to Mohr-Coulomb failure criterion (Figure 8-1).

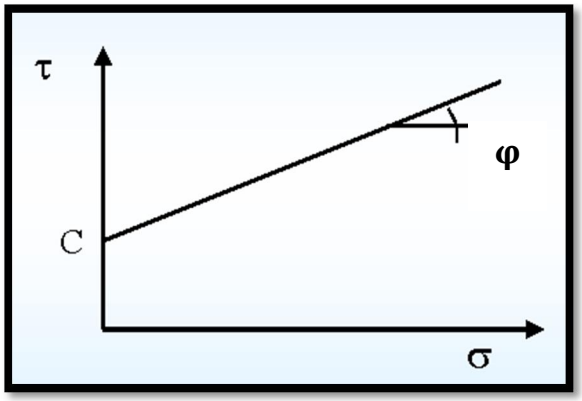

***Figure 8-1**. Mohr-Coulomb failure criterion (Michiel 2005).*

The Mohr-Coulomb failure criterion is based on the Mohr-Coulomb theory. This theory presents a mathematical model which describes the shear response of materials to the applied normal stresses. Most classical engineering materials behave according to this theory. In general, the theory is valid to the materials that have high compressive strength than tensile strength. The theory explains that a material fails due to a critical combination of normal stress and shear stress, and not because of the maximum normal or shear stress alone. (Das 2010).

The Mohr-Coulomb Failure Criterion represents a linear envelope that is obtained from a plot of the shear strength of a material versus the applied normal stress. This relation is expressed in equation (2):

$$\tau = \sigma \cdot \tan(\varphi) + c \qquad (2)$$

Where:

τ - Shear strength (kPa)

σ - Normal stress or consolidation stress (kPa)

φ - Friction angle (°)

c - Cohesion (kPa)

Figures 8-2 to Figure 8-8 show a series of graphs with the combination of normal and shear stress according to the Mohr-Coulomb criterion for each one of the interfaces. The equation of the failure line in each test is also shown.

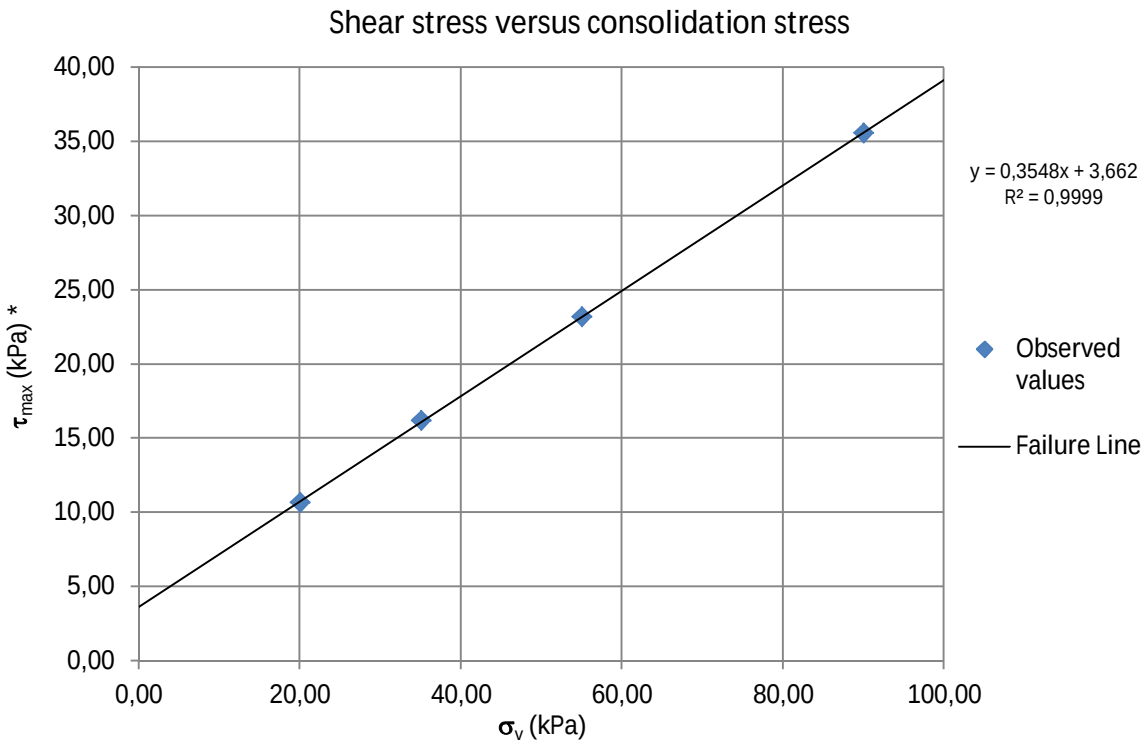

***Figure 8-2**. Shear stress against normal stress in block/block interface.*

**Note: Residual values for shear stress were used due to only few points reaching the maximum shear stress (see Figure 7-1).*

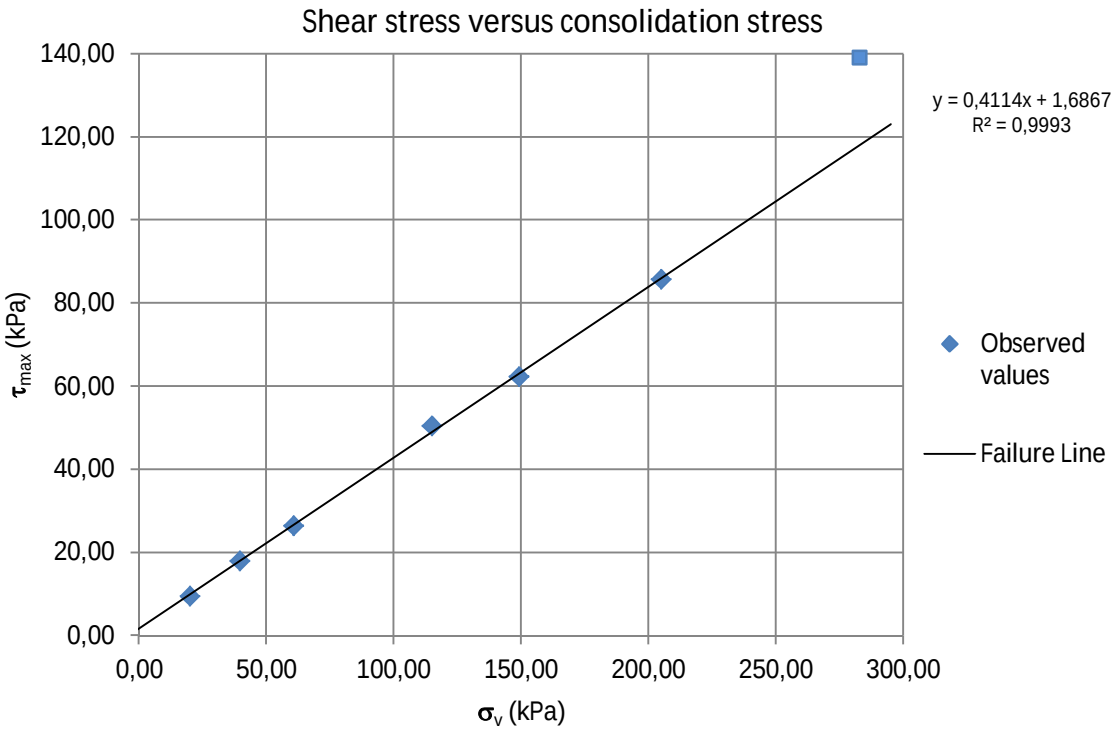

***Figure 8-3**. Shear stress against normal stress in block/pellets interface.*

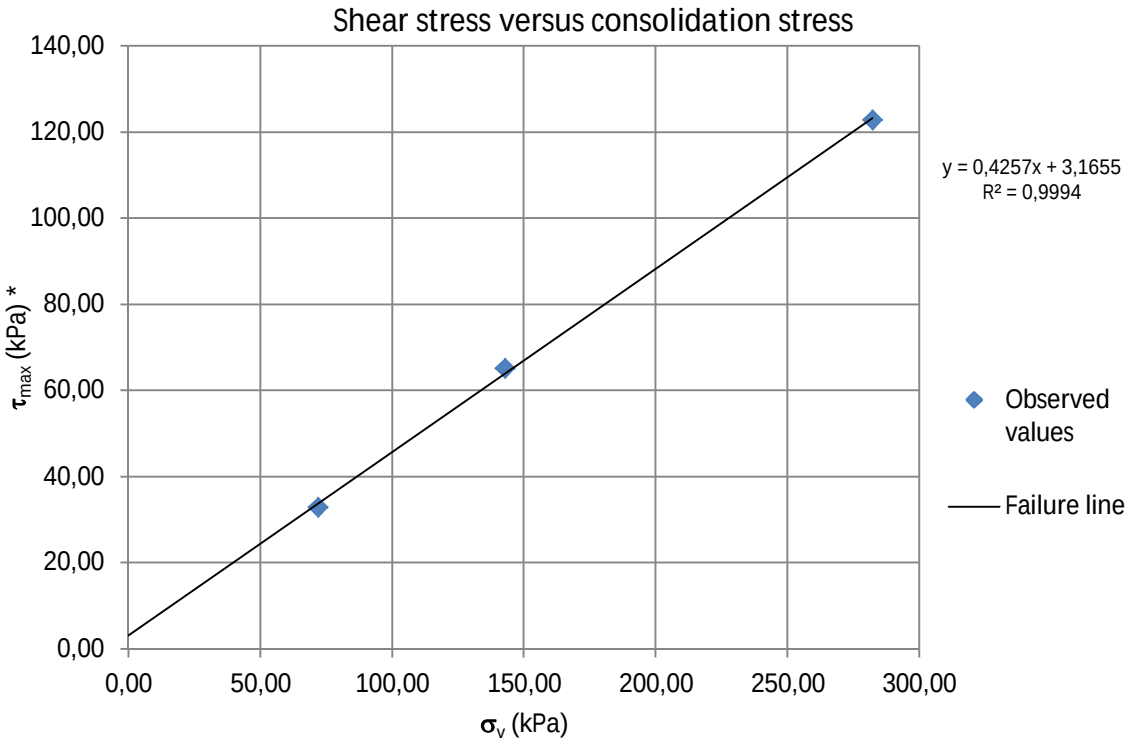

***Figure 8-4**. Shear stress against normal stress in block/granulated bentonite interface.*

**Note: Residual values for shear stress were used due to only few points reaching the maximum shear stress (see Figure 7-3).*

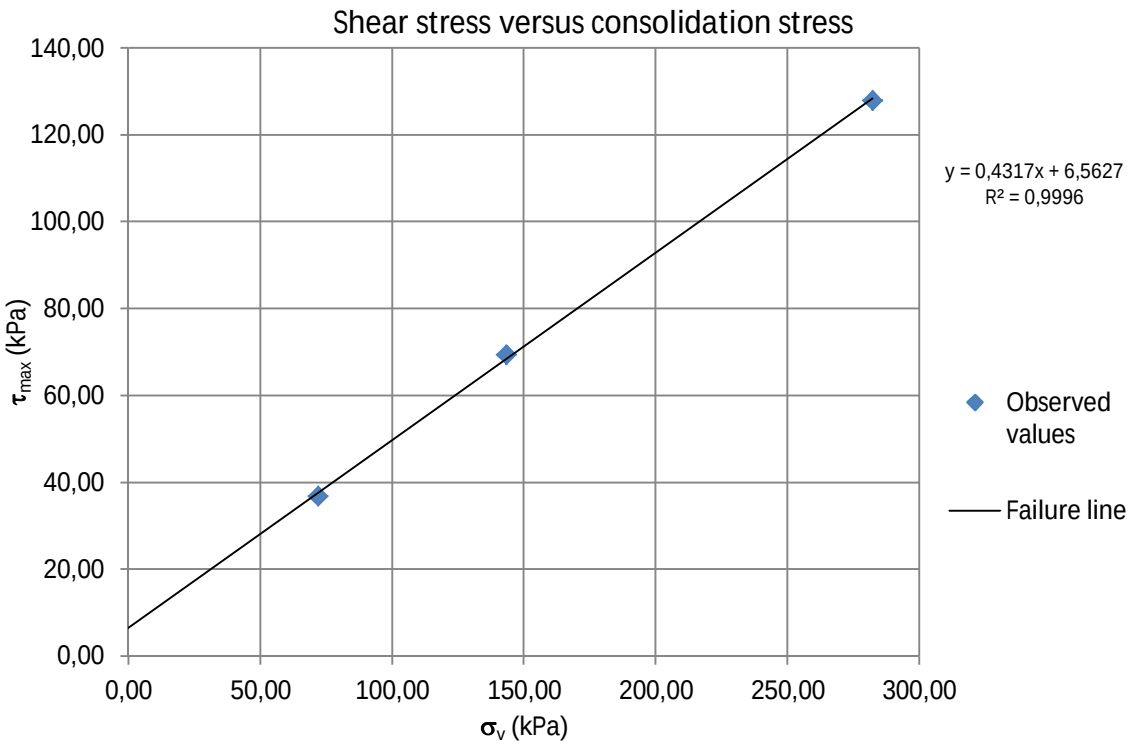

***Figure 8-5**. Shear stress against normal stress in block/foundation bed material interface.*

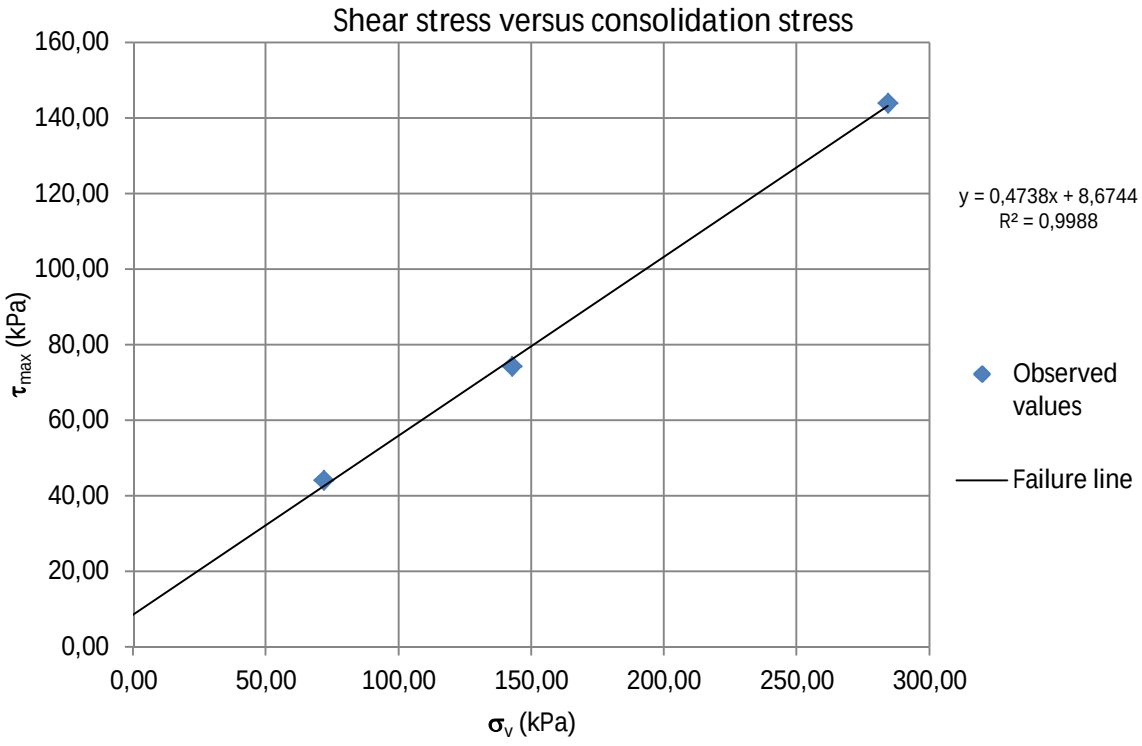

***Figure 8-6**. Shear stress against normal stress in smooth granite stone/pellets interface.*

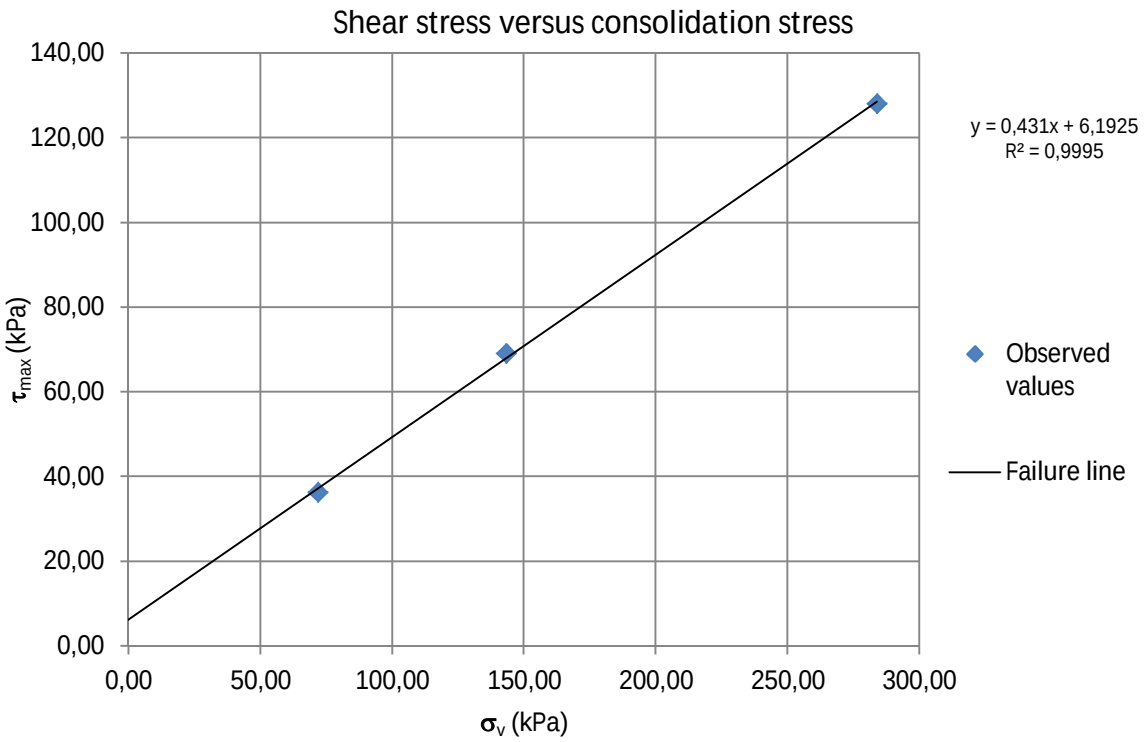

***Figure 8-7**. Shear stress against normal stress in intermediate roughness granite stone/pellets interface.*

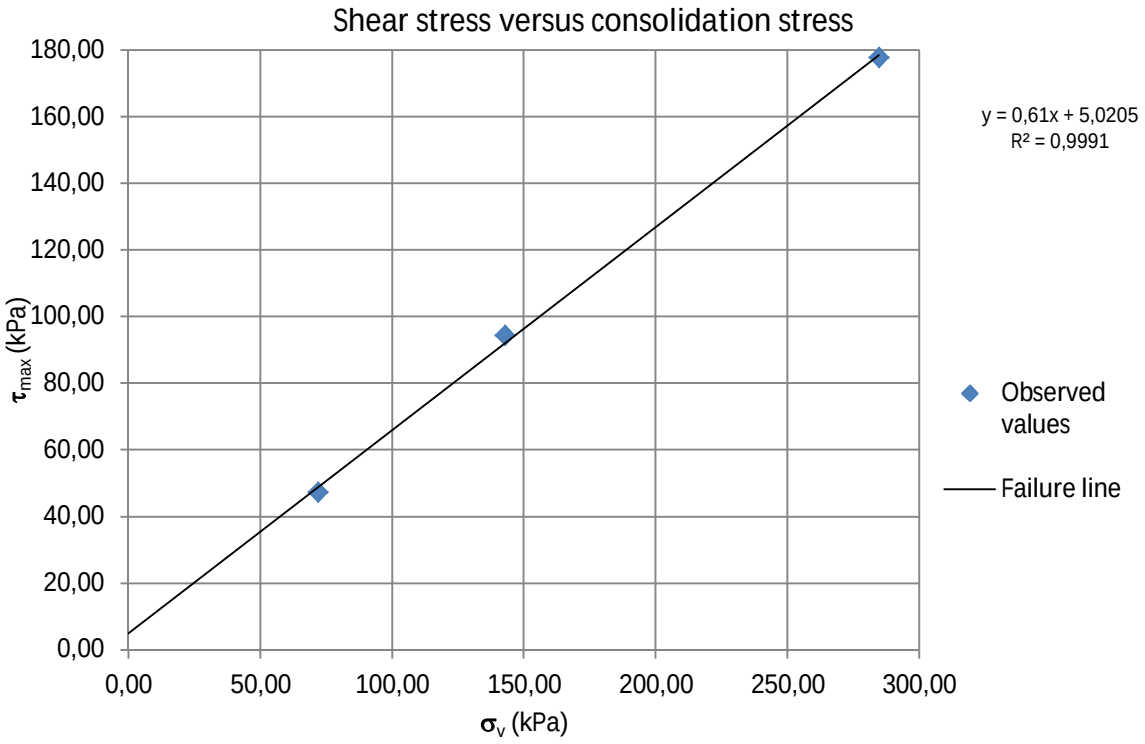

***Figure 8-8**. Shear stress against normal stress in rough granite stone/pellets interface.*

Based on the above graphs, friction angle and cohesion can be calculated using the equation of the failure line as follows:

Equation of trendline (3):

$$y = A * x + B \quad (3)$$

Cohesion (kPa) (4):

$$c = B \quad (4)$$

Friction angle (°) (5):

$$\varphi = \frac{360}{2\pi} * (\tan^{-1}(A)) \quad (5)$$

Cohesion and friction angle for different interfaces are shown in Table 8-1.

***Table 8-1**. Strength parameters for each interface.*

TESTS	φ (°)	c (kPa)	R^2
Block/block	19.50	3.70	0.9999
Block/pellets *	22.36	1.69	0.9993
Block/granulated bentonite	23.06	3.17	0.9994
Block/foundation bed material	23.35	6.56	0.9996
Smooth granite stone/pellets	25.35	8.67	0.9988
Intermediate roughness stone/pellets	23.32	6.19	0.9995
Rough granite stone/pellets	31.38	5.02	0.9991

**Note: The cohesion that can be observed in block/pellet interface was determined without taking into account the point of test 21 (Figure 8-3) because it was performed with similar but not same material and different water content (Table 6.5). So, it was more reliable not considering the point of test 21 in the failure line.*

8.2. Discussion

Following points must be discussed regarding the values in the table 8.1:

1- The regression correlation coefficient (R^2) explains how exact the adjustment of the failure line is to the observed points. In "Eurocode 7: Geotechnical design. Part 2: Ground investigation and testing" there is an additional informative annex for triaxial tests which compares the value of R^2 with some limit values. It states, if the R^2 value is higher than 0.98, no more tests are needed, provided that there is enough experience in this kind of test. Although this study is related with shear box tests and not with triaxial tests, this informative annex can be considered in order to know the number of tests that have to be done. In this study, all the values for the regression correlation coefficients are higher than 0.98, hence the number of tests performed for each interface is acceptable (SFS 1997).

2- Special attention was paid to obtain the cohesion in the interfaces involving granular materials. The calculated cohesions in those tests are very small (in the range of 3-9 kPa) as it can be observed in Table 8-1. Nevertheless, c=0 was expected because granular soils are considered as cohesionless since they do not exhibit cohesive behavior. The reason for the cohesions in granular material could be an "apparent cohesion" which means it is not real cohesion. Apparent cohesions result from the tendency of soil to expand when sheared. This apparent cohesion may also appear due to the capillarity attractive forces in unsaturated soils which bind particles together (Moayed & Alizadeh 2001).

3- Another important factor that has to be taken into consideration is the tilting of the load plate during shearing. This tilting can affect the reliability of the results because it causes a non-uniform distribution normal stress which could cause non-uniform density in the soil mass. Of course, this can only happen in granular soils because the particles are continuously relocating during the shearing. Although the tilting of the load plate was observed in some of the shear box tests in this study, no influence has been detected in the results. This could be because the tilting was not large enough to affect to verticality of the applied compression loads.

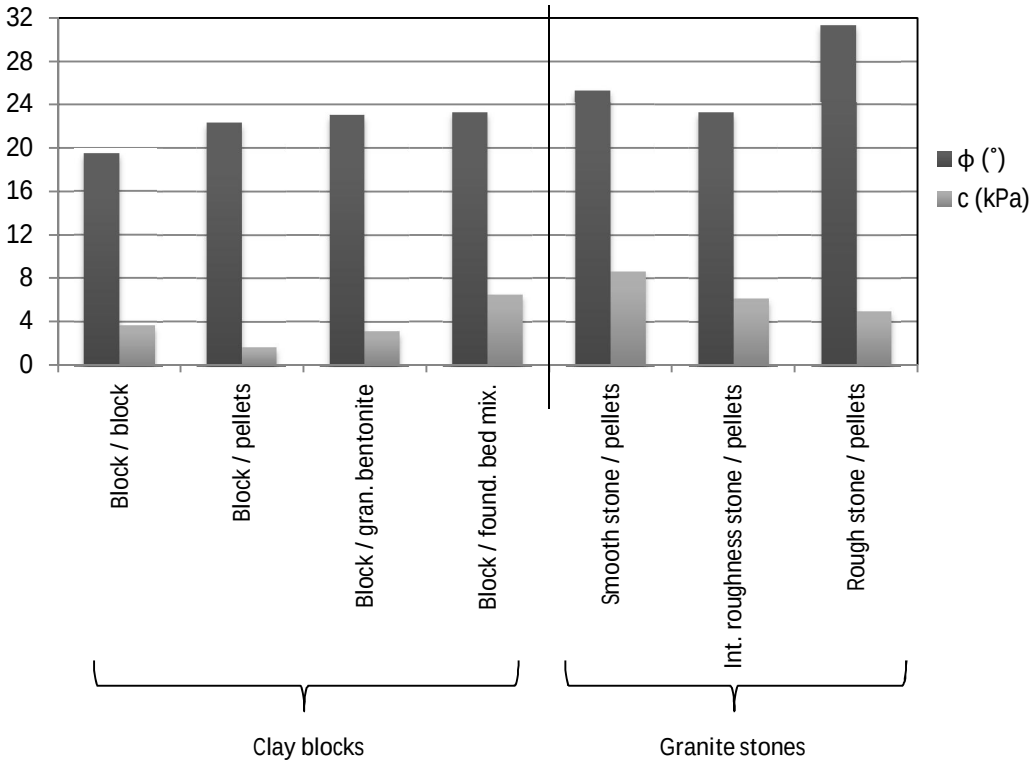

Figure 8-9*. The strength parameters in the evaluated interfaces.*

On the other hand**,** the main findings of the shear box tests results can be summarized as follows:

1- The highest value of friction angle was calculated in the interface between rough granite stone and pellets while the respective value determined for block/block interface is clearly lower (Figure 8-9).

2- No significant differences were observed in the interfaces with pellets, granulated bentonite and foundation bed material. This is because of the granular nature of all these materials. Also, their densities and water contents are very similar; see sections 6.3, 6.4 and 6.5.

3- The highest friction angle was calculated in the interface between rough granite stone and pellets due to the roughness of this granite stone. As it can be seen in Figure 8-11, the average roughness parameter (Ra) is clearly higher than the other two types of granite stones. The roughness of the block surface was also

tested as the stone surface in order to know the differences between the surface of the stone and the surface of the blocks and their influence in the shear strength parameters of the interfaces. (Figure 8-10). The determined value for the Friedland-clay block (following the same calculations as in the stones) was Ra=5.148, really close to the value of the smooth granite stone. Figure 8-10 shows the friction component and the average roughness parameter against different interfaces.

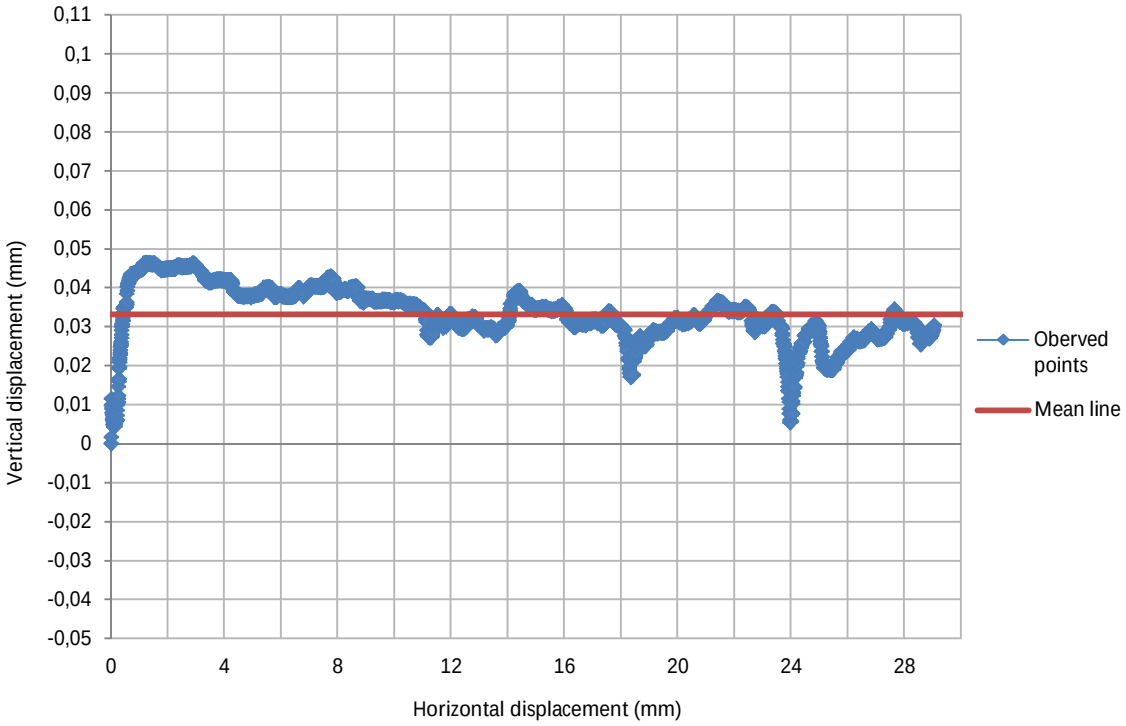

***Figure 8-10**. Horizontal displacement against vertical displacement in Friedland-clay block.*

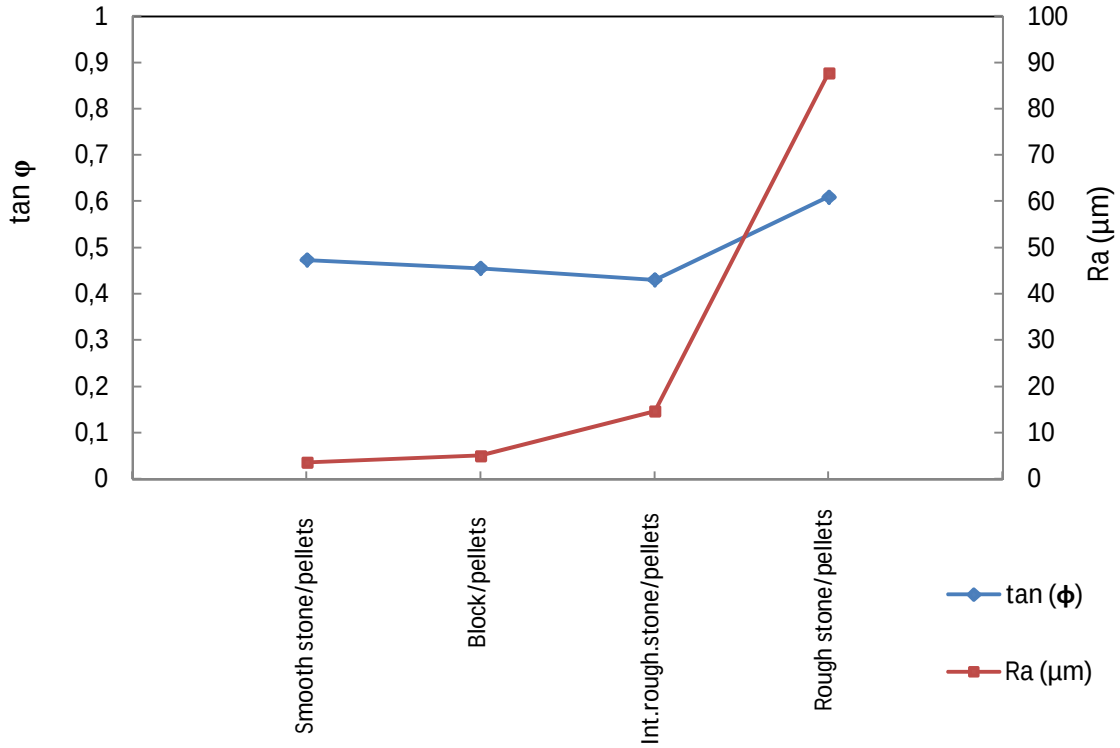

***Figure 8-11**. Friction component and average roughness parameter versus block/pellets and stone/pellets interfaces.*

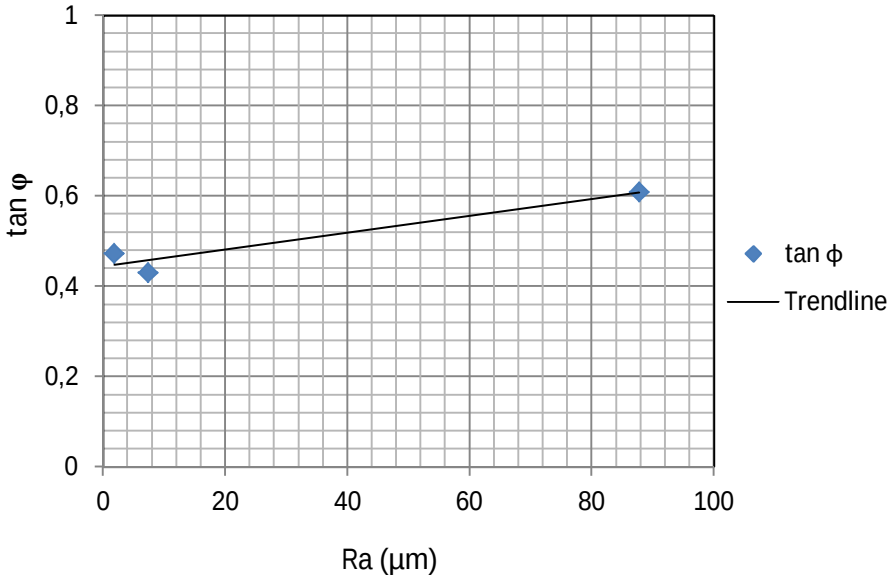

***Figure 8-12**. Average roughness parameter versus friction component.*

According to Figure 8-12, there is a relation between the friction component of the shear strength and the roughness of the surface. The friction component is increasing

with the average roughness parameter of the surface. That means, the interfaces with high roughness yield high shear strength.

When comparing the results from this study with previous studies some differences can be observed. In a similar study which was carried out at Tampere University (Kuula-Väisänen 2008), different compacted materials, blocks and other granular materials were used and the findings are reported below.

Kuula Väisänen et al. (2008) reported a friction angle of φ=24.4° in Friedland-clay blocks with dry block/block interface in the shear box test and a friction angle of φ=19.5° was obtained from the present study for a similar surface. This shows a difference of approximately 5° in the interface friction angled. This could be due to the difference in the equipment that was used to perform the tests and the sample surfaces; however, no significant differences were found in the water content and the density of the clay blocks. Moayed & Alizadeh (2001) reported that the friction angle from a shear box test could decrease with the increase in the box dimension (i.e. increase in the size of the sample). The other friction angles obtained in block/block interface tests in Tampere for other materials were similar to the value for Friedland-clay (Kuula-Väisänen 2008).

The lowest friction angles in the performed tests in Tampere were reached with the pellets. For triaxial tests, a value of φ=21.9° was determined and φ=26.9° for shear box tests. The difference between those results and the results of the present shear box tests are not significant (φ=24.5 ° for block/pellets). Also the results for the interfaces involving foundation bed material and granulated bentonite are in a range of 23°-30°. The interpretation of these results is based on the behaviour of the granular materials as materials formed by particles. The only difference between pellets in both studies was their size due to the size of the pellets in Tampere tests was bigger (Kuula-Väisänen et al. 2008).

Other shear box tests from Tampere cannot directly be compared with the present study as those tests were performed in single materials and not surfaces were involved. The friction angle obtained from a single material shear box texts represent the internal friction angle of a material and does not represent the interface behavior (Kuula-Väisänen et al. 2008).

Börgesson (2001) conducted a series of similar large shear box tests with buffer and backfill materials that were used in a Prototype repository. Crushed TBM muck and different mixtures of bentonite and crushed TBM muck with different proportions (10/90, 20/80, 30/70) were used in this study. Material was manually compacted into the lower half of the shear box before the shearing implemented under drained conditions in a saturated sample. Table 8-2 summarises the finding of Börgesson (2001):

Table 8-2*. Results from shear box tests (Börgesson 2001).*

Material	σ (kPa)	ρ_d (kg/m^3)	τ (kPa)	φ (°)
Crushed TBM muck	1000	2210	1425	54.9
10/90 mixture	1000	2160	625	32.0
20/80 mixture	1000	1970	450	24.2
30/70 mixture	1000	1850	320	17.7

Different bentonite contents were uses in mixtures and it was found that the interface friction angle inversely proportional to the bentonite content due to the smaller grain size distribution of bentonite. Comparing with the present studies, it can be observed that the values for the friction angle in the interfaces with block and granular material (pellets, granulated bentonite and foundation bed material) are really closed to the value of the 20/80 mixture. These similarities between the friction values are associated with the similitude in the grain size distribution. However, the value φ=54.9° from the crushed TBM muck is higher than the φ=31.38° from the rough granite stone/pellets which is the maximum value of the performed tests. This is explained because there is only a single granular material in those tests meanwhile there was an interface between block and granular material in the present direct shear box tests. That means that the tests reported by Börgesson (2001) were studying the internal friction angle and this project is the friction angle of the interface between materials.

All the tests in the present study were carried-out in dry state. However, in situ conditions of these materials in the deep rock repository environment could vary significantly from the tested conditions. The conditions at a depth of 420 m below the ground surface could be significantly wet and the shear behaviour of the interfaces of tunnel backfilling materials under these conditions could be completely different from what was observed in the laboratory tests. In general, the higher the water content, the

lower the interface shear strength (Tonnizamm et al. 2011).Therefore, it is strongly advisable to carry out further tests with different water content at the interfaces of these materials.

Finally, it should be noted that some measuring and evaluation errors could also have influenced the results from this study and some of them are listed below:

1- Errors in applying the normal stress to the sample due a number of mechanical components of the equipment that are involved in transmitting the loads from the load system to the sample.

2- Errors in aligning the interfaces perfectly inside the shear box.

3- Although the tilting of the load plate was not significant, better results can be achieved by using modern techniques that prevent tilting.

4- The accuracy of the strength parameters obtained in these can be verified by conducting a series of triaxial tests and comparing the shear strength parameters (c, φ) from both techniques.

9. CONCLUSIONS

Safety aspects of the deep rock nuclear waste disposal repositories in Finland have been one of the most discussed topics in the recent years. This study was carried out to investigate the mechanical interface behaviour of the deposition tunnel components of the disposal facility. Different kinds of interfaces in the tunnel backfilling components were studied by means of direct shear box tests. Up to seven different dry interfaces were tested including clay and granite stone materials.

Tests results showed that the highest interface shear strength parameters were obtained with the interface between Cebogel QSE pellets and rough granite stone. Although tested granular materials are cohesionless (c=0), low values of cohesion were obtained. A conservative approach of assuming c=0 in modelling might be considered but the experience shows that a small cohesion appears in granular materials, so the modelling of those interface could also assume this small cohesion.

Further tests have to be carried out with other interfaces such as bentonite blocks and granite stone and other backfill mixtures. It would also be useful to study the shearing behavior under different temperatures and by changing the water content at the interface.

10. REFERENCES

Alden, A., n.d. Granite and Its Geology, viewed 17 August 2012, <http://geology.about.com/od/more_igrocks/a/granite.htm>

Börgesson, L., 2001. Compilation of laboratory data for buffer and backfill materials in the Prototype Repository. Äspö Hard Rock Laboratory. International Progress Report IPR-01-34. SKB.

Börgesson, L., Hernelind, J., 2009. Mechanical interaction buffer/backfill. Finite element calculations of the upward swelling of the buffer against both dry and saturated backfill. Report R-09-42. SKB.

Carlson, L. 2004. Bentonite mineralogy, Part 1: Methods of investigation – a literature review, Part 2: Mineralogical research of selected bentonites, Working report 2004–02. Posiva Oy.

CEN ISO/TS 17892-10:2004. Geotechnical investigation and testing – Laboratory testing of soil. Part 10: Direct shear tests.

CEN ISO/TS 17892-4:2004. Geotechnical investigation and testing. Laboratory testing soil. Part 4: Determination of particle size distribution.

Das, B.M., 2010. Principles of Geotechnical Engineering. Seventh edition.

Decher, A., Bechtel, A., Echle, W., Friedrich, G. & Hoernes, S. 1996. Stable Isotope Geochemistry of Bentonites from the Island of Milos (Greece). Chemical Geology.

Dixon, D., Sandén, T., Jonsson, E., Hansen, J. . 2011. Backfilling of deposition tunnels: Use of bentonite pellets. Report P-11-44. SKB.

Edy Tonnizamm, M., Badee Abdulqawi, A., Khairul Anuar, K., Rosli, S., 2011. Shear strength behavior for older alluvium under different moisture content. http://www.ejge.com/2011/Ppr11.038/Ppr11.038ar.pdf

Eurocode 7. Geotechnical design. Part 2: Ground investigation and testing.

Gadelmawla, E.S., Koura, M.M., Maksoud, T.M.A., Elewa, I.M., Soliman, H.H., 2002. Roughness parameters. Journal of Materials Processing Technology. Volume 123, issue 1. http://www.sciencedirect.com/science/article/pii/S0924013602000602

Gunnarsson, D., Morés, L., Sellin, P., Keto, P., 2007. Deep Repository – Engineered Barrier Systems. Assessments of Backfill Materials and Methods for Deposition Tunnels. Working Report 2006-64. Posiva Oy.

Gunnarsson, D., Börgesson, L., Keto, P., Tolppannen, P., Hansen, J., 2004. Backfilling and Closure of the Deep Repository. Assessment of Backfill Concepts. Working Report 2003-77. Posiva Oy.

Head, K.H., 1982. Manual of soil laboratory testing. Volume 2: Permeability, Shear Strength and Compressibility Tests.

Hansen, J., Korkiala-Tanttu, L., Keski-Kuha, E., Keto, P., 2010. Deposition Tunnel Backfill Design for a KBS-3V Repository. Working Report 2009-129. Posiva Oy.

ISO 3310-1:2000. Test sieves- Technical requirements and testing. Part 1: Test sieves of metal cloth.

ISO 565:1990. Test sieves – Metal wire cloth, perforated metal plate and electroformed sheet – Nominal sizes of openings.

Juvankoski, M., Marcos N., 2010. Design basis for buffer components. Working Report 2009-132. Posiva Oy.

Karnland, O., Clay Technology AB, 2010. Chemical and mineralogical characterization of the bentonite buffer for the acceptance control procedure in a KBS-3 repository. Technical Report TR-10-60. SKB.

Keto, P., 2004. Natural Clays as Backfilling Materials in Different Backfilling Concepts. Working Report 2003-79. Posiva Oy.

Keto, P., Kuula-Väisänen, P., Ruuskanen, J., 2006. Effect of Material Parameters on the Compactibility of Backfill Materials. Working Report 2006-34. Posiva Oy.

Keto, P., 2007. Backfilling of Deposition Tunnels, In Situ Alternative. Working Report 2006-90. Posiva Oy.

Keto, P., Dixon, D., Jonsson, E., Gunnarsson, D., Börgesson, L., Hansen, J., 2009. Assessment of backfill design for KBS-3V repository. Report R-09-52. SKB.

Korkiala-Tanttu, L., 2009. Finite Element Modelling of Deformation of Unsaturated Backfill Due to Swelling of the Buffer. Working Report 2008-88. Posiva Oy.

Kuula-Väisänen, P., Leppänen, M., Kolisoja, P. 2008. Backfilling and closure of deep repository. Processes during saturation of the block backfill. Mechanical properties and saturation of the block backfill. Tampere University of Technology, Earth and Foundation Structures.

Kumpulainen, S., L. Kiviranta, 2011. Mineralogical, chemical and physical study of Potential buffer and backfill materials from the ABM test package 1. Working Report 2011-41. Posiva Oy.

Leoni, M., 2012. 2D and 3D finite element analysis of buffer-backfill interaction. Working Report (Draft). Posiva Oy.

Moayed, R.Z., Alizadeh, A., 2001. Effect of the shear box size on the strength for different type of silty sands in directs shear tests.

Marjavaara, P., Kivikoski, H., 2011. Fillig the Gap Between Buffer and Rock in the Deposition Hole. Working Report 2011-33. Posiva Oy.

Michiel. (2005). Teoría de Mohr-Coulomb. Available: www.wikipedia.org. Last accessed 17th Aug 2012.

Nemlander, R. & Keski-Kuha, E. 2012. BACEKO II Flow-through, open-front and saturation tests of pre-compacted backfill blocks in a quarter-scale test tunnel, Posiva working report draft version 3.2.2012.

Posiva, 2010. Nuclear Waste Management at Olkiluoto and Loviisa Power Plants. Review of Current Status and Future Plans for 2010-2012. TKS-2009. Posiva Oy.

Rautioaho, E., Korkiala-Tanttu, L., 2009. Bentomap: Survey of bentonite and tunnel backfill knowledge. State-of-the-art. VTT.

Riikonen, E., 2009. Flow-through and wetting tests of pre-compacted backfill blocks in a quarter-scale test tunnel. Working Report 2008-89. Posiva Oy.

Snelling, C. , 2008. Handbook of Chemistry and Physics, 53rd Edition. *Density of Water (g/mL) vs. Temperature (°C)*. Retrieved August 1, 2012, from http://www2.volstate.edu/CHEM/Density_of_Water.htm

Suomen Standardisoimisliitto SFS 1997. Eurokoodi 7: Geotekninen suunnittelu. Osa 2: Pohjatutkimus ja koestus, SFS-EN 1997-2. Liite P. Maan lujuuskokeita koskevaa yksityiskohtaista tietoa. Suomen Standardisoimisliitto, Helsinki.

Svensk Kärnbränslehantering AB, 1998. RD & D-Programme 98. Treatment and final disposal of nuclear waste. Programme for research, development and demonstration of encapsulation and geological disposal. SKB.

Svensk Kärnbränslehantering AB, 2010. Choice of method – evaluation of strategies and systems for disposal of spent nuclear fuel. Report P-10-47. SKB.

APPENDICES

Appendix 1. Normal stress versus Δh in consolidation phase.

Test 21. Block / pellets	Test 22. Block / foundation bed material
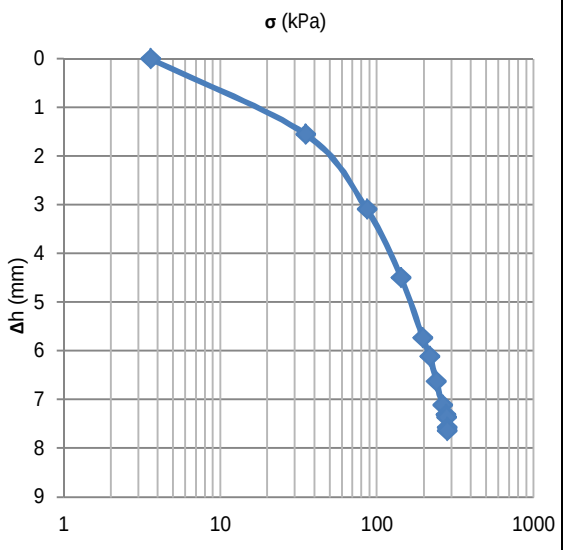	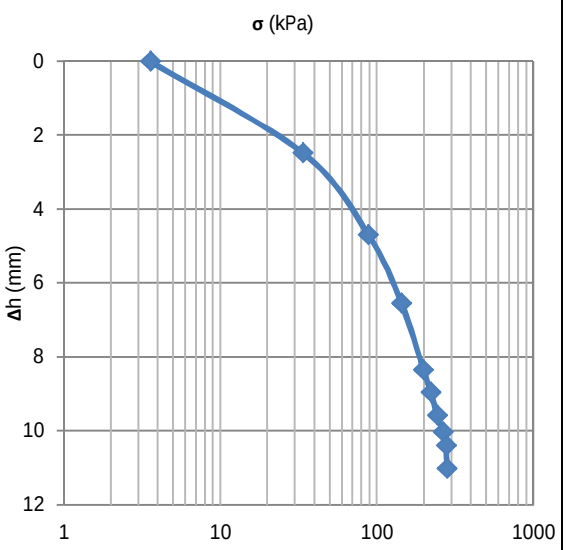
Test 23. Block / foundation bed material	**Test 24. Block / foundation bed material**
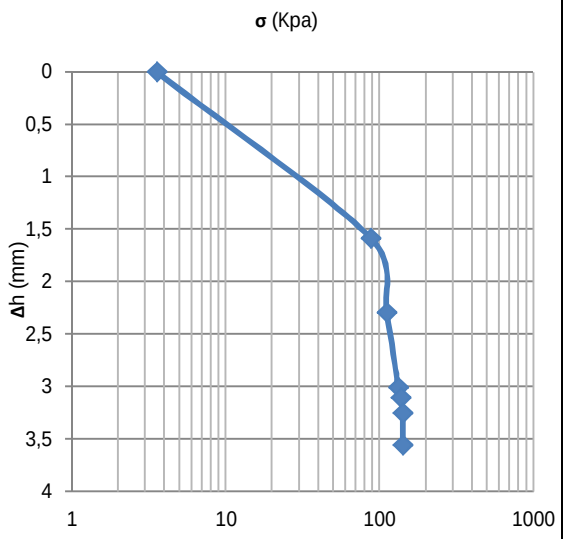	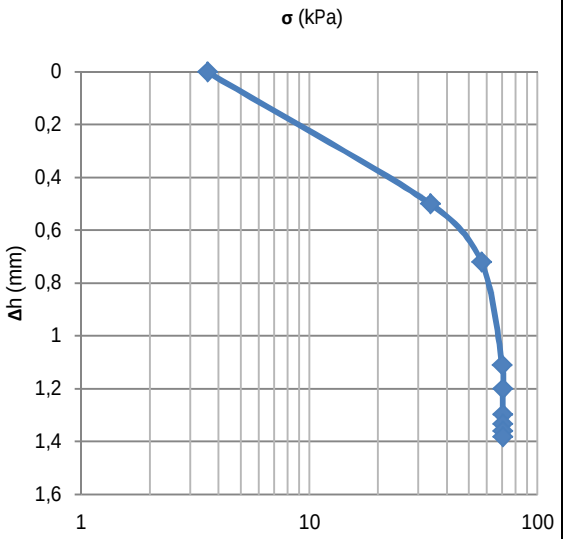

Test 25. Block / granulated bentonite	Test 26. Block / granulated bentonite
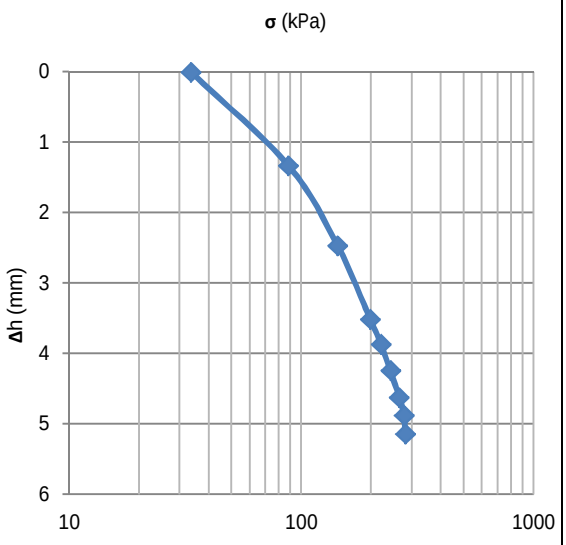	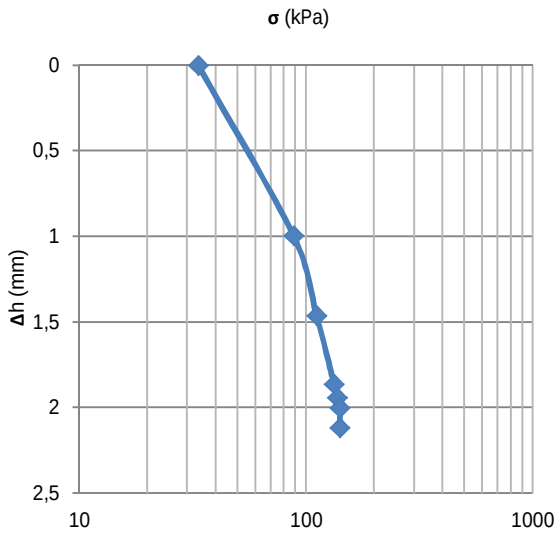
Test 27. Block / granulated bentonite	**Test 28. Block / intermediate roughness granite stone**
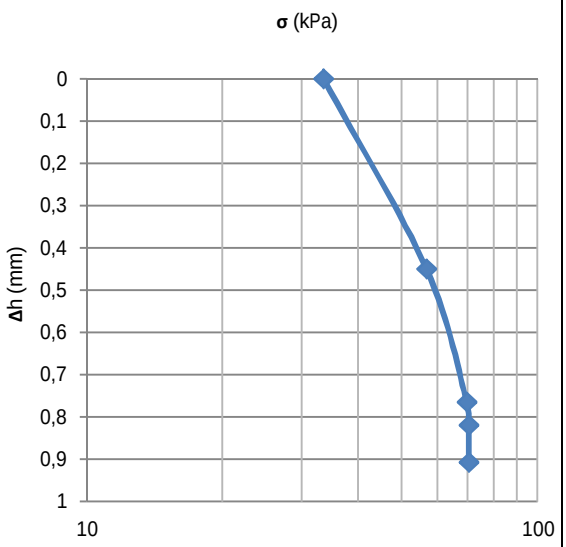	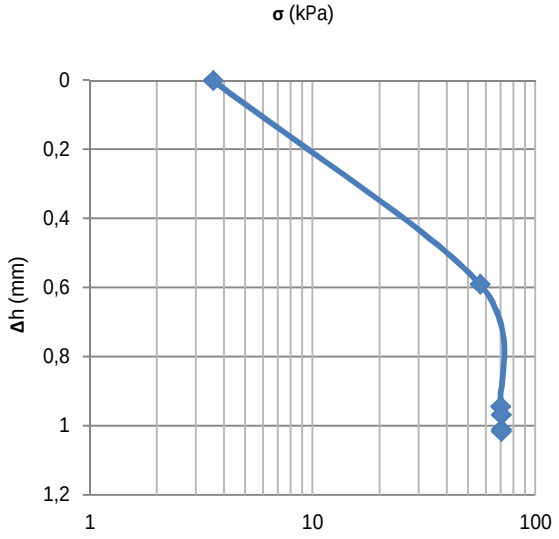

Test 29. Block / smooth granite stone	Test 30. Block / rough granite stone
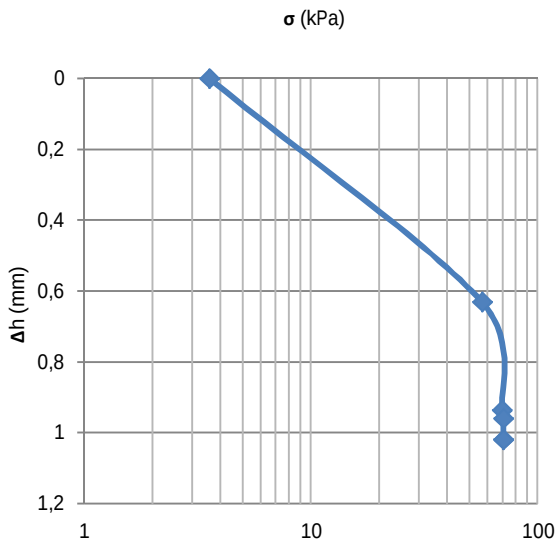	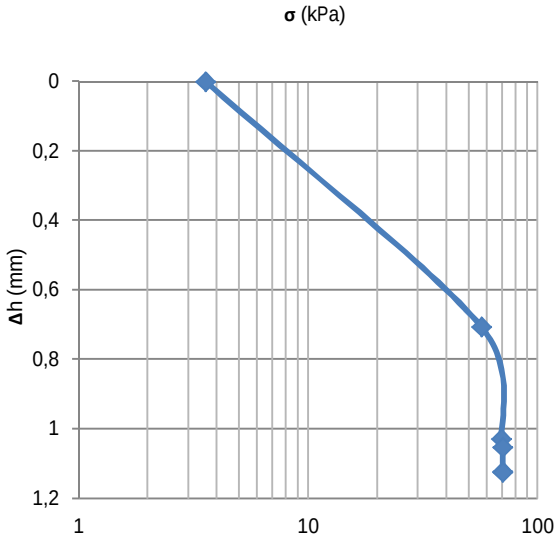
Test 31. Block / intermediate roughness granite stone	**Test 32. Block / smooth granite stone**
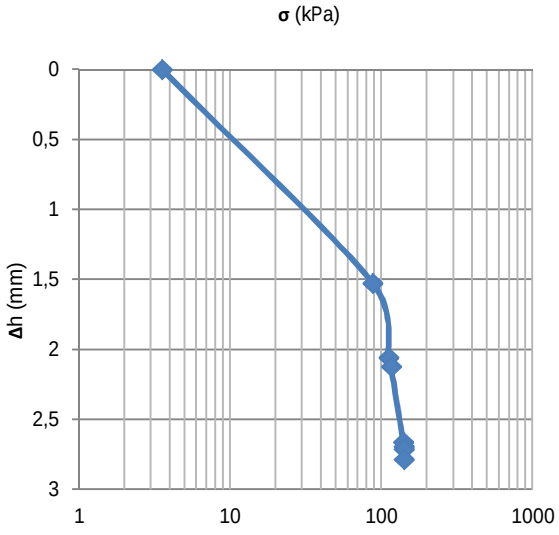	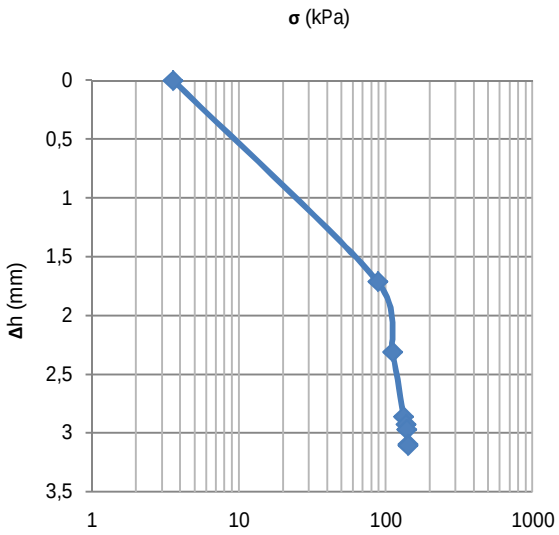

Test 33. Block / rough granite stone	Test 34. Block / intermediate roughness granite stone
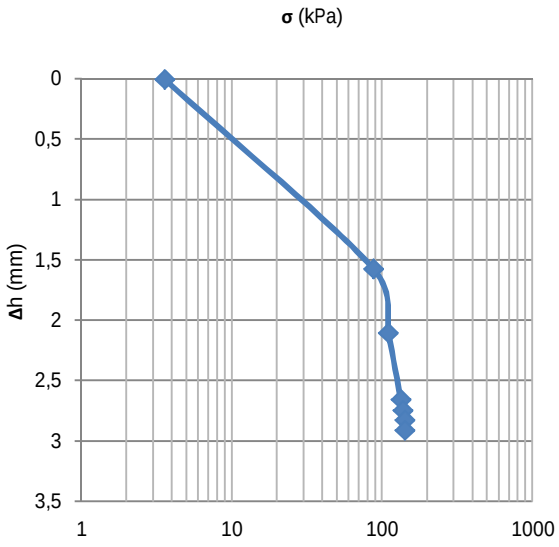	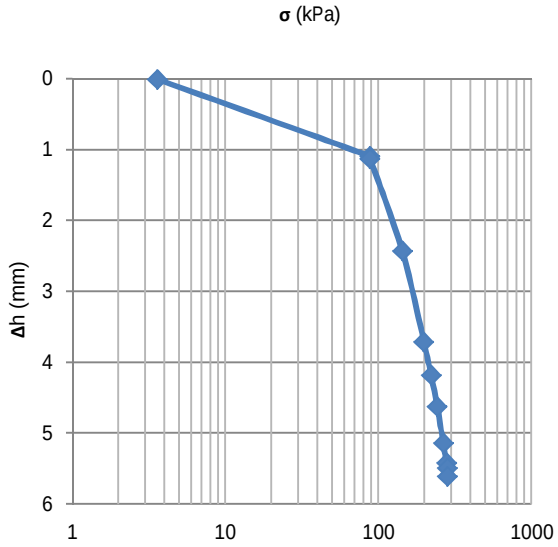
Test 35. Block / smooth granite stone	**Test 37. Block / rough granite stone**
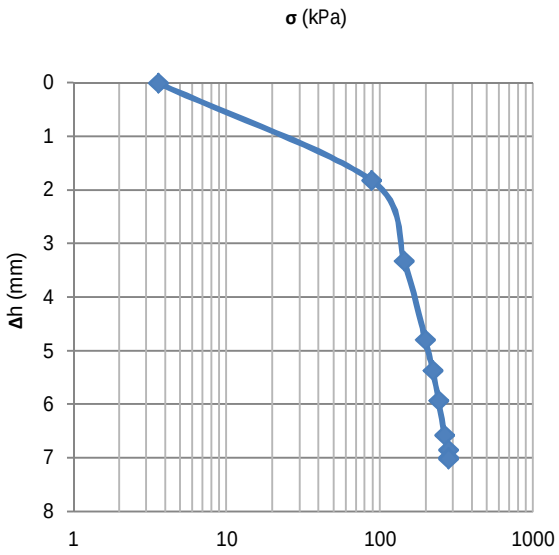	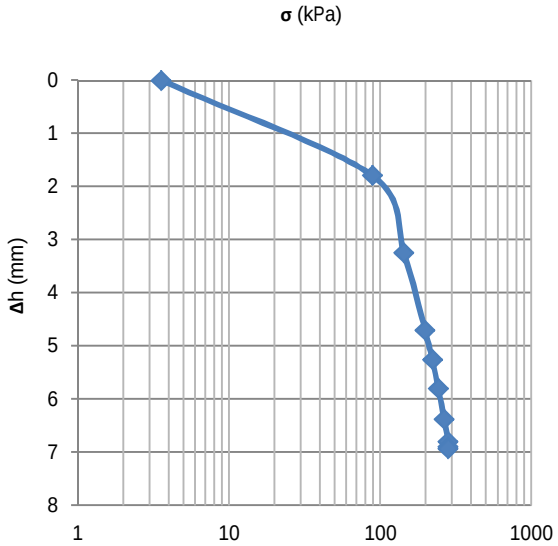

Appendix 2. Time versus Δh in consolidation phase.

Test 21. Block / pellets	Test 22. Block / foundation bed material
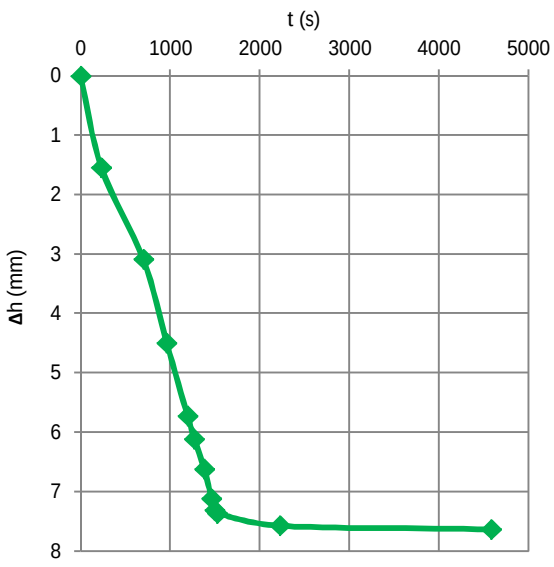	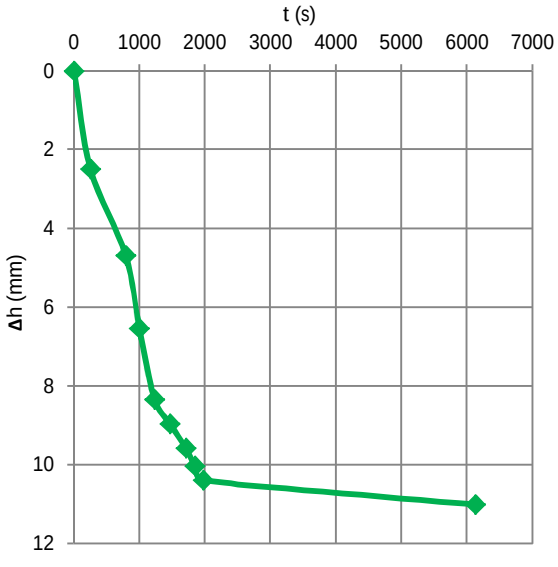
Test 23. Block / foundation bed material	**Test 24. Block / foundation bed material**
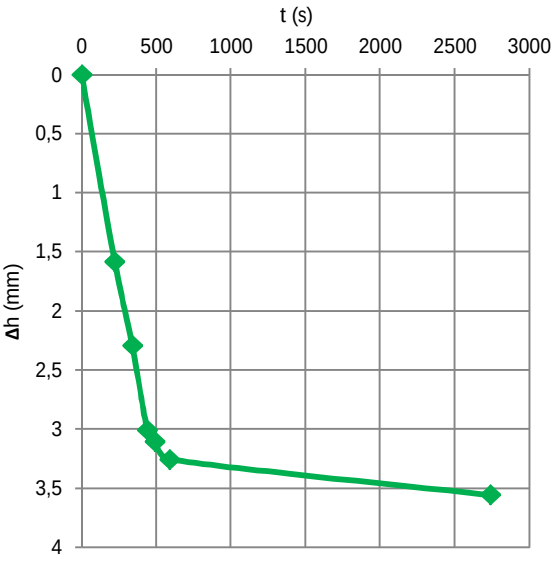	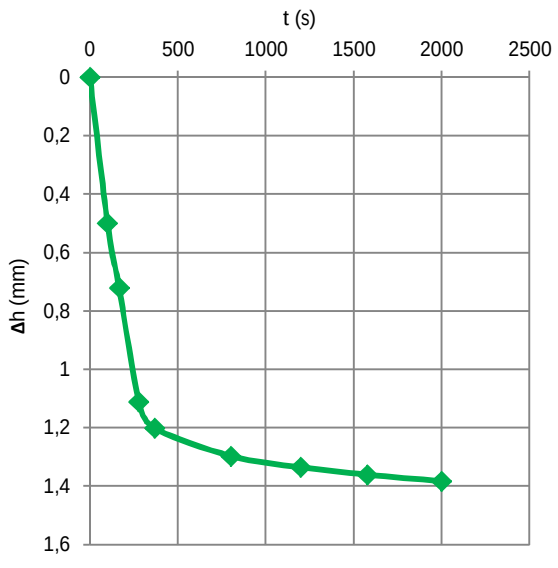

Test 25. Block / granulated bentonite	Test 26. Block / granulated bentonite
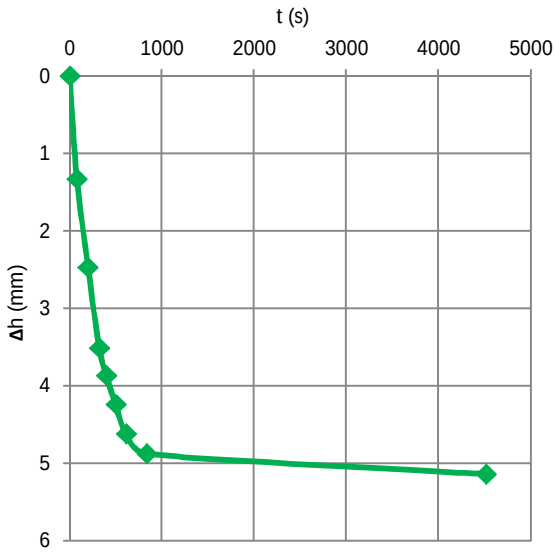	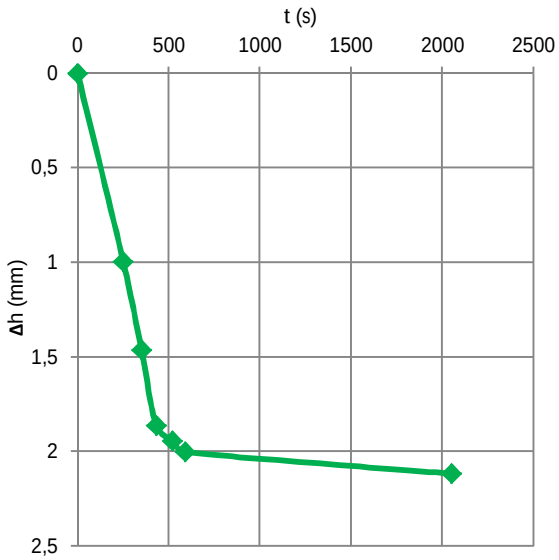
Test 27. Block / granulated bentonite	**Test 28. Block / intermediate roughness granite stone**
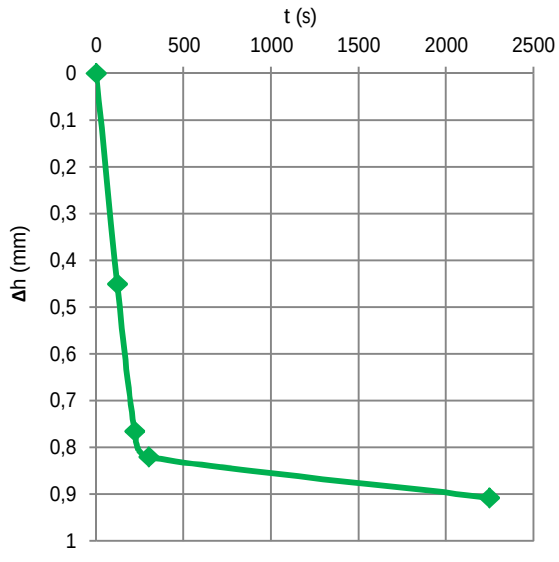	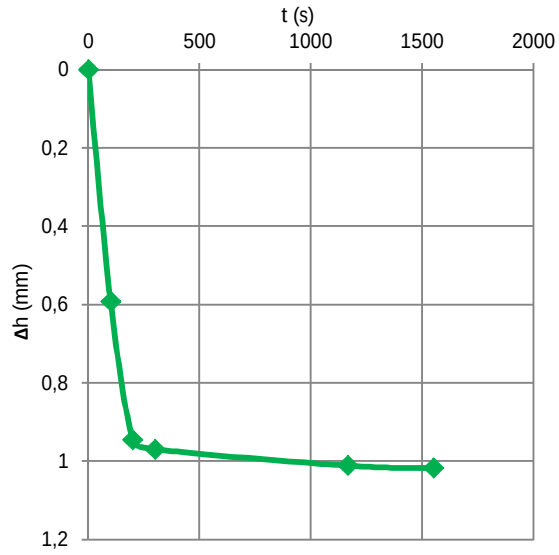

Test 29. Block / smooth granite stone	Test 30. Block / rough granite stone
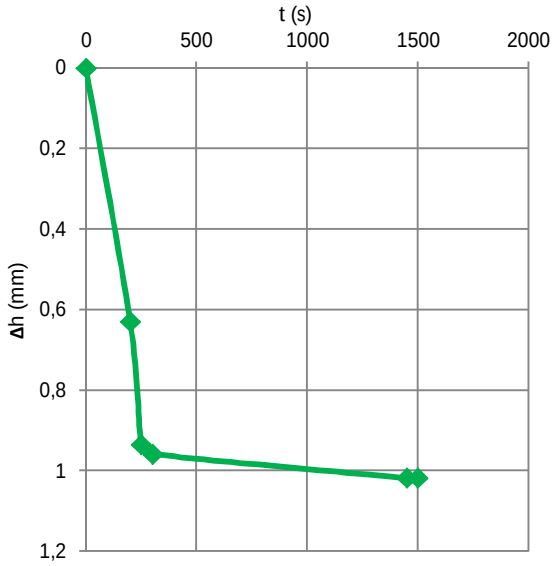	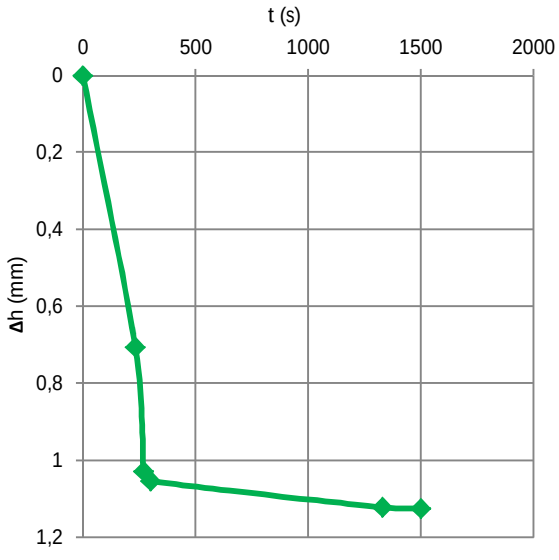
Test 31. Block / intermediate roughness granite stone	**Test 32. Block / smooth granite stone**
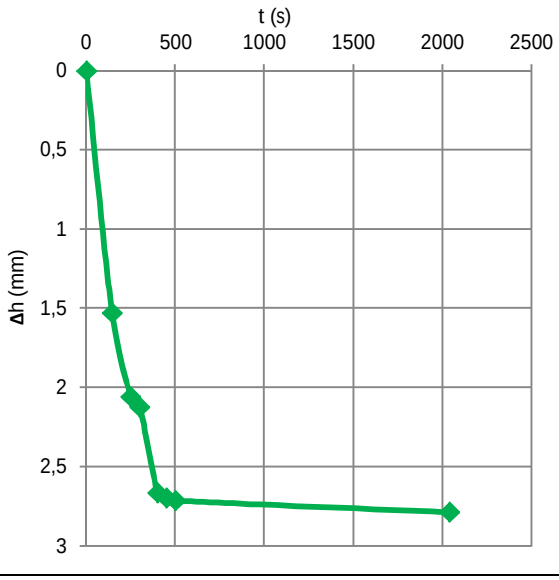	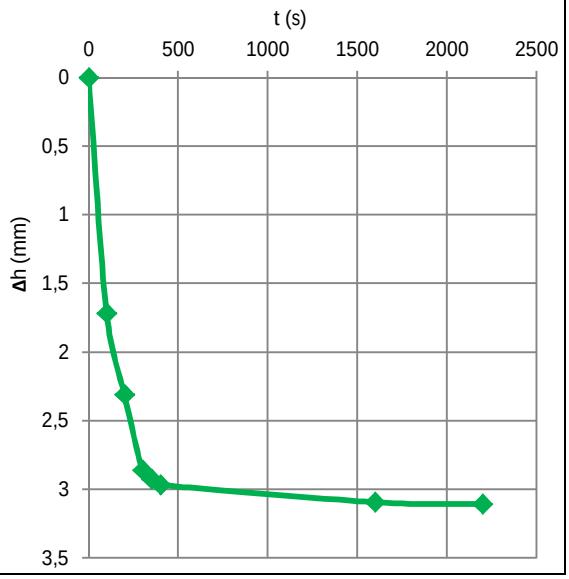

Test 33. Block / rough granite stone	Test 34. Block / intermediate roughness granite stone
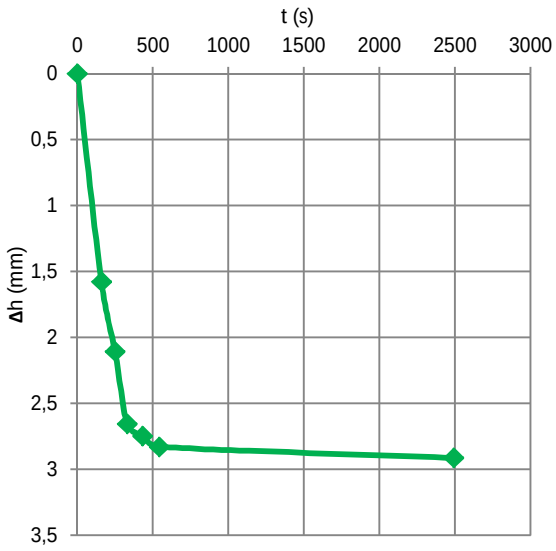	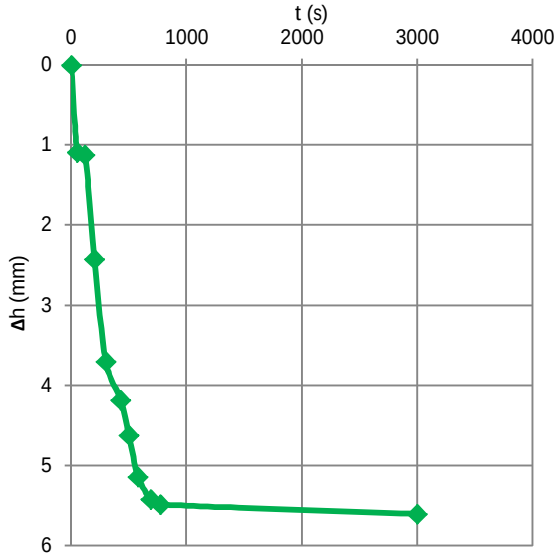
Test 35. Block / smooth granite stone	**Test 37. Block / rough granite stone**